ACUTE EXPOSURE TO TCDD INCREASES LIVER DISEASE PROGRESSION IN MICE WITH CARBON TETRACHLORIDE-INDUCED LIVER INJURY

by

Giovan N. Cholico

A dissertation

Submitted in partial fulfillment

of the requirements for the degree of

Doctor of Philosophy in Biomolecular Sciences

Boise State University

December 2019

BOISE STATE UNIVERSITY GRADUATE COLLEGE

DEFENSE COMMITTEE AND FINAL READING APPROVALS

of the dissertation submitted by

Giovan N. Cholico

Dissertation Title: Acute Exposure to TCDD Increases Liver Disease Progression In Mice With Carbon Tetrachloride-Induced Liver Injury

Date of Final Oral Examination: 2 December 2019

The following individuals read and discussed the dissertation submitted by student Giovan N. Cholico, and they evaluated the student's presentation and response to questions during the final oral examination. They found that the student passed the final oral examination.

Kristen A. Mitchell, Ph.D.	Chair, Supervisory Committee
Kenneth A. Cornell, Ph.D.	Member, Supervisory Committee
Allan R. Albig, Ph.D.	Member, Supervisory Committee
Daniel Fologea, Ph.D.	Member, Supervisory Committee
Denise G. Wingett, Ph.D.	Member, Supervisory Committee

The final reading approval of the dissertation was granted by Kristen A. Mitchell, Ph.D., Chair of the Supervisory Committee. The dissertation was approved by the Graduate College.

DEDICATION

This dissertation is dedicated to my father and mother, Pedro and Angelica Cholico, my grandparents, Miguel and Irene Martin, and Pedro and Maria de Jesus Cholico, and my surrogate grandparents, Salvador and Carolyn Romero. Thank you for your never-ending love and support, as well as your efforts to raise a wonderful and successful family.

Esta disertación está dedicada a mi padre y mi madre, Pedro y Angélica Cholico, mis abuelos, Miguel e Irene Martin, y Pedro y María de Jesus Cholico, y mis abuelos suplentes, Salvador y Carolina Romero. Gracias por su amor y apoyo sin fin, y también por sus esfuerzos para formar una familia maravillosa y exitosa.

ACKNOWLEDGEMENTS

First and foremost, I would like to thank my advisor and mentor, Dr. Kristen Mitchell for her continuing guidance as I strive to become a scientific professional. I am eternally grateful for the guidance she gave me that helped me become the scientist I am today. In addition to my mentor, I would like to thank the members of my defense committee, Drs. Kenneth Cornell, Allan Albig, Daniel Fologea, and Denise Wingett, for also giving me valuable scientific input.

I am also incredibly grateful for members of the Mitchell lab that helped get my project off the ground. A special thanks to Wendy Harvey, Sarah Kobernat, Shivakumar Rayavara Veerabadriah and Dr. Cheri Lamb. I would also like to thank the many students that worked in our lab and helped me with my work; these include Megan Sarmenta, Madison Dupper, Deb Weakly, Samantha Peterson, Justin Nelson, Jade VanTrease, Bradley Heidemann, Cooper Hensen, Paul Stegelmeier, David Maldonado, Victoria Davidson and Natalie Johnson. I would also like to thank Brynne Coulam for all her hard work on investigating melanoma induction mechanisms in our lab.

My mouse work could not have been possible without the help of the Boise State Research Vivarium staff, with special thanks to the Sarah McCusker. Many thanks for the technical expertise of researchers at the Biomolecular Research Center, including Drs. Shin Pu, Cindy Keller-Peck, and Julie Oxford. The histopathological scoring could not have been done without the help of researchers at the Idaho Veterans Research and Education Foundation including Victoria Galarza and Dr. Frederick Bauer.

Funding for this project was supported by Institutional Development Awards (IDeA) from the National Institute of General Medical Sciences of the National Institutes of Health under Grants #P20GM103408 and P20GM109095, as well as support from the Biomolecular Research Center at Boise State with funding from the National Science Foundation, Grants #0619793 and #0923535; the MJ Murdock Charitable Trust; the Idaho State Board of Education; and a bioinformatics seed grant through the Idaho INBRE program.

I would like to give a special thanks to the scientists at the University of Nevada School of Medicine that sparked my interest in research in the first place. This includes my former graduate student mentor, Scott Barnett, my former post-doctoral fellow mentors, Drs. Chad Cowles and Craig Ulrich, and my former principal investigator mentors, Drs. Heather Burkin and Iain Buxton. May you continue to inspire the next generation of scientific researchers.

I would also like to thank the many friends that have given me constant support and encouragement. These include my longtime childhood friends, Camille Lyon and Alyssa Parks. As well as the many friends I made in college, but most importantly Taylor Cohen, and Nick and Lara Vargas. I would like to give a special thanks to Steven Burden and the Burden-Kartchner family for inviting me into their family, as I encountered many hurdles in graduate school. I would like to thank the many other friends I made in Boise that helped me get to where I am today, including Jonathan Reeck, Clémentine Gibard-Bohachek, Hagen Shults, Jessica Roberts, Mary Witucki, Blaire Anderson, Kate Grosswiler, Desiree Self, Phil Moon, Mila Lam, Ashley Poppe, and Jerrett and Kelsey Holdaway.

I would also like to thank the many members of my family that have helped get me to this point in life. A special thanks to my two brothers, Steven and Bryan for the time they gave me in the summers and winters to go on a myriad of adventures. I also thank my grandparents, Miguel and Irene Martin, for letting me spend part of my summers at their home in Mexico. Thanks to my surrogate grandparents, Sal and Carolyn Romero, for their constant financial and recreational support, and truly defining and exemplifying the phrase “spoil the grandkids”.

Finally, I would like to thank my parents, Pedro and Angelica Cholico, for putting their children’s well-being above anything else. From their leap of faith in immigrating to the United States in search of a better life, to the constant sacrifice that they endured during my childhood to raise a family. The push for their kids to obtain a higher education has truly made their dreams a reality in which their kids and grandkids will live a more comfortable life. May they always know that I hold a deep appreciation for their hard work and sacrifice.

ABSTRACT

Liver disease is a worldwide problem and the 9th leading cause of death in the United States. Common causes of liver disease include alcohol abuse, virus infection, and nonalcoholic fatty liver. Regardless of etiology, liver damage elicits inflammation and drives the activation of hepatic stellate cells (HSCs), which deposit collagen throughout the liver. During chronic injury, excessive collagen deposition, referred to as fibrosis or "scarring", can progress to cirrhosis, cancer, and organ failure. Emerging evidence indicates a strong association between liver disease and exposure to environmental chemicals. This research investigated mechanisms by which exposure to the environmental contaminant 2,3,7,8-tetrachlorodibenzo-*p*-dioxin (TCDD) impacts liver disease. TCDD is representative of a family of chemicals that elicit toxicity through the aryl hydrocarbon receptor (AhR). A mouse model system was used in which liver damage was first induced with carbon tetrachloride, and TCDD was administered as a "second hit." We used mice with the AhR selectively removed from either HSCs or hepatocytes. Results indicate that TCDD treatment exacerbated injury, inflammation and HSC activation through a mechanism that required AhR signaling in hepatocytes. Furthermore, TCDD treatment produced changes in gene expression consistent with a condition called non-alcoholic fatty liver disease. The results raise the intriguing possibility that exposure to environmental contaminants may facilitate liver disease progression in an already-injured liver.

TABLE OF CONTENTS

LIST OF TABLES

LIST OF FIGURES

LIST OF ABBREVIATIONS

αSMA	Alpha-Smooth Muscle Actin
AhR	Aryl Hydrocarbon Receptor
AhRR	Aryl Hydrocarbon Receptor Repressor
Alb	Albumin
ALT	Alanine Aminotransferase
ARNT	Aryl Hydrocarbon Receptor Nuclear Translocator
BDL	Bile Duct Ligation
bHLH	Basic Helix-Loop-Helix
CCl_4	Carbon Tetrachloride
ChIP	Chromatin Immunoprecipitation
Cre	Cre-recombinase
CYP	Cytochrome P450
DEG	Differentially Expressed Gene
ECM	Extracellular Matrix
GAPDH	Glyceraldehyde 3-phosphate Dehydrogenase
GFAP	Glial Fibrillary Acidic Protein
H&E	Hematoxylin and Eosin
HABP	Hyaluronic Acid Binding Protein
HAH	Halogenated Aromatic Hydrocarbons
HFD	High Fat Diet
HSC	Hepatic Stellate Cell
IL	Interleukin
KO	Knockout
LD50	Lethal Dose, 50%
NAFLD	Non-alcoholic Fatty Liver Disease

PAS	Per-ARNT-Sim
PCR	Polymerase Chain Reaction
RNA	Ribonucleic Acid
TCDD	2,3,7,8-Tetrachlorodibenzo-*p*-dioxin
SAhRM	Selective AhR Modulator
WT	Wild-type
XRE	Xenobiotic Response Element

CHAPTER ONE: INTRODUCTION

The Aryl Hydrocarbon Receptor

The aryl hydrocarbon receptor (AhR) is a transcription factor that regulates gene expression during a wide variety of physiological processes, including xenobiotic metabolism, development, and adaptation to environmental and cellular stress (Mulero-Navarro & Fernandez-Salguero, 2016). This receptor is widely recognized for its role in mediating the toxicity associated with exposure to environmental contaminants, such as polycyclic aromatic hydrocarbons and halogenated aromatic hydrocarbons, but mechanisms of toxicity remain poorly understood. While the physiological role of the AhR is unclear, recent evidence indicates that targeting the AhR with therapeutic ligands may prove useful in treating autoimmune diseases, inflammation, and cancer (Safe *et al.*, 2017; Burezq, 2018; Neavin *et al.*, 2018). The goal of this research was to investigate the cellular and molecular mechanisms by which AhR activation impacts wound healing responses in the liver, including the regulation of gene expression important for inflammation, metabolism, and fibrogenesis.

AhR Structure

The AhR is a ligand-activated transcription factor that belongs to the basic helix-loop-helix (bHLH), Per-ARNT-Sim (PAS) family. Proteins in the PAS superfamily share a conserved dimerization domain that was originally identified in the three founding

proteins (Gu *et al.*, 2000). The “period” protein Per was originally discovered in *Drosophila melanogaster* and found to control basic circadian rhythm functions (Reddy *et al.*, 1986; Citri *et al.*, 1987). The aryl hydrocarbon receptor translocator (ARNT) protein was determined to be a vital component of transcription regulation (Hoffman *et al.*, 1991). The Drosophila single-minded (Sim) protein was shown to regulate midline cell lineage in the central nervous system (Jackson *et al.*, 1986; Nambu *et al.*, 1991). Typically containing 250-300 amino acids, the PAS domain contains two highly conserved, 50-amino acid subdomains termed A and B (Jackson *et al.*, 1986; Hoffman *et al.*, 1991; Nambu *et al.*, 1991). In eukaryotes, PAS domains serve as recognition sites for interactions with other PAS proteins and cellular chaperones. In general, bHLH-PAS proteins function as transcription factors that detect and respond to environmental and physiological signals, such as xenobiotic exposure, hypoxia and circadian rhythm (Kolonko & Greb-Markiewicz, 2019).

Within the bHLH PAS family, the AhR is unique because it is the only protein that is conditionally activated by ligand binding (Lamas *et al.*, 2018). As shown in Figure 1.1, the PAS-B domain of the AhR includes a ligand-binding domain, where binding of endogenous and exogenous ligands initiates AhR activation (Coumailleau *et al.*, 1995). The AhR is the only bHLH-PAS protein that functions as a receptor.

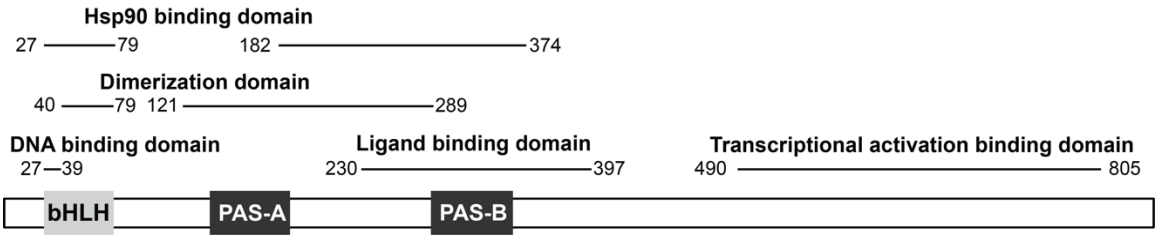

Figure 1.1 Functional Domains of the AhR

The functional domains and corresponding amino acids of the mouse AhR protein are shown above. Hsp90, heat shock protein 90.

Yet another important domain in the AhR protein is the heat shock protein 90 (Hsp90) binding domain, which enables the AhR to interact with two Hsp90 proteins (Coumailleau *et al.*, 1995; Fukunaga *et al.*, 1995). Binding of Hsp90 proteins to the AhR occurs in the cytoplasm and prevents the unliganded AhR from translocating into the nucleus (Soshilov & Denison, 2011). Upon ligand binding, the AhR undergoes a conformational change that releases the Hsp90 complex and reveals a nuclear localization signal, which results in AhR translocation to the nucleus (Ikuta *et al.*, 1998; Petrulis *et al.*, 2003).

AhR Allelic Variations

In humans and mice, the AhR gene (*Ahr*) is located on chromosome 7p15 (Micka *et al.*, 1997) and 12 (Schmidt *et al.*, 1993), respectively. In both organisms, *Ahr* has 11 exons that span about 50 kilobases. Once fully translated, the corresponding AhR protein has a molecular weight of about 96 kDa (Dolwick *et al.*, 1993; Bennett *et al.*, 1996). Four *Ahr* alleles have been identified in mice, and they are distinguished based on the ligand binding affinity of the AhR proteins they encode. Three of these alleles are variants of a

"b" allele and encode AhR proteins with high binding affinity (K_D ~7 pM) for the radioligand 2-[^{125}I]iodo-7,8-dibromo-*p*-dioxin. These allelic variants, which are referred to as *Ahr*$^{b-1}$, *Ahr*$^{b-2}$, *Ahr*$^{b-3}$, produce proteins that differ in length at the C-terminus. In contrast, the AhR protein encoded by the fourth "d" allele possesses a ligand-binding affinity that is 4-5 times lower (K_D ~35 pM), due to a point mutation in the ligand-binding domain. The most prominent mutation in the *Ahr*^{d} allele is an A^{375}V mutation, in which an alanine residue is replaced by a valine residue at position 375 of the primary protein sequence (Poland *et al.*, 1994). Although four *Ahr* alleles have been identified in mice, only one has been identified in humans, and it appears to most closely resemble the *Ahr*^{d} allele found in mice (Moriguchi *et al.*, 2003).

Classical AhR Activation

In the absence of ligand, the AhR resides in the cytoplasm in a complex that includes an Hsp90 dimer (Denis *et al.*, 1988), an Hsp90 co-chaperone called p23 (Cox & Miller, 2004), and the AhR interacting protein (AIP), also known as ARA9 and XAP-2 (Carver & Bradfield, 1997; Ma & Whitlock, 1997; Meyer *et al.*, 1998) (Figure 1.2). Association of the AhR with Hsp90 and AIP prevents proteolysis and nuclear translocation of AhR in the absence of ligand (Ikuta *et al.*, 1998; Kazlauskas *et al.*, 2000; Petrulis *et al.*, 2003; Pappas *et al.*, 2018). The p23 protein functions as an Hsp90 co-chaperone and stabilizes the interaction between AhR and the Hsp90 proteins (Cox & Miller, 2004). Upon binding to a ligand, the AhR undergoes a conformational shift that causes the Hsp90 dimer to dissociate (Ikuta *et al.*, 1998). This process exposes a novel,

bipartite nuclear translocation signal (NLS) that allows the AhR to migrate to the nucleus (Ikuta *et al.*, 1998; Lees & Whitelaw, 1999).

Upon translocation to the nucleus, the AhR forms a heterodimer with ARNT, which is another bHLH-PAS protein (Card *et al.*, 2005). The name ARNT is a misnomer, as this protein does not function in translocating the AhR to the nucleus but instead binds to AhR in the nucleus (Evans *et al.*, 2008). Binding of ARNT to the AhR confers DNA-binding ability, which consequently retains AhR in the nucleus (Pollenz *et al.*, 1994). The AhR/ARNT complex binds to DNA at a conserved sequence, 5'-GCGTG-3'. This sequence has been termed the xenobiotic response element (XRE) or dioxin response element (DRE) (Shen & Whitlock, 1992). It has been shown that residues in both AhR and ARNT interact with this core sequence. If dimerization between AhR and ARNT is prevented, then the AhR cannot binding to the XRE, and transcriptional regulation of AhR-dependent genes ceases.

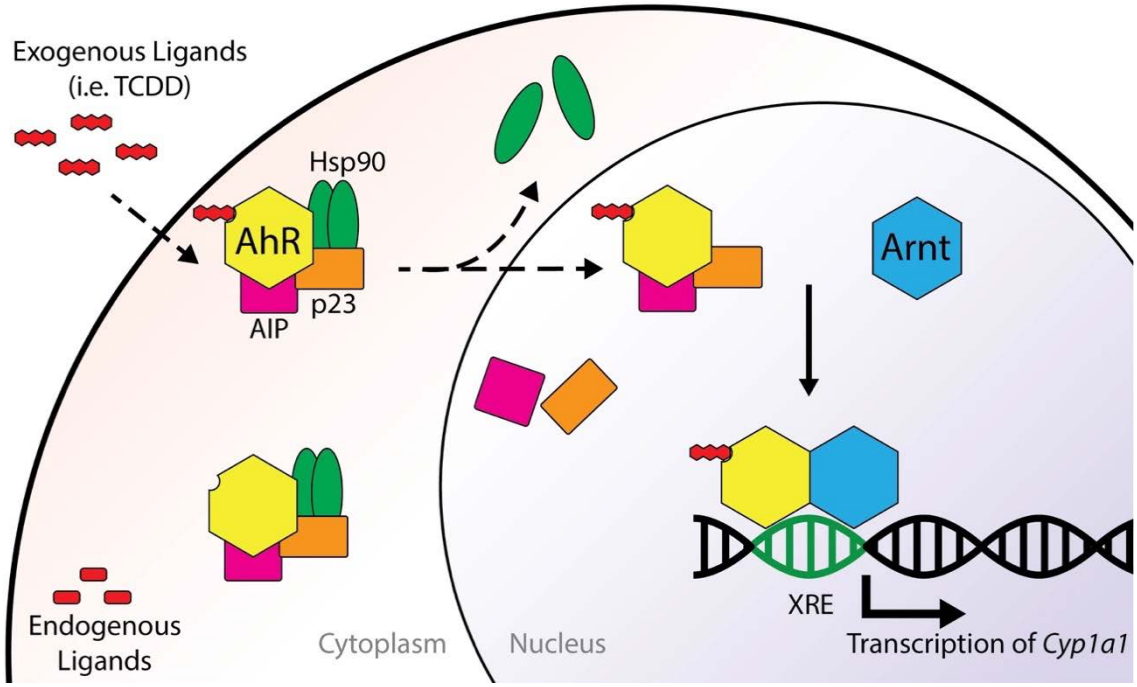

Figure 1.2 Classical AhR Activation.

When a ligand is absent, the AhR is localized to the cytosol in a complex with co-chaperone proteins, which include an HSP90 dimer, p23 protein, and the AhR interacting protein (AIP). Upon binding to ligand, the AhR releases the HSP90 dimer, translocates into the nucleus, where it forms a heterodimer with ARNT, and sheds the remaining co-chaperones. The AhR/ARNT heterodimer then binds to one or more xenobiotic response elements (XREs) to modulate expression of AhR target genes.

The molecular events involved in AhR-mediated transactivation have been particularly well studied in the AhR-mediated induction of *Cyp1a1* expression in response to the AhR ligand 2,3,7,8-tetrachlorodibenzo-*p*-dioxin (TCDD), which is depicted in Figure 1.2. *Cyp1a1* encodes the xenobiotic metabolizing enzyme, cytochrome P4501A1, and its expression is considered a hallmark of AhR activation. The events that lead to expression of this AhR-regulated gene represent what is often referred to as "classical AhR activation." However, studies over the past two decades add significant complexity to the mechanisms of AhR-regulated gene expression. For example, the

transcription of some AhR-regulated genes occurs when the AhR/ARNT complex associates with transcription factors bound to DNA at other, non-XRE-containing response elements. This has been shown for the AhR-dependent induction of NAD(P)H:quinone oxidoreductase-1 (NQO1) in response to the AhR ligand benzo[a]pyrene (Lin *et al.*, 2011). In this instance, induction of NQO1 gene expression requires the interaction between the AhR/ARNT heterodimer and another protein complex comprised of nuclear factor erythroid 2-related factor-2 (Nrf2) and Maf, which binds to a nearby antioxidant response element (ARE) (Lin *et al.*, 2011). Another example of non-classical AhR activation occurs when the AhR/ARNT heterodimer binds to the XRE and then interacts with protein complexes at other response elements, such as the estrogen receptor (ER) complex bound to the estrogen receptor element (ERE) (Safe & Wormke, 2003). In this example, the activated AhR indirectly impacts gene expression by inhibiting the transcription of ER-dependent genes (Safe & Wormke, 2003).

To further add to the complexity of AhR transcriptional activity, it was recently demonstrated that the AhR can initiate the transcription of genes that do not contain XREs (Jackson *et al.*, 2015). This is not entirely surprising because TCDD treatment reportedly modulated the expression of 5307 genes in mouse liver, yet chromatin immuno-precipitation studies revealed that only 3369 of these genes contained a functional XRE (Dere *et al.*, 2011). For example, *Serpine1* was found to be a TCDD-induced gene and yet, it does not contain an XRE (Son & Rozman, 2002). Subsequent studies demonstrated that, in response to TCDD, the AhR interacts with the *Serpine1* gene promoter at a novel sequence comprised of a tetranucleotide repeat of 5'-GGGA-3'.

This sequence is now referred to as non-consensus XRE (NC-XRE) (Huang & Elferink, 2012). Subsequent studies have shown that the AhR interacts with the NC-XRE independently of ARNT and instead partners with Krueppel-like factor 6 (Wilson *et al.*, 2013).

Non-Genomic AhR Activation

In addition to regulating gene transcription, AhR activation has also been shown to induce non-genomic cellular events. For example, TCDD-induced AhR activation has been shown to mitigate an influx of extracellular Ca^{2+} in various cell types through opening T-type calcium channels (Hanneman *et al.,* 1996; Karras *et al.*, 1996; Dale & Eltom, 2006; Kim *et al.*, 2009). In addition, the activated AhR has been shown to initiate activation of the tyrosine kinase c-Src through a transcription-independent method (Tomkiewicz *et al.*, 2013). c-Src has been shown to associate with the AhR complex in the cytoplasm (Mehta & Vezina, 2011). When TCDD binds to the AhR, c-Src is activated and is released from the complex (Mehta & Vezina, 2011). Downstream signaling events mediated by c-Src include the activation of focal adhesion kinase, restructuring of integrins and, ultimately, increased cell migration (Tomkiewicz *et al.*, 2013). Collectively, these examples demonstrate that AhR-mediated activity extends beyond transcriptional control of gene expression.

Regulation of the AhR Activity and Expression

AhR activity can be repressed by a protein called the AhR repressor (AhRR). The gene encoding this protein contains an XRE and is expressed in response to AhR

activation (Sakurai *et al.*, 2017). The AhRR functions as a repressor by competing with AhR to form a heterodimer complex with ARNT, which prevents formation of the transcriptionally active AhR/ARNT complex (Mimura *et al.*, 1999; Vogel *et al.*, 2016). The AhRR/ARNT heterodimer can then bind XRE sites, where this protein complex recruits Ankyrin-repeat protein2 and histone deacetylases (HDAC4 and HDAC5) to induce chromosomal remodeling and prevent AhR/ARNT complexes from binding to the XRE (Gradin *et al.*, 1999; Oshima *et al.*, 2007).

AhR expression is regulated post-translationally through proteasomal degradation (Ma *et al.*, 2000). For example, activation of the AhR by TCDD induces AhR degradation through ubiquitination of AhR (Ma *et al.*, 2000). After being tagged with ubiquitin, the AhR is translocated into a proteasome for degradation and recycling of amino acids (Ma *et al.*, 2000). Treatment of mouse hepatoma cells with TCDD has been shown to increase AhR degradation via this mechanism (Ma *et al.*, 2000). In this study, AhR was determined to have a half-life of 28 hours before being ubiquitinated for proteasomal degradation, and treatment with 1 nM TCDD decreased the half-life of AhR to 3 hours (Ma *et al.*, 2000). Regulation of AhR activity is a complex process that occurs through many molecular mechanisms.

Phenotype of the AhR Knockout Mouse

In an attempt to discover the endogenous role of the receptor, AhR knockout mice were produced independently in three separate labs (Fernandez-Salguero *et al.*, 1995; Schmidt *et al.*, 1996; Mimura *et al.*, 1997). Global AhR knockout produced no overt consequences on the organism but did result in several physiological and anatomical

anomalies. The most prominent feature in these mice were livers that were 50% smaller than those of wild-type counterparts (Schmidt *et al.*, 1996; Mimura *et al.*, 1997). AhR knockout mice also exhibited subtle portal liver fibrosis and decreased body size during the first 4 weeks of age. Additionally, these mice showed a decrease in fertility and had litters that were smaller and less viable than wild-type mice. Another feature common to all three lines of AhR knockout mice was the reduction of gene expression for constitutively expressed xenobiotic metabolizing enzymes, such as cytochrome P4501A2 (Lahvis & Bradfield, 1998). AhR knockout mice also exhibited a myriad of vascular deformities, which included a patent ductus venosus, a persistent hyaloid artery in the eye, and abnormal vascularization in the kidneys (Lahvis *et al.*, 2000; Lin *et al.*, 2001; Walker *et al.*, 2002). Reproductive organs also showed abnormalities in terms of development and function of the prostate and ovaries (Lin *et al.*, 2002; Hernández-Ochoa *et al.*, 2009). The final abnormality that was observed in these strains of AhR knockout mice was the severe alteration of hematopoietic stem cell development (Lindsey & Papoutsakis, 2011).

AhR Ligands

Endogenous AhR Ligands

Over the past several decades, the search for endogenous agonists of the AhR has been the subject of intense investigation. Five classes of endogenous AhR ligands have been identified: indigoids (indigo and indirubin), heme metabolites (bilirubin, hemin, and bilirubin), eicosanoids (lipoxin A4 and prostaglandin G2), tryptophan derivatives

(tryptamine) and equilenin (Figure 1.3) (Stejskalova *et al.*, 2011). These compounds have diverse chemical structures and have several origins. For example, dietary sources such as plant matter are the origin for indigoids (Stejskalova *et al.*, 2011). Heme metabolites, such as biliverdin and bilirubin, are byproducts of heme degradation (Otterbein *et al.*, 2003). Eicosanoids, such as the anti-inflammatory compounds lipoxin A4 and prostaglandins, are derivatives of arachidonic acid, a fatty acid that is a major component of the cell membrane (in phospholipid form) (Stejskalova *et al.*, 2011).

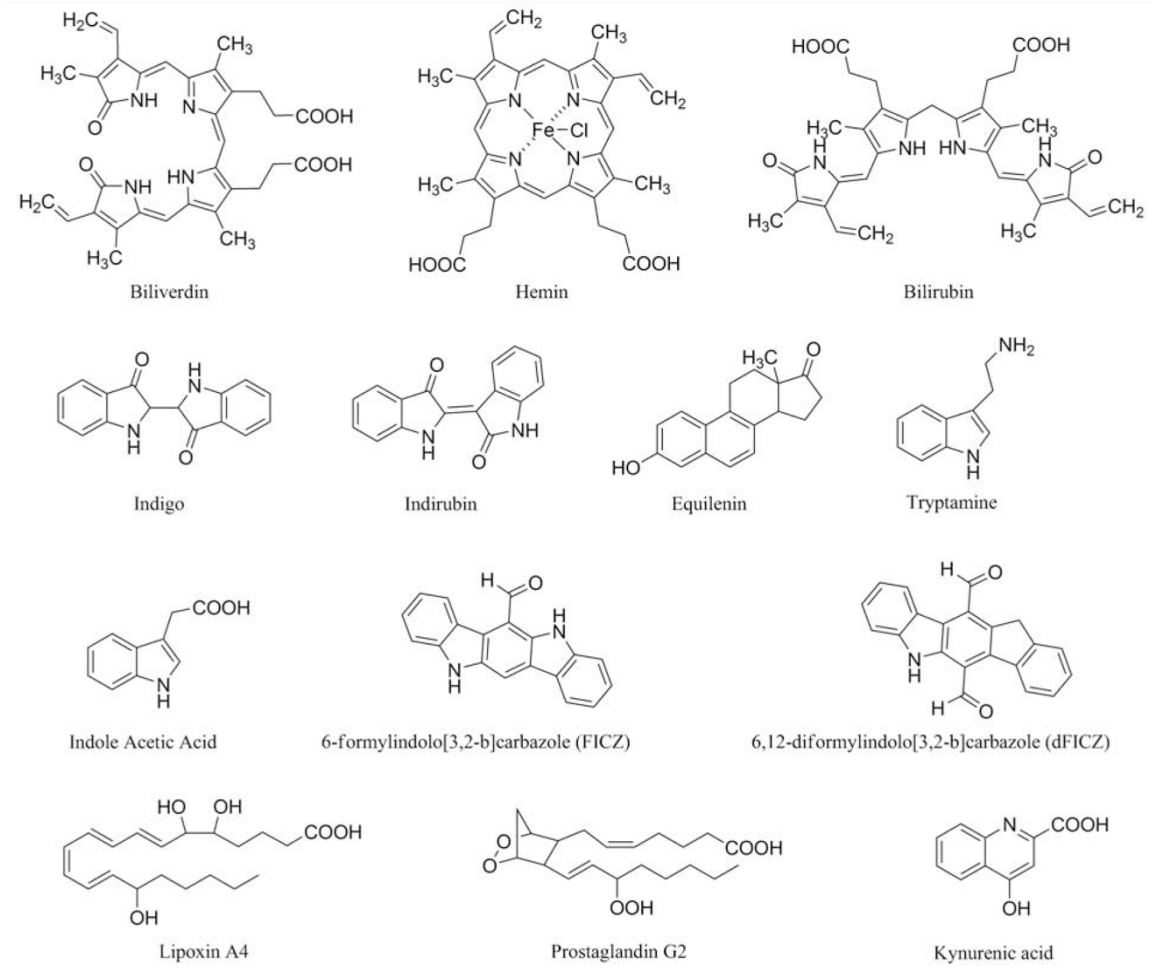

Figure 1.3 Structures of Endogenous AhR Ligands.

Figure adapted from Stejskalova et al., 2011.

Exogenous AhR Ligands

The AhR is activated in response to many xenobiotic compounds including halogenated aromatic hydrocarbons (HAHs) and polycyclic aromatic hydrocarbons (PAHs) (Stejskalova *et al.*, 2011). Examples of HAH compounds include dioxins, furans, and biphenyls (Figure 1.4). In contrast to known endogenous ligands, these exogenous ligands are structurally similar, possessing aromatic carbon rings with differences in secondary chemical structures and halogenation. The large family of HAH compounds represent environmental contaminants, that in most cases, originate from industrial processes (Kearney *et al.*, 1973). These compounds find their way into the food chain of many ecosystems and are resistant to degradation (Poland & Knutson, 1982). The most toxic HAH is 2,3,7,8-tetrachlorodibenzo-*p*-dioxin (TCDD) (Figure 1.5), which serves as the prototypical compound for studying HAH toxicity because of its high binding affinity for the AhR as well as being non-metabolizable (Poland & Knutson, 1982).

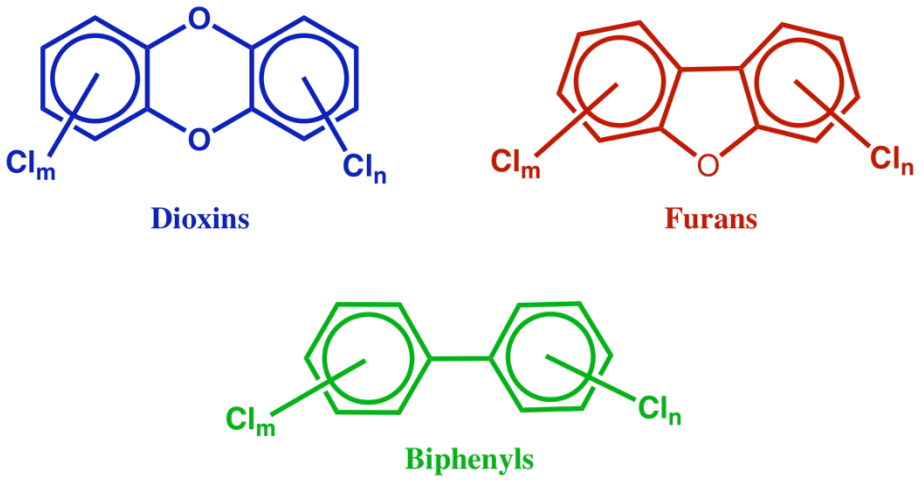

Figure 1.4 Structures of HAHs

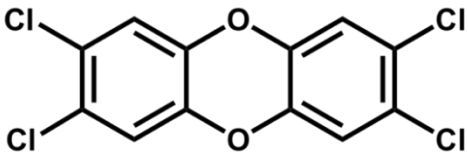

Figure 1.5 Structure of TCDD

Selective Aryl Hydrocarbon Receptor Modulators

Another class of AhR ligands is selective aryl hydrocarbon receptor modulators (SAhRMs). In general, SAhRMs function as an agonist in one tissue and an antagonist in another (Smith & O'Malley, 2004). One of the first compounds identified as a SAhRM was 1,3,8-trichloro-6-methyldibenzofuran (6-MCDF) (Pearce *et al.*, 2004). Initially, this compound was identified as an AhR antagonist that prevented TCDD-induced expression of *Cyp1a1*, TCDD-induced immunotoxicity, and hepatic porphyria (Astroff *et al.*, 1987; Harris *et al.*, 1988; Bannister *et al.*, 1989). However, later studies showed that 6-MCDF also functions as an AhR agonist by activating inhibitory crosstalk between the AhR and ERα (McDougal *et al.*, 2001). Recent studies have suggested that SAhRMs can potentially modulate AhR activity through non-canonical mechanisms (Narayanan *et al.*, 2012). Furthermore, because SAhRM-induced AhR activity does not occur through XRE-dependent mechanisms, potentially cytotoxic gene expression changes seen with canonical AhR activation are absent (Patel *et al.*, 2009; Narayanan *et al.*, 2012). These novel mechanisms of mediating AhR activity have potential therapeutic use.

The Exogenous AhR Ligand, TCDD

TCDD possesses one of the highest binding affinities of any ligand for the AhR (Poland & Knutson, 1982). Although TCDD induces the transcription of *Cyp1a1*, TCDD is not a viable substrate for this enzyme and therefore cannot be degraded. This accounts for the long half-life of TCDD within cells, which can be up to ten days in hepatocytes (Håkansson & Hanberg, 1989). TCDD has never intentionally been produced but is instead generated as an unintentional byproduct of several industrial and manufacturing processes, such as the chlorine bleaching of paper pulp, incineration of biomedical and municipal waste, and herbicide manufacturing (Schecter, 1994; Silkworth & Brown, 1996). For example, TCDD was found to be a contaminant in the herbicide Agent Orange, which was sprayed from 1961 to 1971 during the Vietnam war. Agent Orange contained a mixture of two herbicides, 2,4-D and 2,4,5-D, the latter of which was found to contain trace amounts of TCDD as a byproduct of the manufacturing reaction (Institute of Medicine, 1994).

TCDD Toxicity in Humans

As a persistent environmental contaminant, TCDD poses a potential health risk to humans. As a lipophilic compound, TCDD is stored in adipose tissue for extended periods of time leading to an overall increased health risk. Most of what is known about TCDD toxicity in humans is limited to retrospective epidemiological studies of people who were exposed to the chemical during industrial accidents. Throughout history there have been several industrial accidents that led to high exposure of TCDD. For example,

in 1976, TCDD was released during an explosion at a trichlorophenol manufacturing facility in Seveso, Italy (Bertazzi *et al.*, 1998). It was estimated that several kilograms of TCDD were released into the atmosphere, which resulted in the exposure of 220,100 people in the surrounding communities (Caramaschi *et al.*, 1981). In the United States, in 1949, 226 employees of Monsanto Company were exposed to dioxin after an herbicide storage container exploded (Tucker *et al.*, 1981). Finally, one of the most infamous cases of human TCDD exposure is that of former Ukrainian president Victor Yushchenko, who was poisoned with TCDD during a state dinner in 2004. Based on measurement of TCDD in Yushchenko's bodily fluids, the half-life of TCDD in humans was determined to be about 15 months (Sorg *et al.*, 2009).

TCDD Toxicity in Rodents

Reproductive/Developmental Toxicity

Acute toxicity of TCDD in mice and rats has been studied for several decades. Results indicate that all TCDD toxicity is mediated through the AhR (Mimura & Fujii-Kuriyama, 2005). In mice expressing the b allele and d allele of *Ahr*, the LD_{50} has been reported to be 159 µg/kg and 3351 µg/kg, respectively (Birnbaum *et al.*, 1990). In other studies, chronic administration of TCDD has been reported to elicit hepatomegaly (enlargement of the liver), steatosis, and thymic atrophy (Gupta *et al.*, 1973; Tucker *et al.*, 1981). Studies dating back to the 1970s characterized the fetotoxicity of TCDD on both mice and rats. These studies found that TCDD could lead to cleft palate, irregular kidneys, intestinal hemorrhages, and prenatal mortality (Courtney & Moore, 1971;

Sparschu *et al.*, 1971; Khera & Ruddick, 1973; Moore *et al.*, 1973; Smith *et al.*, 1976). Fertility was also found to be hindered in cohorts that had been treated with TCDD. Decreases in fertility, postnatal pup survival, and litter size were all common characteristics in female rats that were exposed to 0.01 µg/kg/day TCDD 90 days prior to pregnancy (Murray *et al.*, 1979).

Carcinogenicity

Experiments using rodent systems have demonstrated carcinogenic effects of TCDD. In studies dating back several decades, it was discovered that chronic administration of 0.001 µg/kg/week for 78 weeks led to cancerous tumors in male rats (Van-Miller *et al.*, 1977). The types of cancer that were characterized include ear duct carcinoma, leukemia, kidney adenocarcinoma, peritoneal histiocytoma, skin angiosarcoma, and hard palate, tongue and nasal carcinoma (Van-Miller *et al.*, 1977). Female rats that were dosed with 0.1 µg/kg/day for two years had increased incidence of liver and squamous cell carcinoma of the lungs, hard palate, tongue and nasal carcinoma (Kociba *et al.*, 1978). Similar studies were conducted in male mice treated with 0.05 µg/kg/week of TCDD for two years and demonstrated that TCDD caused liver cancer (National Toxicology Program, 1982b). Female mice of the same study develop both liver cancer and thyroid adenomas (National Toxicology Program, 1982b). In studies where TCDD was applied topically for two years, female mice showed increased levels of a fibrosarcoma type of skin cancer (National Toxicology Program, 1982a). TCDD is listed as a group 1 human carcinogen based on the IARC (Steenland *et al.*, 2004).

Liver Toxicity

One of the hallmarks of acute TCDD toxicity is hepatomegaly, a condition in which the liver weight increases in comparison to an organism's body weight (Safe, 1986). TCDD also increases serum levels of alanine aminotransferase (ALT) (Triebig *et al.*, 1998) which is a hepatocyte-specific enzyme that is released into circulation upon necrosis (Giboney, 2005). Although hepatomegaly and increased serum ALT are the two major indicators of acute liver toxicity, other physiological and pathological anomalies are present in the liver of TCDD-treated mice.

Inflammation

Exposure to TCDD induces hepatic inflammation. For instance, C57BL/6J female mice that were treated with a single dose of 30 μg/kg showed histological patterns of inflammatory foci (Shen *et al.*, 1991). Upon closer investigation it was discovered that these foci were primary composed of mononuclear and neutrophil cells (Olivero-Verbel *et al.*, 2011). TCDD-induced focal inflammation has been reported to be localized in the periportal region of the hepatic lobules (Vos *et al.*, 1974; Jones & Greig, 1975). The influx of inflammatory cells into the liver of TCDD-treated mice appears to be driven by increased production of pro-inflammatory cytokines, such as interleukin (IL)-1β and tumor necrosis factor (TNF)α (Fan *et al.*, 1997; Vogel *et al.*, 1997). Increased levels of the pro-inflammatory keratinocyte chemoattractant (KC) and monocyte chemoattractant protein-1 (MCP-1) were also reported in mice treated with TCDD (Vogel *et al.*, 2007).

Dysregulation of Vitamin A Homeostasis

Vitamin A contributes to the regulation of numerous important physiological functions, such as the transduction of light into nerve signals (Saari, 1994), maintenance of epithelial cell integrity (Gudas *et al.*, 1994), embryonic development (Hofmann & Eichele, 1994; McCaffery & Drager, 1995), and maintenance of the immune system (Trechsel *et al.*, 1985; Katz *et al.*, 1987). The liver stores as much as 90% of the body's vitamin A (Raica Jr. *et al.*, 1972). Most of the vitamin A storage occurs in lipid droplets within hepatic stellate cells (HSCs), which are non-parenchymal cells that comprise about 8% of the cells in the liver (Hendriks *et al.*, 1985). TCDD treatment disrupts vitamin A homeostasis. For example, administration of TCDD to rats reduced vitamin A stores in the liver (Thunberg *et al.*, 1980). Following TCDD treatment, vitamin A concentrations increase in the kidneys, serum, testes and epididymis (Håkansson & Hanberg, 1989).

Steatosis

Hepatic steatosis is defined as the accumulation of triglycerides in vacuoles within hepatocytes. Chronic administration of TCDD (25 μg/kg/week) has been shown to induce hepatic steatosis in mice, with initial occurrence observed at day 4 and maximal effect observed at week 4 (Jones *et al.*, 1981). Hepatic steatosis most likely occurs because TCDD enhances the uptake of triglycerides in hepatocytes through upregulation of fatty acid transporters, such as CD36 (Lee *et al.*, 2010). Furthermore, mice that had a double CD36 knockout were protected against TCDD-induced steatosis (Lee *et al.*, 2010). TCDD also suppresses the secretion of very low density lipoproteins (VLDL), which are lipoproteins that form complexes with triglycerides to circulate fats throughout

the body (Lee *et al.*, 2010). Therefore, TCDD increases uptake of lipids while inhibiting their secretion in mice.

Aberrant Wound Healing – Regeneration

TCDD exposure suppressed the ability of cultured mouse hepatoma cells to proliferate (Weiss *et al.*, 1996; Kolluri *et al.*, 1999). Furthermore, studies conducted using a murine model system found that treatment of TCDD stunted the regenerative ability of livers (Bauman *et al.*, 1995; Mitchell *et al.*, 2006). In these cases, suppression of liver regeneration occurred due to an AhR-mediated G_1 cell cycle arrest in hepatocytes (Kolluri et al., 1999; Jackson *et al.*, 2014). The AhR interacts with retinoblastoma protein (pRb) to regulate G_1/S phase progression in the cell cycle. Exposure to TCDD elicits a G_1 cell cycle arrest in primary hepatocytes, mouse hepatoma cells, and in the regenerating mouse liver (Bauman *et al.*, 1995; Kolluri *et al.*, 1999). Possible mechanisms include the TCDD-induced upregulation of p21 and p27, which are Cip/Kip family proteins that regulate the G_1/S phase checkpoint. Furthermore, endogenous AhR signaling has been linked to cell cycle progression, as primary mouse embryonic fibroblasts from AhR knockout mice proliferate more slowly than their wild-type counterparts (Elizondo *et al.*, 2000). However, TCDD has also been shown to increase proliferation of liver cells. For example, AhR activation by TCDD increased hepatocyte proliferation during mitogen-induced hyperplasia induced by 1,4-Bis-[2-(3,5-dichloropyridyloxy)]benzene,3,3′,5,5′-tetrachloro-1,4-bis(pyridyloxy)benzene (TCPOBOP), an agonist for the constitutive androstane receptor (Mitchell *et al.*, 2010). This was attributed to increased assembly of cyclin/Cyclin-dependent kinase (CDK) complexes that facilitate S-phase progression.

Based on these results, it stands to reason that the mechanisms by which AhR signaling impacts cell cycle progression may depend on the type of model system (e.g., compensatory hyperplasia induced by partial hepatectomy or direct hyperplasia in response to mitogens). As a result, it has been difficult to understand how exogenous AhR ligands could impact the human liver.

Aberrant Wound Healing – Fibrogenesis

In addition to hepatocyte proliferation, another physiological response to liver damage is fibrogenesis, which is a normal wound-healing mechanism characterized by deposition of extracellular matrix (ECM) proteins (Kisseleva & Brenner, 2008). Fibrogenesis is initiated by tissue injury and inflammation (Wynn, 2008). During fibrogenesis, ECM proteins, such as collagens, are synthesized and secreted into the ECM. Upon removal of the injurious stimulus, the ECM is degraded. However, in the presence of chronic injury and unresolved inflammation, the deposition of ECM proteins exceeds turnover, resulting in a pathological condition referred to as *fibrosis* (Wynn, 2008).

TCDD has been shown to increase collagen gene expression in the liver, increase soluble mediators important for fibrogenesis (TGFβ), and modulate expression and activity of enzymes important for ECM remodeling (Pierre *et al.*, 2014; Nault *et al.*, 2016; Han *et al.*, 2017; Lamb *et al.*, 2016a). Understanding how TCDD and AhR signaling impact liver fibrosis is a relatively new area of research, and it is the focus of the research described in this dissertation. The processes involved in liver fibrosis are described in further detail below.

Liver Fibrosis

Liver disease is a broad term that refers to any pathology of the liver. Generally speaking, it occurs in response to chronic injury and/or inflammation (Pellicoro *et al.*, 2014). A multitude of insults can produce liver disease, including viral infection, toxicant exposure, idiosyncratic drug reactions, chronic alcohol consumption, autoimmune disease, cholestasis, and metabolic diseases (Pellicoro *et al.*, 2014). Regardless of etiology, the progression of chronic liver disease occurs through similar stages. In response to injury and inflammation, myofibroblast precursors, namely hepatic stellate cells (HSCs), become activated and secrete ECM proteins. During chronic injury and inflammation, the deposition of ECM proteins exceeds ECM turnover, which produces a pathological condition in the liver called fibrosis. Fibrosis could potentially progress into cirrhosis, which is characterized by impeded blood flow and pockets of regeneration that result in nodules that could progress to cancer (Ginès *et al.*, 2004). The only type of clinical intervention for cirrhosis is liver transplantation (Figure 2.1).

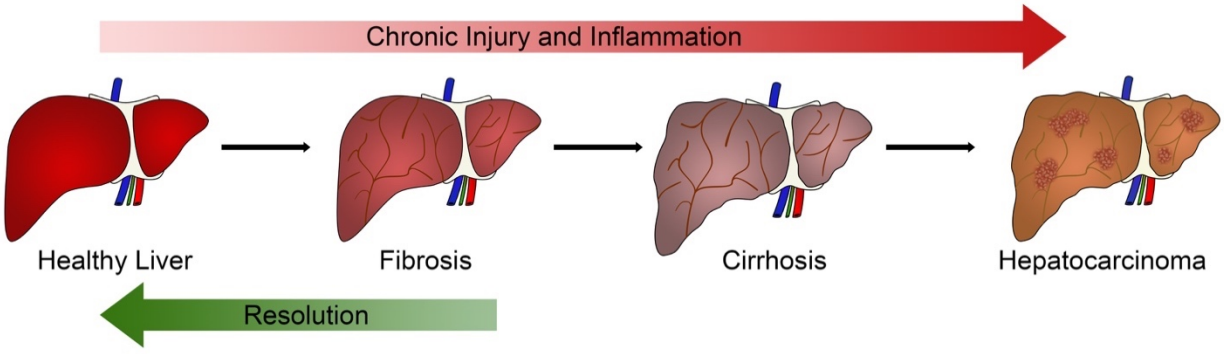

Figure 2.1 Stages of Liver Disease

The first stage of liver disease, liver fibrosis, can be characterized by gross deposition of ECM proteins such as fibrillar collagens (types I and III) (Pellicoro et al., 2014). Excessive collagen deposition results in portal hypertension that is characterized by elevated blood pressure of the portal vein (Sherman *et al.*, 1990). Liver fibrosis is mediated by a population of non-parenchymal liver cells called hepatic stellate cells (HSCs) (Wells, 2008). In the healthy liver, HSCs function to store vitamin A (Blomhoff *et al.*, 1992). However, in response to injury, HSCs become activated and transition to a myofibroblast-like phenotype (Wells, 2008). This phenotype is characterized by loss of vitamin A stores, proliferation, motility, secretion of chemokines and production of extracellular matrix proteins, such as collagen (Friedman, 2000; Wells, 2008). In addition to secreting ECM proteins, activated HSCs also synthesize a myriad of proteases that lead to the turnover and remodeling of the ECM (Duarte *et al.*, 2015). It is believed that increased protease secretion and subsequent ECM remodeling allow for better myofibroblast and inflammatory cell mobilization during liver repair (Han, 2006).

Evidence that TCDD/AhR contributes to the regulation of liver fibrosis

TCDD increases HSC activation

Several studies have shown TCDD treatment reduces the level of vitamin A that is stored in the liver (Thunberg *et al.,* 1980; Håkansson & Ahlborg, 1985; Håkansson & Hanberg, 1989; Hanberg *et al.*, 1998). Vitamin A loss is one of the hallmark features of HSC activation. *In vitro* studies using human HSC lines have also demonstrated that TCDD promotes the activation of HSCs (Harvey *et al.*, 2016; Han *et al.*, 2017). In one of these studies, TCDD-treated HSCs were shown to proliferate and produce alpha-smooth muscle actin (αSMA), both indicators of HSC activation (Harvey *et al.*, 2016). In addition to this evidence, other studies show that TCDD treatment of mice induces the production of activated HSC markers such as αSMA and collagen type I (Pierre *et al.*, 2014; Lamb *et al.*, 2016b). It is possible that HSCs may be a direct cellular target for TCDD in the mouse liver. The half-life of TCDD in hepatocytes in about 13 days, while the half-life of TCDD in HSCs is about 52 days (Håkansson & Hanberg, 1989). The shear fact that it takes HSCs about 4 times longer than hepatocytes to eliminate TCDD could give TCDD a longer timespan to modulate gene expression in HSCs.

TCDD impacts ECM remodeling

ECM-related genes that are known to be modulated by AhR activation include those that encode collagens, matrix metalloproteases (MMPs), tissue inhibitor of metalloproteases (TIMPs) and profibrotic cytokines (Andreasen *et al.*, 2007; Pierre *et al.*,

2014). As previously mentioned, there is some evidence that TCDD induces fibrogenesis in the liver. However, there is also evidence to suggest that TCDD modulates MMP activity directly which could limit fibrogenesis (Haque *et al.*, 2005; Villano *et al.*, 2006; Andreasen *et al.*, 2007; Lamb *et al.*, 2016a).

Chronic TCDD administration elicits fibrosis.

In 2014, it was reported that chronic exposure of mice to TCDD produced liver fibrosis (Pierre *et al.*, 2014). In these experiments, male mice were treated with 25 µg/kg of TCDD once a week for 6 weeks. Mice were euthanized after 42 days. Results indicated that TCDD treatment increased the deposition of collagen protein in the liver and promoted hepatic inflammation. Production of the inflammatory cytokines IL1β and MCP-1 were also observed in TCDD treated samples. Another study used mice that were treated with varying concentrations (0-30 µg/kg) of TCDD every 4 days for 28 or 92 days (Nault *et al.*, 2016). The results of those studies indicated that at 28 days, 30 µg/kg of TCDD elicited portal fibrosis. Inflammation was observed at 28 days with only 10 µg/kg of TCDD. Steatosis was also observed in this model upon TCDD treatment. This study indicated that a TCDD dose of 0.3 µg/kg was sufficient to elicit hepatic lipid accumulation after 28 days.

TCDD increases fibrogenesis in bile duct ligation-induced liver fibrosis

Cholestasis is a type of liver disease characterized by the accumulation of bile acids and bilirubin in the liver, which induces liver damage and fibrosis (Hirschfield *et*

al., 2010). An experimental model used to induce cholestasis is bile duct ligation (BDL), in which the common bile duct is ligated to prevent bile acid export. The accumulation of bile acids in the liver causes injury and inflammation, which promotes the activation of portal fibroblasts and HSCs, leading to fibrosis (Hirschfield *et al.*, 2010). TCDD treatment was shown to increase liver damage in mice subjected to BDL (Ozeki *et al.*, 2011). Additionally, TCDD-treated BDL mice showed increased hepatic accumulation of bile acids and bilirubin compared to vehicle-treated BDL mice. Histopathological assessment identified widespread necrosis, which was attributed to the accumulation of bile acids.

TCDD increases pathology in liver of mice fed a high fat diet

Consuming a Western diet high in sugar and fat can promote steatosis in the liver (Arisqueta *et al.*, 2018; Jensen *et al.*, 2018). A recent study examined how AhR activation might exacerbate liver disease in mice that had steatosis (Duval *et al.*, 2017). This study utilized mice that were fed a high fat diet (HFD) to promote steatosis. It was reported that treatment with TCDD exacerbated steatosis and hepatic triglyceride stores in the liver of HFD mice. However, it remains unclear what mechanism leads to elevated fat stores in the liver. TCDD treatment of HFD mice also increased serum ALT levels and promoted inflammatory cell infiltration, which was accompanied by increased mRNA levels of inflammatory marker genes *CCl2*, *Il1b*, *Itgam*, and *Cd68*. TCDD was also shown to increase expression of the fibrosis-related genes *Tgfb1*, *Col1a1* and *Col3a1* (Duval *et al.*, 2017) and increase collagen protein deposition (Pierre *et al*., 2014).

Overall, this study supports the notion that TCDD treatment exacerbates steatosis and promotes liver fibrosis.

TCDD increases fibrogenesis during CCl_4-induced liver fibrosis.

One model system that is widely used to study liver fibrosis is chronic administration of carbon tetrachloride (CCl_4) (Weber *et al.*, 2003). In this model system, mice are typically exposed twice weekly to CCl_4 for 4-8 weeks. CCl_4 is metabolized by the enzyme cytochrome P450E1 to a trichloromethyl radical, which elicits lipid peroxidation in the cell membrane (Wong *et al.*, 1998). Chronic exposure to CCl_4 elicits widespread centrilobular necrosis and inflammation in the liver, which ultimately drive the activation of HSCs and the promotion of liver fibrosis (Mederacke *et al.*, 2013). Using a "two-hit" system of chronic CCl_4 treatment followed by TCDD, Lamb *et al.* showed that TCDD treatment increased HSC activation and liver fibrosis in CCl_4-treated mice (Lamb *et al.*, 2016a; Lamb *al.*, 2016b). Results obtained with this model system are described in further detail in Chapter 2 of this dissertation.

Conclusion

In mouse models of liver fibrosis, AhR activation by TCDD promotes liver injury, inflammation, HSC activation, and ECM deposition and turnover. Studies described in this dissertation determined the cellular and molecular mechanisms by which AhR signaling mediates the effects of TCDD on these endpoints.

References

Andreasen, E. A., Mathew, L. K., Löhr, C. V., Hasson, R. and Tanguay, R. L. (2007). Aryl hydrocarbon receptor activation impairs extracellular matrix remodeling during zebra fish fin regeneration. *Toxicol. Sci.*, **95**(1), pp. 215–226.

Arisqueta, L., Navarro-Imaz, H., Labiano, I., Rueda, Y. and Fresnedo, O. (2018). High-fat diet overfeeding promotes nondetrimental liver steatosis in female mice. *Am. J. Physiol. Gastrointest. Liver Physiol.*, **315**(5), pp. G772–G780.

Astroff, B., Zachaewski, T., Safe, S., Arlotto, M. P., Parkinson, A., Thomas, P. and Levin, W. (1987). Tetrachlorodibenzo-p-dioxin antagonist : inhibition of the induction of rat cytochrome P-450 isozymes and related monooxygenase activities. *Mol. Pharmacol.*, **33**, pp. 231–236.

Bannister, R., Biegel, L., Davis, D., Astroff, B. and Safe, S. (1989). 6-Methyl-1,3,8-trichlorodibenzofuran (MCDF) as a 2,3,7,8-tetrachlorodibenzo-p-dioxin antagonist in C57BL/6 mice. *Toxicology*, **54**, pp. 139–150.

Bauman, J. W., Goldsworthy, T. L., Dunn, C. S. and Fox, T. R. (1995). Inhibitory effects of 2,3,7,8-tetrachlorodibenzo-p-dioxin on rat hepatocyte proliferation induced by 2/3 partial hepatectomy. *Cell Prolif.*, **28**(8), pp. 437–451.

Bennett, P., Ramsden, D. B. and Williams, A. C. (1996). Complete structural characterization of the human aryl hydrocarbon receptor gene. *J. Clin. Pathol.*, **49**, pp. 12–16.

Bertazzi, P. A., Bernucci, I., Brambilla, G., Consonni, D. and Pesatori, A. C. (1998). The Seveso studies on early and long-term effects of dioxin exposure: A review. *Environ. Health Perspect.*, **106**(SUPPL. 2), pp. 625–633.

Birnbaum, L. S., Mcdonald, M. M., Blair, P. C., Clark, A. M. and Harris, M. W. (1990). Differential toxicity of 2,3,7,8-tetrachlorodibenzo-p-dioxin (TCDD) in C57BL/6J Mice Congenic at the Ah locus. *Toxicol. Sci.*, **15**(1), pp. 186–200.

Blomhoff, R., Green, M. H. and Norum, K. R. (1992). Vitamin A: physiological and biochemical processing. *Ann. Rev. Nutr.*, **12**, pp. 37–57.

Burezq, H. (2018). Role of Aryl hydrocarbon-ligands in the regulation of autoimmunity. *Intech*, pp. 1-15.

Caramaschi, F., Del Corno, G., Favaretti, C., Giambelluca, S. E., Montesarchio, E. and Fara, G. M. (1981). Chloracne following environmental contamination by TCDD in Seveso, Italy. *Int. J. Epidemiol.*, **10**(2), pp. 135–143.

Card, P. B., Erbel, P. J. A. and Gardner, K. H. (2005). Structural basis of ARNT PAS-B dimerization: Use of a common beta-sheet interface for hetero- and homodimerization. *J. Mol. Biol.*, **353**(3), pp. 664–677.

Carver, L. A. and Bradfield, C. A. (1997). Ligand-dependent interaction of the aryl hydrocarbon receptor with a novel immunophilin homolog in vivo. *J. Biol. Chem.*, **272**(17), pp. 11452–11456.

Citri, Y., Colot, H. V., Jacquier, A. C., Yu, Q., Hall, J. C., Baltimore, D. and Rosbash, M. (1987). A family of unusually spliced biologically active transcripts encoded by a Drosophila clock gene. *Nature*, **326**(6108), pp. 42–47.

Coumailleau, P., Poellinger, L., Gustafsson, J.-Å. and Whitelaw, M. L. (1995). Definition of a minimal domain of the dioxin receptor that is associated with Hsp90 and maintains wild type ligand binding affinity and specificity. *J. Biol. Chem.*, **270**(42), pp. 25291–25300.

Courtney, K. D. and Moore, J. A. (1971). Teratology studies with 2,4,5-trichlorophenoxyacetic acid and 2,3,7,8-tetrachlorodibenzo-P-dioxin. *Toxicol. Appl. Pharmacol.*, **20**(3), pp. 396–403.

Cox, M. B. and Miller III, C. A. (2004). Cooperation of heat shock protein 90 and p23 in aryl hydrocarbon receptor signaling. *Cell Stress Chaperones*. Springer, **9**(1), pp. 4–20.

Dale, Y. R. and Eltom, S. E. (2006). Calpain mediates the dioxin-induced activation and down-regulation of the aryl hydrocarbon receptor. *Mol. Pharmacol.*, **70**(5), pp. 1481–1487.

Denis, M., Cuthill, S., Wikström, A.-C., Poellinger, L. and Gustafsson, J.-Å. (1988). Association of the dioxin receptor with the Mr 90,000 heat shock protein: A

structural kinship with the glucocorticoid receptor. *Biochem. Biophys. Res. Commun.* Academic Press, **155**(2), pp. 801–807.

Dere, E., Lo, R., Celius, T., Matthews, J. and Zacharewski, T. R. (2011). Integration of genome-wide computation DRE search, AhR ChIP-chip and gene expression analyses of TCDD-elicited responses in the mouse liver. *BMC Genomics*, **12**(1), p. 365.

Dolwick, K. M., Schmidt, J. V., Carver, L. A., Swanson, H. I. and Bradfield, C. A. (1993). Cloning and expression of a human Ah receptor cDNA. *Mol. Pharmacol.*, (44), pp. 911–917.

Duarte, S., Baber, J., Fujii, T. and Coito, A. J. (2015). Matrix metalloproteinases in liver injury, repair and fibrosis. *Matrix Biol.*, **0**, pp. 147–156.

Duval, C., Teixeira-Clerc, F., Leblanc, A. F., Touch, S., Emond, C., Guerre-Millo, M., Lotersztajn, S., Robert Barouki, Aggerbeck, M. and Coumoul, and X. (2017). Chronic exposure to low doses of dioxin promotes liver fibrosis development in the C57BL/6J diet-induced obesity mouse model. *Environ. Health Perspect.*, **125**(3), pp. 428–436.

Elizondo, G., Fernandez-Salguero, P., Sheikh, M. S., Kim, G. Y., Fornace, A. J., Lee, K. S. and Gonzalez, F. J. (2000). Altered cell cycle control at the G2/M phases in aryl hydrocarbon receptor-null embryo fibroblast. *Mol. Pharmacol.*, **57**(5), pp. 1056–1063.

Evans, B. R., Karchner, S. I., Allan, L. L., Pollenz, R. S., Tanguay, R. L., Jenny, M. J., Sherr, D. H. and Hahn, M. E. (2008). Repression of aryl hydrocarbon receptor (AHR) signaling by AHR repressor: role of DNA binding and competition for AHR nuclear translocator. *Mol. Pharmacol.*, **73**(2), pp. 387–398.

Fan, F., Yan, B., Wood, G., Viluksela, M. and Rozman, K. K. (1997). Cytokines (IL-1β and TNFα) in relation to biochemical and immunological effects of 2,3,7,8-tetrachlorodibenzo-p-dioxin (TCDD) in rats. *Toxicology*, **116**(1–3), pp. 9–16.

Fernandez-Salguero, P. M., Pineau, T., Hilbert, D. M., McPhail, T., Lee, S. S. T., Kimura, S., Nebert, D. W., Rudikoff, S., Ward, J. M. and Gonzalez, F. J. (1995).

Immune system impairment and hepatic fibrosis in mice lacking the dioxin-binding Ah receptor. *Science*, **268**, pp. 722–726.

Friedman, S. L. (2000). Molecular regulation of hepatic fibrosis, an integrated cellular response to tissue injury. *J. Biol. Chem.*, **275**, pp. 2247–2250.

Fukunaga, B. N., Probst, M. R., Reisz-Porszasz, S. and Hankinson, O. (1995). Identification of functional domains of the aryl hydrocarbon receptor. *J. Biol. Chem.*, **270**(49), pp. 29270–29278.

Giboney, P. T. (2005). Mildly elevated liver transaminase levels in the asymptomatic patient. *Am. Fam. Physician*, **71**(6), pp. 1105–1110.

Ginès, P., Cárdenas, A., Arroyo, V. and Rodés, J. (2004). Management of cirrhosis and ascites. *N. Engl. J. Med.*, **350**(16), pp. 1646–1654.

Gradin, K., Toftgård, R., Poellinger, L. and Berghard, A. (1999). Repression of dioxin signal transduction in fibroblasts. Identification of a putative repressor associated with Arnt. *J. Biol. Chem.*, **274**(19), pp. 13511–13518.

Gu, Y.-Z., Hogenesch, J. B. and Bradfield, C. A. (2000). The PAS superfamily: sensors of environmental and developmental signals. *Annu. Rev. Pharmacol. Toxicol.*, **40**, pp. 519–561.

Gudas, L. J., Sporn, M. B. and Roberts, A. (1994). Cellular biology and biochemistry of the retinoids. In *The Retinoids: Biology, Chemistry and Medicine, 2nd ed*. Raven Press, NY, pp. 443–520.

Gupta, B. N., Vos, J. G., Moore, J. A., Zinkl, J. G. and Bullock, B. C. (1973). Pathologic effects of 2,3,7,8-tetrachlorodibenzo-p-dioxin in laboratory animals. *Environ. Health Perspect.*, (5), pp. 125–140.

Håkansson, H. and Ahlborg, U. G. (1985). The effect of 2,3,7,8-tetrachlorodibenzo-p-dioxin (TCDD) on the uptake, distribution and excretion of a single oral dose of [11,12-3H]retinyl acetate and on the vitamin A status in the rat. *J. Nutr.*, **115**(6), pp. 759–771.

Håkansson, H. and Hanberg, A. (1989). The distribution of [14C]-2,3,7,8-

tetrachlorodibenzo-p-dioxin (TCDD) and its effect on the vitamin A content in parenchymal and stellate cells of rat liver. *J. Nutr.*, **119**(4), pp. 573–580.

Han, M., Liu, X., Liu, S., Su, G., Fan, X., Chen, J., Yuan, Q. and Xu, G. (2017). 2,3,7,8-tetrachlorodibenzo-p-dioxin (TCDD) induces hepatic stellate cell (HSC) activation and liver fibrosis in C57BL6 mouse via activating Akt and NF-κB signaling pathways. *Toxicol. Lett.*, **273**, pp. 10–19.

Han, Y.-P. (2006). Matrix metalloproteinases, the pros and cons, in liver fibrosis. *J. Gastroenterol. Hepatol.*, **21**(Suppl 3), pp. S88–S91.

Hanberg, A., Nilsson, C. B., Trossvik, C. and Håkansson, H. (1998). Effect of 2,3,7,8-tetrachlorodibenzo-p-dioxin on the lymphatic absorption of a single oral dose of [3H]retinol and on the intestinal retinol esterification in the rat. *J. Toxicol. Environ. Health Part A*, **55**(5), pp. 331–344.

Hanneman, W. H., Legare, M. E., Barhoumi, R., Burghardt, R. C., Safe, S. and Tiffany-Castiglioni, E. (1996). Stimulation of calcium uptake in cultured rat hippocampal neurons by 2,3,7,8-tetrachlorodibenzo-p-dioxin. *Toxicology*, **112**(1), pp. 19–28.

Haque, M., Francis, J. and Sehgal, I. (2005). Aryl hydrocarbon exposure induces expression of MMP-9 in human prostate cancer cell lines. *Cancer Lett.*, **225**(1), pp. 159–166.

Harris, M., Zacharewski, T., Astroff, B. and Safe, S. (1988). Partial antagonism of 2,3,7,8-tetrachlorodibenzo-p-dioxin-mediated induction of aryl hydrocarbon hydroxylase by 6-methyl-1,3,8-trichlorodibenzofuran: mechanistic studies. *Mol. Pharmacol.*, **35**, pp. 729–735.

Harvey, W. A., Jurgensen, K., Pu, X., Lamb, C. L., Cornell, K. A., Clark, R. J., Klocke, C. and Mitchell, K. A. (2016). Exposure to 2,3,7,8-tetrachlorodibenzo-p-dioxin (TCDD) increases human hepatic stellate cell activation. *Toxicology*, **344**, pp. 26–33.

Hendriks, H. F. J., Verhoofstad, W. A. M. M., Brouwer, A., De Leeuw, A. M. and Knook, D. L. (1985). Perisinusoidal fat-storing cells are the main vitamin A storage sites in rat liver. *Exp. Cell Res.*, **160**, pp. 138–149.

Hernández-Ochoa, I., Karman, B. N. and Flaws, J. A. (2009). The role of the aryl hydrocarbon receptor in the female reproductive system. *Biochem. Pharmacol.*, **77**(4), pp. 547–559.

Hirschfield, G. M., Heathcote, E. J. and Gershwin, M. E. (2010). Pathogenesis of cholestatic liver disease and therapeutic approaches. *Gastroenterology*, **139**(5), pp. 1481–1496.

Hoffman, E. C., Reyes, H., Chu, F.-F., Sander, F., Conley, L. H., Brooks, B. A. and Hankinson, O. (1991). Cloning of a factor required for activity of the Ah (dioxin) receptor. *Science*, **252**(5008), pp. 954–958.

Hofmann, C. and Eichele, G. (1994). Retinoids in development. In *The Retinoids: Biology, Chemistry and Medicine, 2nd ed*. Raven Press, NY, pp. 387–441.

Huang, G. and Elferink, C. J. (2012). A novel nonconsensus xenobiotic response element capable of mediating aryl hydrocarbon receptor-dependent gene expression. *Mol. Pharmacol.*, **81**(3), pp. 338–347.

Ikuta, T., Eguchi, H., Tachibana, T., Yoneda, Y. and Kawajiri, K. (1998). Nuclear localization and export signals of the human aryl hydrocarbon receptor. *J. Biol. Chem.*, **273**(5), pp. 2895–2904.

Institute of Medicine. (1994). *Veterans and Agent Orange: Health Effects of Herbicides Used in Vietnam*. Washington, DC: The National Academies Press.

Jackson, D. P., Joshi, A. D. and Elferink, C. J. (2015). Ah receptor pathway intricacies; signaling through diverse protein partners and DNA-motifs. *Toxicol. Res.* Royal Society of Chemistry, **4**(5), pp. 1143–1158.

Jackson, D. P., Li, H., Mitchell, K. A., Joshi, A. D. and Elferink, C. J. (2014). Ah receptor-mediated suppression of liver regeneration through NC-XRE-driven p21Cip1 expression. *Mol. Pharmacol.*, **85**(4), pp. 533–541.

Jackson, F. R., Bariello, T. A., Yun, S.-H. and Young, M. W. (1986). Product of per locus of Drosophila shares homology with proteoglycans. *Nature*, **320**, pp. 185–188.

Jensen, T., Abdelmalek, M. F., Sullivan, S., Nadeau, K. J., Green, M., Roncal, C., Nakagawa, T., Kuwabara, M., Sato, Y., Kang, D.-H., Tolan, D. R., Sanchez-Lozada, L. G., Rosen, H. R., Lanaspa, M. A., Diehl, A. M. and Johnson, R. J. (2018). Fructose and sugar: A major mediator of nonalcoholic fatty liver disease. *J. Hepatol.*, **68**(5), pp. 1063–1075.

Jones, G. and Greig, J. B. (1975). Pathological changes in the liver of mice given 2,3,7,8-tetrachlorodibenzo-p-dioxin. *Experientia*, **31**(11), pp. 1315–1317.

Jones, K. G., Cole, F. M. and Sweeney, G. D. (1981). The role of iron in the toxicity of 2,3,7,8-tetrachlorodibenzo-(p)-dioxin (TCDD). *Toxicol. Appl. Pharmacol.*, **88**, pp. 74–88.

Karras, J. G., Morris, D. L., Matulka, R. A., Kramer, C. M. and Holsapple, M. P. (1996). 2,3,7,8-tetrachlorodibenzo-p-dioxin (TCDD) elevates basal B-cell intracellular calcium concentration and suppresses surface Ig- but not CD40-induced antibody secretion. *Toxicol. Appl. Pharmacol.*, **137**(2), pp. 275–284.

Katz, D. R., Drzymala, M., Turton, J. A., Hicks, R. M., Hunt, R., Palmer, L. and Malkovský, M. (1987). Regulation of accessory cell function by retinoids in murine immune responses. *Br. J. Exp. Path.*, **68**(3), pp. 343–50.

Kazlauskas, A., Poellinger, L. and Pongratz, I. (2000). The immunophilin-like protein XAP2 regulates ubiquitination and subcellular localization of the dioxin receptor. *J. Biol. Chem.*, **275**(52), pp. 41317–41324.

Kearney, P. C., Woolson, E. A., Isensee, A. R. and Helling, C. S. (1973). Tetrachlorodibenzodioxin in the environment: sources, fate, and Decontamination. *Environ. Health Perspect.*, **5**, pp. 273-277.

Khera, K. S. and Ruddick, J. A. (1973). Polychlorodibenzo-p-dioxins: Perinatal effects and the dominant lethal test in wistar rats. In *Chlorodioxins—Origin and Fate*, American Chemical Society, Washington D.C., pp. 70–84.

Kim, Y. H., Shim, Y. J., Shin, Y. J., Sul, D., Lee, E. and Min, B. H. (2009). 2,3,7,8-tetrachlorodibenzo-p-dioxin (TCDD) induces calcium influx through T-type calcium channel and enhances lysosomal exocytosis and insulin secretion in INS-

1 cells. *Int. J. Toxicol.*, **28**(3), pp. 151–161.

Kisseleva, T. and Brenner, D. A. (2008). Mechanisms of fibrogenesis. *Exp. Biol. Med.*, **233**(2), pp. 109–122.

Kociba, R. J., Keyes, D. G., Beyer, J. E., Carreon, R. M., Wade, C. E., Dittenber, D. A., Kalnins, R. P., Frauson, L. E., Park, C. N., Barnard, S. D., Hummel, R. A. and Humiston, C. G. (1978). Results of a two-year chronic toxicity and oncogenicity study of 2,3,7,8-tetrachlorodibenzo-p-dioxin in rats. *Toxicol. Appl. Pharmacol.*, **46**(2), pp. 279–303.

Kolluri, S. K., Weiss, C., Koff, A. and Göttlicher, M. (1999). Induction and inhibition of proliferation by the intracellular Ah receptor in developing thymus and hepatoma cells. *Genes Dev.*, (13), pp. 1742–1753.

Kolonko, M. and Greb-Markiewicz, B. (2019). bHLH–PAS proteins: Their structure and intrinsic disorder. *Int. J. Mol. Sci.*, **20**(15), p. 3653.

Lahvis, G. P. and Bradfield, C. A. (1998). Ahr null alleles: Distinctive or different?. *Biochem. Pharmacol.*, **56**(7), pp. 781–787.

Lahvis, G. P., Lindell, S. L., Thomas, R. S., McCuskey, R. S., Murphy, C., Glover, E., Bentz, M., Southard, J. and Bradfield, C. A. (2000). Portosystemic shunting and persistent fetal vascular structures in aryl hydrocarbon receptor-deficient mice. *Proc. Natl. Acad. Sci. U.S.A.*, **97**(19), pp. 10442–10447.

Lamas, B., Natividad, J. M. and Sokol, H. (2018). Aryl hydrocarbon receptor and intestinal immunity. *Mucosal Immunol.*, **11**(4), pp. 1024–1038.

Lamb, C. L., Cholico, G. N., Perkins, D. E., Fewkes, M. T., Oxford, J. . T., Morrill, E. E. and Mitchell, K. A. (2016a). Aryl hydrocarbon receptor activation by TCDD modulates expression of extracellular matrix remodeling genes during experimental liver fibrosis. *Biomed Res. Int.*, **2016**.

Lamb, C. L., Cholico, G. N., Pu, X., Hagler, G. D., Cornell, K. A. and Mitchell, K. A. (2016b). 2,3,7,8-tetrachlorodibenzo-p-dioxin (TCDD) increases necro-inflammation and hepatic stellate cell activation but does not exacerbate experimental liver fibrosis in mice. *Toxicol. Appl. Pharmacol.* Elsevier Inc., **311**,

pp. 42–51.

Lee, J. H., Wada, T., Febbraio, M., He, J., Matsubara, T., Jae, M., Gonzalez, F. J. and Xie, W. (2010). A novel role for the dioxin receptor in fatty acid metabolism and hepatic steatosis. *Gastroenterology*, **139**(2), pp. 653–663.

Lees, M. J. and Whitelaw, M. L. (1999). Multiple roles of ligand in transforming the dioxin receptor to an active basic helix-loop-helix/PAS transcription factor complex with the nuclear protein Arnt. *Mol. Cell. Biol.*, **19**(8), pp. 5811–5822.

Lin, T.-M., Ko, K., Moore, R. W., Buchanan, D. L., Cooke, P. S. and Peterson, R. E. (2001). Role of the aryl hydrocarbon receptor in the development of control and 2,3,7,8-tetrachlorodibenzo-p-dioxin exposed male mice. *J. Toxicol. Environ. Health Part A*, **64**(4), pp. 327–342.

Lin, T.-M., Ko, K., Moore, R. W., Simanainen, U., Oberley, T. D. and Peterson, R. E. (2002). Effects of aryl hydrocarbon receptor null mutation and in utero and lactational 2,3,7,8-tetrachlorodibenzo-p-dioxin exposure on prostate and seminal vesicle development in C57BL/6 mice. *Toxicol. Sci.*, **68**(2), pp. 479–487.

Lin, X., Yang, H., Zhou, L. and Guo, Z. (2011). Nrf2-dependent induction of NQO1 in mouse aortic endothelial cells overexpressing catalase. *Free Radic. Biol. Med.*, **51**(1), pp. 97–106.

Lindsey, S. and Papoutsakis, E. T. (2011). The aryl hydrocarbon receptor (AhR) transcription factor regulates megakaryocytic polyploidization. *Br. J. Haematol.*, **152**(4), pp. 469–484.

Ma, Q., Baldwin, K. T. and Virginia, W. (2000). Hydrocarbon receptor (AhR) by the ubiquitin-proteasome pathway. *J. Biol. Chem.*, **275**(12), pp. 8432–8438.

Ma, Q. and Whitlock, J. P. (1997). A novel cytoplasmic protein that interacts with the Ah receptor, contains tetratricopeptide repeat motifs, and augments the transcriptional response to 2,3,7,8-tetrachlorodibenzo-p-dioxin. *J. Biol. Chem.*, **272**(14), pp. 8878–8884.

McCaffery, P. and Drager, U. C. (1995). Retinoice acid synthesizing enzymes in the embryonic and adult vertebrae. In *Enzymology and Molecular Biology of*

Carbonyl Metabolism 5, Plenum Press, N.Y. pp. 173–183.

McDougal, A., Wormke, M., Calvin, J. and Safe, S. (2001). Tamoxifen-induced antitumorigenic/antiestrogenic action synergized by a selective aryl hydrocarbon receptor modulator. *Cancer Res.*, **61**(10), pp. 3902–3907.

Mederacke, I., Hsu, C. C., Troeger, J. S., Huebener, P., Mu, X., Dapito, D. H., Pradere, J.-P. and Schwabe, R. F. (2013). Fate tracing reveals hepatic stellate cells as dominant contributors to liver fibrosis independent of its aetiology. *Nat. Comm.*, **4**, p. 2823.

Mehta, V. and Vezina, C. M. (2011). Potential protective mechanisms of aryl hydrocarbon receptor (AhR) signaling in benign prostatic hyperplasia. *Differentiation*, **82**(4–5), pp. 211–219.

Meyer, B. K., Pray-Grant, M. G., Vanden Heuvel, J. P. and Perdew, G. H. (1998). Hepatitis B virus X-associated protein 2 is a subunit of the unliganded aryl hydrocarbon receptor core complex and exhibits transcriptional enhancer activity. *Mol. Cell. Biol.*, **18**(2), pp. 978–88.

Micka, J., Milatovich, A., Menon, A., Grabowski, G. A., Puga, A. and Nebert, D. W. (1997). Human Ah receptor (AhR) gene: localization to 7p15 and suggestive correlation of polymorphism with CYP1A1 inducibility. *Pharmacogenetics*, **7**(2), pp. 95–101.

Mimura, J., Ema, M., Sogawa, K. and Fujii-Kuriyama, Y. (1999). Identification of a novel mechanism of regulation of Ah (dioxin) receptor function. *Genes Dev.*, **13**(1), pp. 20–25.

Mimura, J. and Fujii-Kuriyama, Y. (2003). Functional role of AhR in the expression of toxic effects by TCDD. *Biochim. Biophys. Acta*, **1619**(3), pp. 263–268.

Mimura, J., Yamashita, K., Nakamura, K., Morita, M., Takagi, T. N., Nakao, K., Ema, M., Sogawa, K., Yasuda, M., Katsuki, M. and Fujii-Kuriyama, Y. (1997). Loss of teratogenic response to 2,3,7,8-tetrachlorodibenzo-p-dioxin (TCDD) in mice lacking the Ah (dioxin) receptor. *Genes Cells*, **2**(10), pp. 645–654.

Mitchell, K. A., Lockhart, C. A., Huang, G. and Elferink, C. J. (2006). Sustained aryl

hydrocarbon receptor activity attenuates liver regeneration. *Mol. Pharmacol.*, **70**(1), pp. 163–170.

Mitchell, K. A., Wilson, S. R. and Elferink, C. J. (2010). The activated aryl hydrocarbon receptor synergizes mitogen-induced murine liver hyperplasia. *Toxicology*, **276**(2), pp. 103–109.

Moore, J. A., Gupta, B. N., Zinkl, J. G. and Vos, J. G. (1973). Postnatal effects of maternal exposure to 2,3,7,8-tetrachlorodibenzo-p-dioxin (TCDD). *Environ. Health Perspect.*, **5**, p. 81.

Moriguchi, T., Motohashi, H., Hosoya, T., Nakajima, O., Takahashi, S., Ohsako, S., Aoki, Y., Nishimura, N., Tohyama, C., Fujii-Kuriyama, Y. and Yamamoto, M. (2003). Distinct response to dioxin in an arylhydrocarbon receptor (AHR)-humanized mouse. *Proc. Natl. Acad. Sci. U.S.A.*, **100**(10), pp. 5652–5657.

Mulero-Navarro, S. and Fernandez-Salguero, P. M. (2016). New Trends in Aryl Hydrocarbon Receptor Biology. *Front. Cell Dev. Biol.*, **4**(45).

Murray, F. J., Smith, F. A., Nitschke, K. D., Humiston, C. G., Kociba, R. J. and Schwetz, B. A. (1979). Three-generation reproduction study of rats given 2,3,7,8-tetrachlorodibenzo-p-dioxin (TCDD) in the diet. *Toxicol. Appl. Pharmacol.*, **50**(2), pp. 241–252.

Nambu, J. R., Lewis, J. O., Wharton, K. A. and Crews, S. T. (1991). The drosophila single-minded gene encodes a helix-loop-helix protein that acts as a master regulator of CNS midline development. *Cell*, **67**(6), pp. 1157–1167.

Narayanan, G. A., Murray, I. A., Krishnegowda, G., Amin, S. and Perdew, G. H. (2012). Selective aryl hydrocarbon receptor modulator-mediated repression of CD55 expression induced by cytokine exposure. *J. Pharmacol. Exp. Ther.*, **342**(2), pp. 345–355.

National Toxicology Program (1982a). *Bioassay of 2,3,7,8-tetrachlorodibenzo-p- dioxin for possible carcinogenicity (dermal).* Natl. Toxicol. Program Tech. Rep. Ser. **201**:1-113.

National Toxicology Program (1982b). *Carcinogenesis Bioassay of 2,3,7,8-*

Tetrachlorodibenzo-p-dioxin (CAS No. 1746-01-6) in Osborne-Mendel Rats and B6C3F-1 Mice (Gavage Study). Natl. Toxicol. Program Tech. Rep. Ser. **209**:1-195.

Nault, R., Fader, K. A., Ammendolia, D. A., Dornbos, P., Potter, D., Sharratt, B., Kumagai, K., Harkema, J. R., Lunt, S. Y., Matthews, J. and Zacharewski, T. (2016). Dose-dependent metabolic reprogramming and differential gene expression in TCDD-elicited hepatic fibrosis. *Toxicol. Sci.*, **154**(2), pp. 253–266.

Neavin, D. R., Liu, D., Ray, B. and Weinshilboum, R. M. (2018). The role of the aryl hydrocarbon receptor (AhR) in immune and inflammatory diseases. *Int. J. Mol. Sci.*, **19**(12).

Olivero-Verbel, J., Roth, R. A. and Ganey, P. E. (2011). Dioxin alters inflammatory responses to lipopolysaccharide. *Toxicol. Environ. Chem.*, **93**(6), pp. 1180–1194.

Oshima, M., Mimura, J., Yamamoto, M. and Fujii-Kuriyama, Y. (2007). Molecular mechanism of transcriptional repression of AhR repressor involving ANKRA2, HDAC4, and HDAC5. *Biochem. Biophys. Res. Commun.*, **364**(2), pp. 276–282.

Otterbein, L. E., Soares, M. P., Yamashita, K. and Bach, F. H. (2003). Heme oxygenase-1: Unleashing the protective properties of heme. *Trends Immunol.*, **24**(8), pp. 449–455.

Ozeki, J., Uno, S., Ogura, M., Choi, M., Maeda, T., Sakurai, K., Matsuo, S., Amano, S., Nebert, D. W. and Makishima, M. (2011). Aryl hydrocarbon receptor ligand 2,3,7,8-tetrachlorodibenzo-p-dioxin enhances liver damage in bile duct-ligated mice. *Toxicology*, **280**(1–2), pp. 10–17.

Pappas, B., Yang, Y., Wang, Y., Kim, K., Chung, H. J., Cheung, M., Ngo, K., Shinn, A. and Chan, W. K. (2018). p23 protects the human aryl hydrocarbon receptor from degradation via a heat shock protein 90-independent mechanism. *Biochem. Pharmacol.*, **152**, pp. 34–44.

Patel, R. D., Murray, I. A., Flaveny, C. A., Kusnadi, A. and Perdew, G. H. (2009). Ah receptor represses acute phase response gene expression without binding to its cognate response element. *Lab Invest.*, **89**(6), pp. 695–707.

Pearce, S. T., Liu, H., Radhakrishnan, I., Abdelrahim, M., Safe, S. and Jordan, V. C. (2004). Interaction of the aryl hydrocarbon receptor ligand 6-methyl-1,3,8-trichlorodibenzofuran with estrogen receptor α. *Cancer Res.*, **64**(8), pp. 2889–2897.

Pellicoro, A., Ramachandran, P., Iredale, J. P. and Fallowfield, J. A. (2014). Liver fibrosis and repair: Immune regulation of wound healing in a solid organ. *Nat. Rev. Immunol.*, **14**(3), pp. 181–194.

Petrulis, J. R., Kusnadi, A., Ramadoss, P., Hollingshead, B. and Perdew, G. H. (2003). The hsp90 co-chaperone XAP2 alters importin β recognition of the bipartite nuclear localization signal of the Ah receptor and represses transcriptional activity. *J. Biol. Chem.*, **278**(4), pp. 2677–2685.

Pierre, S., Chevallier, A., Teixeira-Clerc, F., Ambolet-Camoit, A., Bui, L. C., Bats, A. S., Fournet, J. C., Fernandez-Salguero, P. M., Aggerbeck, M., Lotersztajn, S., Barouki, R. and Coumoul, X. (2014). Aryl hydrocarbon receptor-dependent induction of liver fibrosis by dioxin. *Toxicol. Sci.*, **137**(1), pp. 114–124.

Poland, A. and Knutson, J. C. (1982). 2,3,7,8-tetrachlorodibenzo-p-dioxin and related halogenated aromatic hydrocarbons: examination of the mechanism of toxicity. *Ann. Rev. Pharmacol. Toxicol.*, **22**, pp. 517–54.

Poland, A., Palen, D. and Glover, E. (1994). Analysis of the four alleles of the murine aryl hydrocarbon receptor. *Mol. Pharmacol.*, **46**, pp. 915–921.

Pollenz, R. S., Sattler, C. A. and Poland, A. (1994). The aryl hydrocarbon receptor and aryl hydrocarbon receptor nuclear translocator protein show distinct subcellular localizations in Hepa 1c1c7 cells by immunfluorescence microscopy. *Mol. Pharmacol.*, **45**(3), pp. 428–438.

Raica Jr., N., Scott, J., Lowry, L. and Sauberlich, H. E. (1972). Vitamin A concentration in human tissues collected from five areas in the United States. *Am. J. Clin. Nutr.*, **25**(March), pp. 291–296.

Reddy, P., Jacquier, A. C., Abovich, N., Petersen, G. and Rosbash, M. (1986). The period clock locus of D. melanogaster codes for a proteoglycan. *Cell*, **46**(1), pp. 53–61.

Saari, J. C. (1994). Retinoids in photosensitive systems. In *The Retinoids: Biology, Chemistry and Medicine, 2nd ed*. Raven Press, NY, pp. 351–385.

Safe, S., Cheng, Y. and Jin, U. H. (2017). The aryl hydrocarbon receptor (AhR) as a drug target for cancer chemotherapy. *Curr. Opin. Toxicol.*, **1**, pp. 24–29.

Safe, S. H. (1986). Mechanism of action of polychlorinated dibenzo-p-dioxins and dibenzofurans. *Annu. Rev. Pharmacol. Toxicol.*, **26**, pp. 371–399.

Safe, S. and Wormke, M. (2003). Inhibitory aryl hydrocarbon receptor-estrogen receptor α cross-talk and mechanisms of action. *Chem. Res. Toxicol.*, **16**(7), pp. 807–816.

Sakurai, S., Shimizu, T. and Ohto, U. (2017). The crystal structure of the AhRR–ARNT heterodimer reveals the structural basis of the repression of AhR-mediated transcription. *J. Biol. Chem.*, **292**(43), pp. 17609–17616.

Schecter, A. (1994). *Dioxins and Health*. Plenum Press, N.Y.

Schmidt, J. V., Carver, L. A. and Bradfield, C. A. (1993). Molecular characterization of the murine Ahr gene. *J. Biol. Chem.*, **268**(29), pp. 22203–22209.

Schmidt, J. V., Su, G. H.-T., Reddy, J. K., Simon, M. C. and Bradfield, C. A. (1996). Characterization of a murine Ahr null allele: involvement of the Ah receptor in hepatic growth and development. *Proc. Natl. Acad. Sci. U.S.A.*, **93**(13), pp. 6731–6736.

Shen, E. S., Gutman, S. I. and Olson, J. R. (1991). Comparison of 2,3,7,8-tetrachlorodibenzo-p-dioxin-mediated hepatotoxicity in C57BL/6J and DBA/2J mice. *J. Toxicol. Environ. Health*, **32**(4), pp. 367–381.

Shen, E. S. and Whitlock, J. P. (1992). Protein-DNA interactions at a dioxin-responsive enhancer. Mutational analysis of the DNA-binding site for the liganded Ah receptor. *J. Biol. Chem.*, **267**(10), pp. 6815–6819.

Sherman, I. A., Pappas, S. C. and Fisher, M. M. (1990). Hepatic microvascular changes associated with development of liver fibrosis and cirrhosis. *Am. J. Physiol.*, **258**(2 27-2).

Silkworth, J. B. and Brown, J. F. (1996). Evaluating the impact of exposure to

environmental contaminants on human health. *Clin. Chem.*, **42**, pp. 1345–1349.

Smith, C. L. and O'Malley, B. W. (2004). Coregulator function: A key to understanding tissue specificity of selective receptor modulators. *Endocr. Rev.*, **25**(1), pp. 45–71.

Smith, F. A., Schwetz, B. A. and Nitschke, K. D. (1976). Teratogenicity of 2,3,7,8-tetrachlorodibenzo-p-dioxin in CF-1 mice. *Toxicol. Appl. Pharmacol.*, **38**(3), pp. 517–523.

Son, D.-S. and Rozman, K. K. (2002). 2,3,7,8-tetrachlorodibenzo-p-dioxin (TCDD) induces plasminogen activator inhibitor-1 through an aryl hydrocarbon receptor-mediated pathway in mouse hepatoma cell lines. *Arch. Toxicol.*, **76**(7), pp. 404–413.

Sorg, O., Zennegg, M., Schmid, P., Fedosyuk, R., Valikhnovskyi, R., Gaide, O., Kniazevych, V. and Saurat, J.-H. (2009). 2,3,7,8-tetrachlorodibenzo-p-dioxin (TCDD) poisoning in Victor Yushchenko: identification and measurement of TCDD metabolites. *The Lancet*, **374**(9696), pp. 1179–1185.

Soshilov, A. and Denison, M. S. (2011). Ligand displaces heat shock protein 90 from overlapping binding sites within the aryl hydrocarbon receptor ligandbinding domain. *J. Biol. Chem.*, **286**(40), pp. 35275–35282.

Sparschu, G. L., Dunn, F. L. and Rowe, V. K. (1971). Study of the teratogenicity of 2,3,7,8-tetrachiorodibenzo-p-dioxin in the rat. *Fd. Cosmet. Toxicol.*, **9**(3), pp. 405–412.

Steenland, K., Bertazzi, P., Baccarelli, A. and Kogevinas, M. (2004). Dioxin revisited: Developments since the 1997 IARC classification of dioxin as a human carcinogen. *Environ. Health Perspect.*, **112**(13), pp. 1265–1268.

Stejskalova, L., Dvorak, Z. and Pavek, P. (2011). Endogenous and exogenous ligands of aryl hydrocarbon receptor: Current state of art. *Curr. Drug Metab.*, **12**(2), pp. 198–212.

Thunberg, T., Ahlborg, U. G., Håkansson, H., Krantz, C. and Monier, M. (1980). Effect of 2,3,7,8-tetrachlorodibenzo-p-dioxin on the hepatic storage of retinol in rats with different dietary supplies of vitamin A (retinol). *Arch. Toxicol.*, **45**(4), pp.

273–285.

Tomkiewicz, C., Herry, L., Bui, L. C., Métayer, C., Bourdeloux, M., Barouki, R. and Coumoul, X. (2013). The aryl hydrocarbon receptor regulates focal adhesion sites through a non-genomic FAK/Src pathway. *Oncogene*, **32**(14), pp. 1811–1820.

Trechsel, U., Evêquoz, V. and Fleisch, H. (1985). Stimulation of interleukin 1 and 3 production by retinoic acid in vitro. *Biochem. J.*, **230**(2), pp. 339–44.

Triebig, G., Werle, E., Päpke, O., Heim, G., Broding, C. and Ludwig, H. (1998). Effects of dioxins and furans on liver enzymes, lipid parameters, and thyroid hormones in former thermal metal recycling workers. *Environ. Health Perspect.*, **106**(SUPPL. 2), pp. 697–700.

Tucker, R. E., Young, A. L. and Gray, A. P. (1981). *Human and Environmental Risks of Chlorinated Dioxins and Related Compounds*. Springer US.

Van-Miller, J. P., Lalich, J. J. and Allen, J. R. (1977). Increased Incidence Of Neoplasms In Rats Exposed To Low Levels Of 2,3,7,8-Tetrachlorodibenzo-P-Dioxin. *Chemosphere*, (9), pp. 537–544.

Villano, C. M., Murphy, K. A., Akintobi, A. and White, L. A. (2006). 2,3,7,8-Tetrachlorodibenzo-p-dioxin (TCDD) induces matrix metalloproteinase (MMP) expression and invasion in A2058 melanoma cells. *Toxicol. Appl. Pharmacol.*, **210**(3), pp. 212–224.

Vogel, C., Donat, S., Döhr, O., Kremer, J., Esser, C., Roller, M. and Abel, J. (1997). Effect of subchronic 2,3,7,8-tetrachlorodibenzo-p-dioxin exposure on immune system and target gene responses in mice: Calculation of benchmark doses for CYP1A1 and CYPIA2 related enzyme activities. *Arch. Toxicol.*, **71**(6), pp. 372–382.

Vogel, C. F. A., Chang, W. L. W., Kado, S., McCulloh, K., Vogel, H., Wu, D., Haarmann-Stemmann, T., Yang, G., Leung, P. S. C., Matsumura, F. and Gershwin, M. E. (2016). Transgenic overexpression of aryl hydrocarbon receptor repressor (AhRR) and AhR-mediated induction of CYP1A1, cytokines, and acute toxicity. *Environ. Health Perspect.*, **124**(7), pp. 1071–1093.

Vogel, C. F. A., Nishimura, N., Sciullo, E., Wong, P., Li, W. and Matsumura, F. (2007). Modulation of the chemokines KC and MCP-1 by 2,3,7,8-tetrachlorodibenzo-p-dioxin (TCDD) in mice. *Arch. Biochem. Biophys.*, **461**(2), pp. 169–175.

Vos, J. G., Moore, J. A. and Zinkl, J. G. (1974). Toxicity of 2,3,7,8-tetrachlorodibenzo-p-dioxin (TCDD) in C57B1/6 mice. *Toxicol. Appl. Pharmacol.*, **29**, pp. 229–241.

Walker, M. K., Thackaberry, E. A., Gabaldon, D. M. and Smith, S. M. (2002). Aryl hydrocarbon receptor null mice develop cardiac hypertrophy and increased hypoxia-inducible factor-1α in the absence of cardiac hypoxia. *Cardiovasc. Toxicol.*, **2**(4), pp. 263–273.

Weber, L. W. D., Boll, M. and Stampfl, A. (2003). Hepatotoxicity and mechanism of action of haloalkanes: carbon tetrachloride as a toxicological model. *Crit. Rev. Toxicol.*, **33**(2), pp. 105–136.

Weiss, C., Kolluri, S. K., Kiefer, F. and Göttlicher, M. (1996). Complementation of Ah receptor deficiency in hepatoma cells: Negative feedback regulation and cell cycle control by the Ah receptor. *Exp. Cell Res.*, **226**(1), pp. 154–163.

Wells, R. G. (2008). Cellular sources of extracellular matrix in hepatic fibrosis. *Clin. Liver Dis.*, **12**(4), pp. 1–10.

Wilson, S. R., Joshi, A. D. and Elferink, C. J. (2013). The tumor suppressor kruppel-like factor 6 is a novel aryl hydrocarbon receptor DNA binding partner. *J. Pharmacol. Exp. Ther.*, **345**(3), pp. 419–429.

Wong, F. W. Y., Chan, W. Y. and Lee, S. S. T. (1998). Resistance to carbon tetrachloride-induced hepatotoxicity in mice which lack CYP2E1 expression. *Toxicol. Appl. Pharmacol.*, **153**(1), pp. 109–118.

Wynn, T. A. (2008). Cellular and molecular mechanisms of fibrosis. *J. Pathol.*, **214**(2), pp. 199–210.

CHAPTER TWO

SUMMARY OF THE EFFECTS OF TCDD DURING CARBON TETRACHLORIDE-INDUCED LIVER FIBROSIS[1]

In previous studies from our lab, male C57BL/6 mice were treated with 0.5 ml/kg CCl_4 twice a week for 8 weeks to induce liver injury. Mice were then treated with 20 μg/kg TCDD once a week during weeks 7 and 8 to activate the AhR. Mice were euthanized at the end of the 8-week experiment. Liver-to-body weight ratios and serum ALT levels measured to characterize the extent of TCDD hepatotoxicity. TCDD treatment was found to elicit hepatomegaly regardless of CCl_4 treatment (Figure 2.2A). Treatment with either CCl_4 or TCDD alone increased serum ALT levels (Figure 2.2B). These results are consistent with other reports of hepatotoxicity in mice treated with CCl_4 or TCDD (Mejia-Garcia *et al.*, 2013; Scholten *et al.*, 2015). Co-treated mice (CCl_4/TCDD) exhibited a 40% mortality rate during the final week of the experiment, while death was not observed in any other treatment group.

---

[1] Data from this chapter were published as part of the following manuscripts:

Lamb, C. L., **Cholico, G. N**., Perkins, D. E., Fewkes, M. T., Oxford, J. T., Morrill, E. E. and Mitchell, K. A. (2016). Aryl hydrocarbon receptor activation by TCDD modulates expression of extracellular matrix remodeling genes during experimental liver fibrosis. *BioMed Res. Int*., **2016**.

Lamb, C. L., **Cholico, G. N**., Pu, X., Hagler, G. D., Cornell, K. A. and Mitchell, K. A. (2016). 2,3,7,8-Tetrachlorodibenzo-*p*-dioxin (TCDD) increases necroinflammation and hepatic stellate cell activation but does not exacerbate experimental liver fibrosis in mice. *Toxicol. Appl. Pharmacol*., **311**, pp. 42–51.

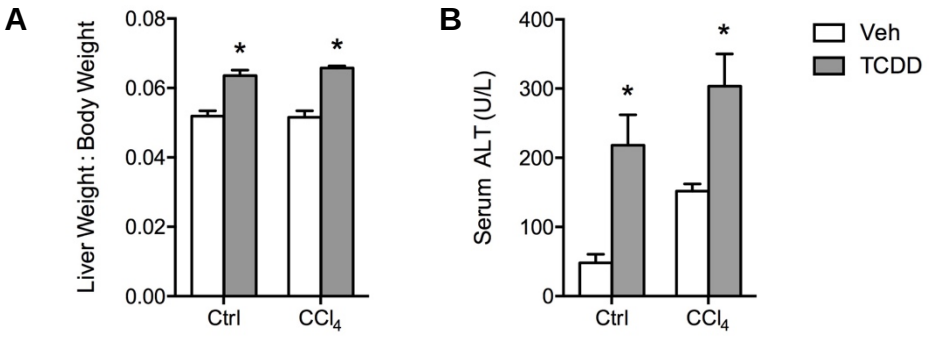

Figure 2.2 Gross Markers of TCDD Hepatoxicity.

(A) Liver-to-body weight ratios. (B) Serum ALT levels. Data represent mean ± SEM from six mice per treatment group. Asterisks (*) denote a significant difference when compared to vehicle-treated mice within same treatment group. ($p < 0.05$)

Liver fibrosis is mediated by myofibroblast precursors that become activated in response to injury and inflammation (Pellicoro et al., 2014). During CCl_4-induced liver fibrosis, the primary type of myofibroblast precursor are hepatic stellate cells (HSCs) (Iwaisako *et al.*, 2014). To test the hypothesis that TCDD increased HSC activation, we measured expression of the HSC activation marker, alpha-smooth muscle actin (αSMA). CCl_4 treatment increased αSMA protein expression in the liver (Figure 2.3A). Whereas TCDD treatment alone had no impact on αSMA expression, it produced a two-fold increase in αSMA immunofluorescence compared to mice treated with CCl_4 alone (Figure 2.3B). Analysis of αSMA mRNA levels revealed that neither TCDD nor CCl_4 treatment alone impacted αSMA transcript levels, but when administered together, a 40-fold increase in αSMA mRNA was detected (Figure 2.3C).

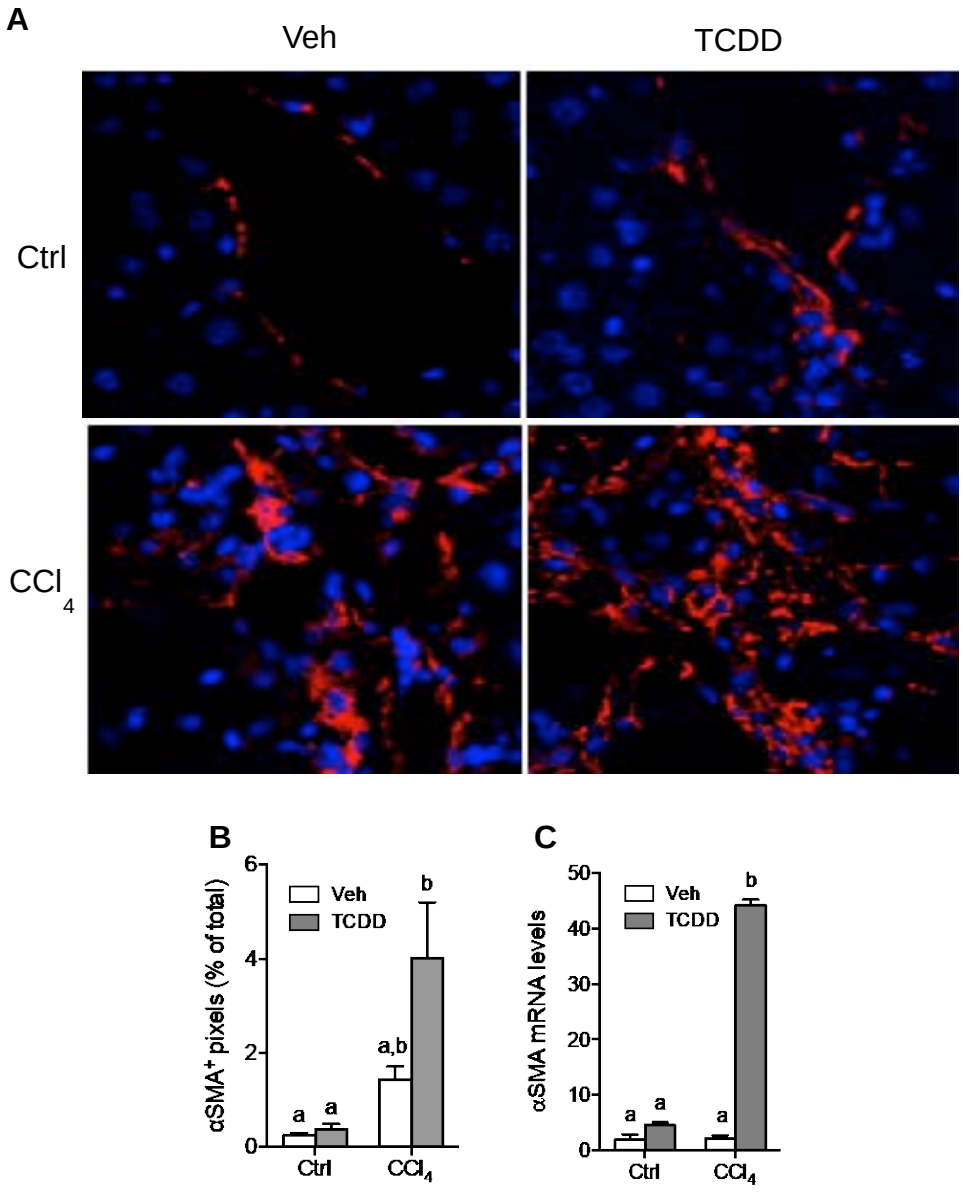

Figure 2.3 TCDD increases markers of HSC activation.

(A) Immunofluorescence was used to measure αSMA expression (red) in paraffin-embedded liver tissues (200X magnification). Cell nuclei were counterstained with DAPI (blue). (B) Pixel densitometry for αSMA immunofluorescence. (C) Hepatic αSMA mRNA levels. Data were normalized to GAPDH and expressed as fold-change relative to the Ctrl/Veh treatment group. Data represent mean ± SEM (n=4). Bars with different letters are significantly different from each other ($p < 0.05$) (Lamb *et al*., 2016b).

Next we investigated how TCDD impacts the extent of fibrogenesis in the CCl_4-injured liver by measuring expression of genes encoding procollagen types I and III, which are the most abundant types of collagen deposited by HSCs during liver injury

(Maher & McGuire, 1990). Treatment with TCDD alone significantly increased mRNA levels of *Col1a1*, while CCl_4 alone significantly increased mRNA levels of both *Col1a1* and *Col3a1*. TCDD treatment in CCl_4 mice increased the expression of these genes even further (Fig. 2.4).

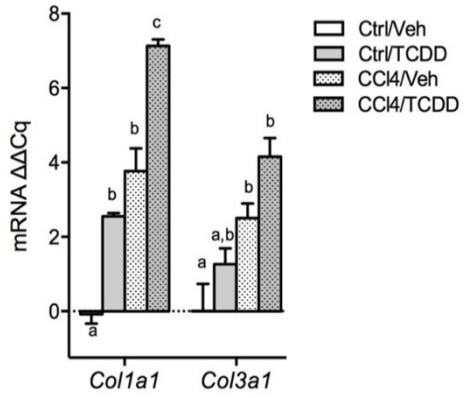

Figure 2.4 TCDD treatment increases collagen gene expression.
Col1a1 and Col3a1 mRNA levels in the mouse liver were measured by qRT-PCR. Data were normalized to GAPDH and expressed relative to the Ctrl/Veh treatment group. Data represent mean ± SEM (n=3). Bars with different letters are significantly different from each other ($p < 0.05$). (Lamb *et al.*, 2016b).

Given that TCDD increased HSC activation and procollagen gene expression in CCl_4-treated mice, we hypothesized that liver fibrosis would likewise be more severe. To visualize the extent of liver fibrosis, paraffin-embedded liver sections were stained with picrosirius red, which specifically binds to collagen fibrils. Collagen deposition was detected in mice treated with CCl_4 but, contrary to our hypothesis, TCDD treatment did not consistently increase deposition (Figure 2.5A, B). Liver fibrosis was further evaluated using the Ishak Modified Histological Activity Index system, which produced similar results (Figure 2.5C) (Ishak *et al.*, 1995). Hepatic collagen protein levels were further measured using Western blot (Figure 2.5D) and mass spectrometry (Figure 2.5E). Results

from these techniques confirm that TCDD treatment did not markedly impact collagen content compared to mice treated with CCl_4 alone.

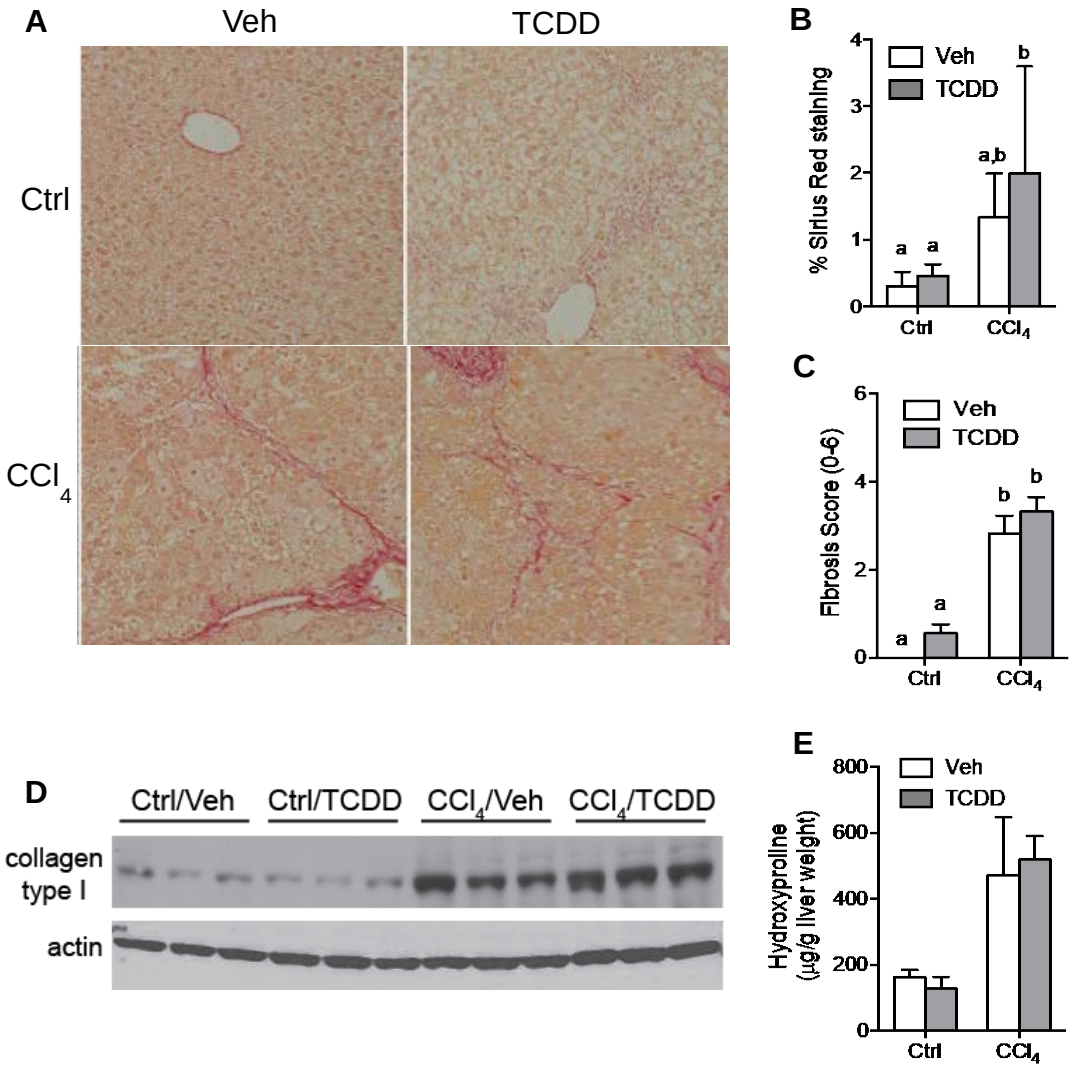

Figure 2.5 TCDD does not increase collagen deposition in the liver of CCl_4-treated mice.

(A) Liver tissue was stained with Sirius red to visualize collagen deposition (100X magnification). (B) Sirius red staining was quantified and expressed as a percentage of total area. (C) Sirius-red-stained liver tissue was scored according to the Ishak Modified Histological Activity Index. Bars for (B, C) represent mean ± SEM for mice (n=6). Bars with a different letter denote a significant difference ($p < 0.05$). (D) Western blot to detect collagen type I in pepsin-digested liver homogenates (n=3). Actin levels were measured in undigested liver homogenates (25 ug protein/lane). (E) Average hydroxyproline content in liver based on mass spectrometry analysis (n=3).

In the CCl_4 model of experimental liver fibrosis, fibrogenesis is driven not only by liver injury, but also by inflammation (Weber *et al.*, 2003). We therefore sought to characterize how TCDD treatment impacted inflammation and subsequent progression of liver disease. Inflammation was evaluated based on the presence of inflammatory foci in H&E-stained liver tissue (Figure 2.6). Foci containing infiltrating leukocytes were detected in the liver of mice treated with TCDD alone (Figure 2.6 C, D). Analysis of the liver of CCl_4-treated mice revealed areas of injury that included ballooning hepatocytes, coagulation necrosis and necrotic bridge formation (Figure 2.6 E, F). Administration of TCDD to CCl_4-treated mice appeared to produce widespread coagulation necrosis and inflammation (Figure 2.6 G, H). We further addressed the extent of hepatic necrosis and inflammation using the Ishak Modified Histological Activity Index system. In this scoring system, necroinflammation is assessed based on four endpoints: 1) periportal or periseptal interface necrosis; 2) confluent necrosis; 3) focal lytic necrosis, apoptosis, and focal inflammation; and 4) portal inflammation (Ishak *et al.*, 1995). Treatment with either TCDD or CCl_4 alone slightly increased all four endpoints, resulting in a "mild" necroinflammation score (Table 2.3). However, co-treatment of mice with CCl_4 and TCDD resulted in a marked increase of confluent necrosis, portal inflammation and periportal or periseptal interface hepatitis, resulting in an overall necroinflammation score that was twice as high.

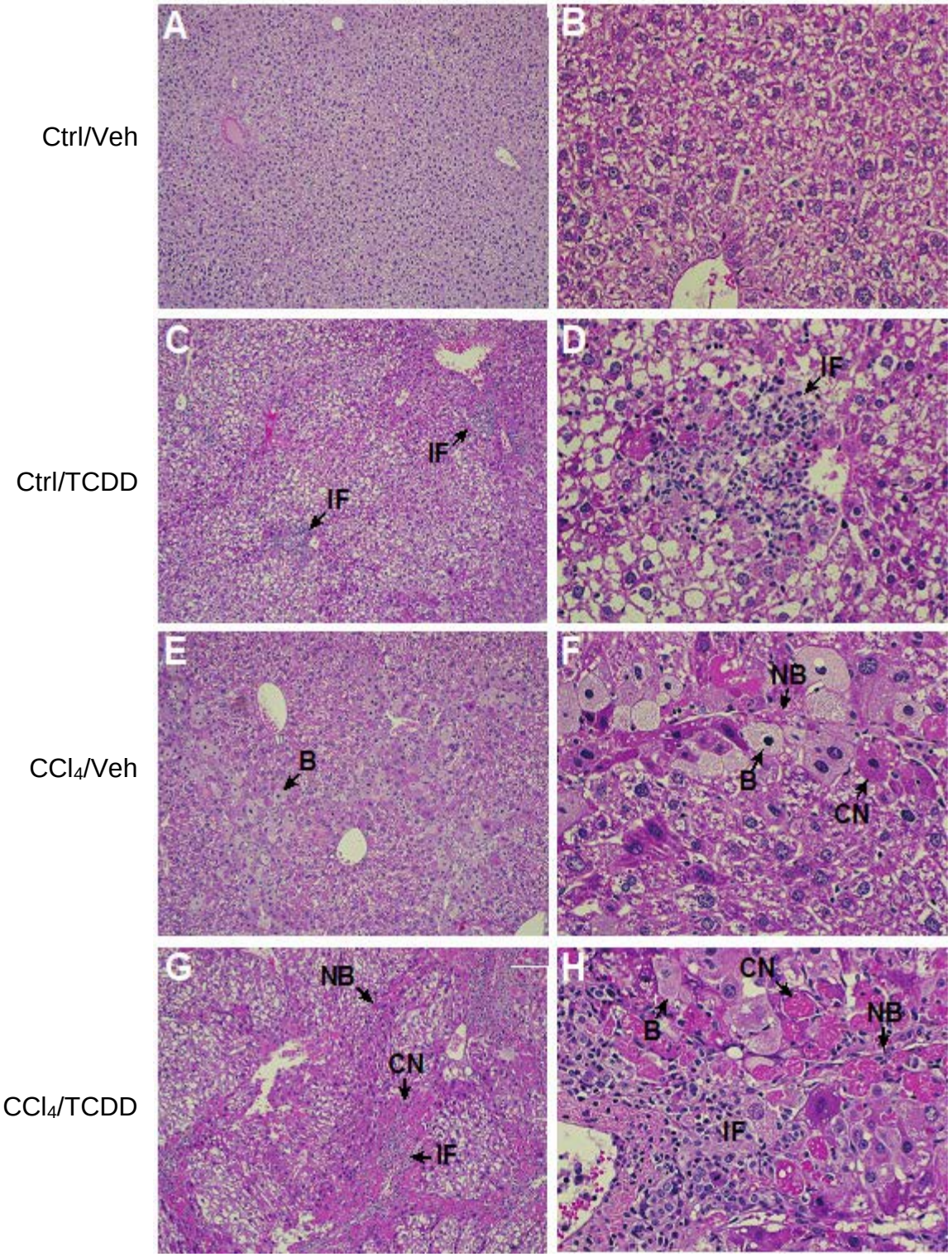

Figure 2.6 TCDD increases liver injury and necroinflammation.

Representative sections of liver tissue stained with H&E were imaged at 100x (A, C, E, G) and 200x (B, D, F, H). H&E-stained liver tissue allows for visualization of necrotic bridges, **NB**; inflammatory foci, **IF**; ballooning hepatocytes, **B**; and coagulation necrosis, **CN**.

Table 2.1 TCDD increased necroinflammation in CCl_4-treated mice.

	Ctrl/Veh	Ctrl/TCDD	CCl_4/Veh	CCl_4/TCDD
Periportal or periseptal interface hepatitis (0-4)	0	1.86 ± 0.34^{a}	1.50 ± 0.22^{a}	$4 \pm 0^{a,b}$
Confluent necrosis (0-6)	0	1.14 ± 0.26^{a}	1.33 ± 0.21^{a}	$5 \pm 0^{a,b}$
Focal lytic necrosis, apoptosis, and focal inflammation (0-4)	0	1.71 ± 0.29^{a}	1 ± 0	1.33 ± 0.33^{a}
Portal inflammation (0-4)	0	1.86 ± 0.34^{a}	1.83 ± 0.17^{a}	$3.33 \pm 0.33^{a,b}$
Combined necroinflammation score:	0	6.57 ± 0.81^{a} (mild)	5.67 ± 0.33^{a} (mild)	13.67 ± 0.33^{a} (severe)

Necroinflammation was assessed using the Ishak Modified Histological Activity Index System. Numbers in parentheses indicate the scoring range for each feature. $^{a}p < 0.05$ when compared to Ctrl/Veh; $^{b}p < 0.05$ when compared to CCl_4/Veh. Six mice were assessed per treatment group.

Objectives and Hypothesis

Previous studies from our laboratory indicate that TCDD treatment increases liver injury, inflammation, and HSC activation during CCl_4-induced liver fibrosis. These results support other reports that TCDD treatment activates HSCs both *in vitro* and *in vivo* (Harvey *et al.*, 2016; Han *et al.*, 2017). However, what remains unclear is whether TCDD increases HSC activation through a **direct** or **indirect** mechanism. For example, it is possible that TCDD directly interacts with AhR in the HSCs to produce transcriptional changes that result in activation of these cells. Alternatively, TCDD could indirectly activate HSCs through other methods, such as by increasing damage to parenchymal hepatocytes and/or by increasing inflammation. These possible mechanisms are depicted in Figure 2.7, which forms the basis for the project described in Chapter 3. The specific goal for this project was to determine the cell-specific consequences of TCDD/AhR signaling on HSC activation and fibrosis in the CCl_4-injured liver. To accomplish this, we used conditional AhR knockout mice, in which the AhR was removed from either hepatocytes or HSCs. Mice were treated with CCl_4 for 5 weeks to elicit initial liver injury, and then a single dose of TCDD was administered during the final week to activate the AhR. Liver damage, inflammation, HSC activation and fibrosis were measured. Understanding the cell-specific role of AhR signaling in fibrosis is important for determining mechanisms of TCDD toxicity. Furthermore, this information could potentially be used for the future development therapeutic AhR ligands to target and diminish HSC activation and alleviate fibrosis.

In Chapter 4, we tested the hypothesis that TCDD elicits a condition similar to non-alcoholic fatty liver disease (NAFLD) in the liver of CCl_4-treated mice. We assessed

histopathological markers of NAFLD, which included steatosis, inflammation, and fibrosis. Transcriptome RNA-sequencing was conducted to identify patterns of gene expression known to be associated with NAFLD, such as metabolic pathways related to insulin signaling, glucose metabolism and lipid metabolism. The extent to which AhR activation contributes to NAFLD progression remains unclear, but this is an important area of research, as NAFLD is a growing health concern that is expected to become the leading cause of liver transplantation by the year 2030. Furthermore, exposure to environmental contaminants, such as those that activate the AhR, has been proposed as a possible mechanism to explain NAFLD progression (Bertot & Adams, 2016).

Results from the studies in Chapter 3 and Chapter 4 are summarized, and future studies are discussed, in the final chapter of this dissertation.

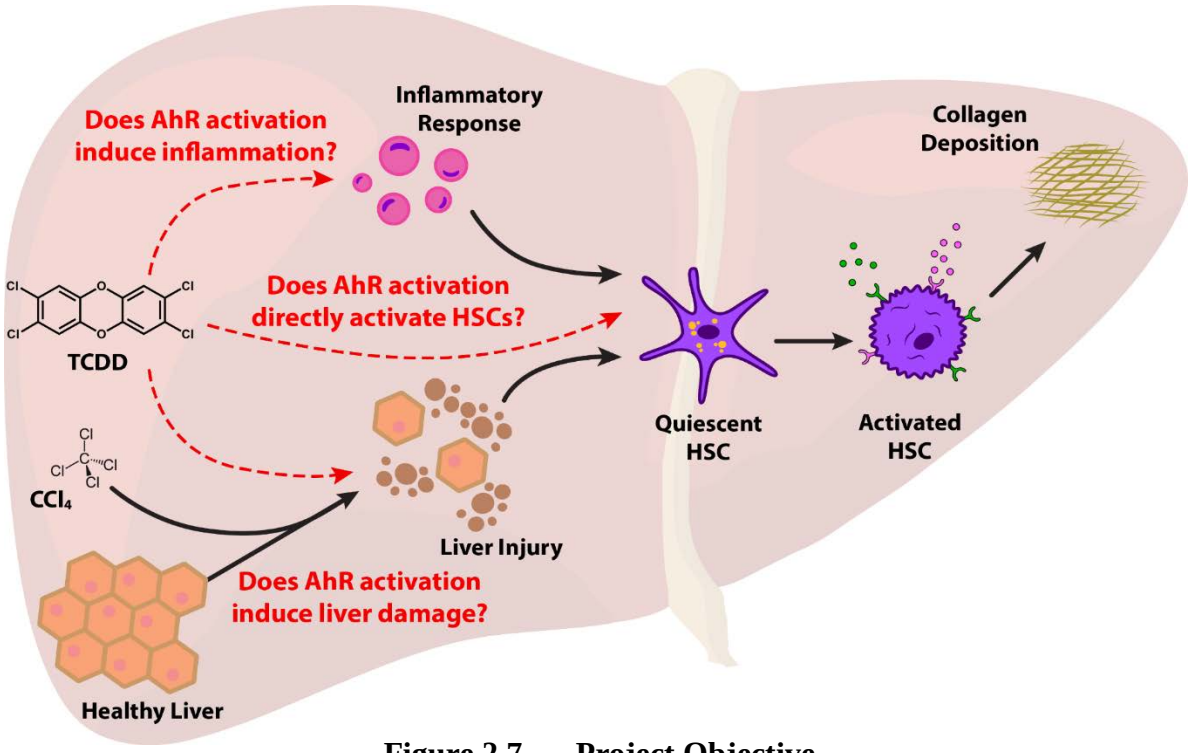

Figure 2.7 Project Objective

The goal of this project is to determine if TCDD directly targets HSCs in mice with CCl_4-induced liver injury. Alternate mechanisms were also assessed, such as the possibility that TCDD enhances liver injury induced by CCl_4, subsequently driving the activation of HSCs. Enhanced liver injury could also elicit an inflammatory response which could indirectly drive HSC activation. It is also possible that TCDD treatment directly elicits an inflammatory response, which could drive HSC activation.

References

Bertot, L. C. and Adams, L. A. (2016). The natural course of non-alcoholic fatty liver disease. *Int. J. Mol. Sci.*, 17(5).

Han, M., Liu, X., Liu, S., Su, G., Fan, X., Chen, J., Yuan, Q. and Xu, G. (2017). 2,3,7,8-Tetrachlorodibenzo-p-dioxin (TCDD) induces hepatic stellate cell (HSC) activation and liver fibrosis in C57BL6 mouse via activating Akt and NF-κB signaling pathways. *Toxicol. Lett.*, 273, pp. 10–19.

Harvey, W. A., Jurgensen, K., Pu, X., Lamb, C. L., Cornell, K. A., Clark, R. J., Klocke, C. and Mitchell, K. A. (2016). Exposure to 2,3,7,8-tetrachlorodibenzo-p-dioxin (TCDD) increases human hepatic stellate cell activation. *Toxicology.*, 344, pp. 26–33.

Ishak, K., Baptista, A., Bianchi, L., Callea, F., De Groote, J., Gudat, F., Denk, H., Desmet, V., Korb, G., MacSween, R. N. M., Phillips, M. J., Portmann, B. G., Poulsen, H., Scheuer, P. J., Schmid, M. and Thaler, H. (1995). Histological grading and staging of chronic hepatitis. *J. Hepatol.*, 22(6), pp. 696–699.

Iwaisako, K., Jiang, C., Zhang, M., Cong, M., Moore-Morris, T. J., Park, T. J., Liu, X., Xu, J., Wang, P., Paik, Y.-H., Meng, F., Asagiri, M., Murray, L. A., Hofmann, A. F., Iida, T., Glass, C. K., Brenner, D. A. and Kisseleva, T. (2014). Origin of myofibroblasts in the fibrotic liver in mice. *Proc. Natl. Acad. Sci. U.S.A.*, 111(32), pp. E3297–E3305.

Lamb, C. L., Cholico, G. N., Perkins, D. E., Fewkes, M. T., Oxford, J. T., Morrill, E. E. and Mitchell, K. A. (2016a). Aryl hydrocarbon receptor activation by TCDD modulates expression of extracellular matrix remodeling genes during experimental liver fibrosis. *BioMed Res. Int.*

Lamb, C. L., Cholico, G. N., Pu, X., Hagler, G. D., Cornell, K. A. and Mitchell, K. A. (2016b). 2,3,7,8-Tetrachlorodibenzo-p-dioxin (TCDD) increases necro-inflammation and hepatic stellate cell activation but does not exacerbate experimental liver fibrosis in mice. *Toxicol. Appl. Pharmacol.*, 311, pp. 42–51.

Maher, J. J. and McGuire, R. F. (1990). Extracellular matrix gene expression increases

preferentially in rat lipocytes and sinusoidal endothelial cells during hepatic fibrosis in vivo. *J. Clin. Invest.*, 86(5), pp. 1641–1648.

Mejia-Garcia, A., Sanchez-Ocampo, E. M., Galindo-Gomez, S., Shibayama, M., Reyes-Hernandez, O., Guzman-Leon, S., Gonzalez, F. J. and Elizondo, G. (2013). 2,3,7,8-Tetrachlorodibenzo-p-dioxin enhances CCl_4-induced hepatotoxicity in an aryl hydrocarbon receptor-dependent manner. *Xenobiotica*, 43(2), pp. 161–168.

Pellicoro, A., Ramachandran, P., Iredale, J. P. and Fallowfield, J. A. (2014). Liver fibrosis and repair: Immune regulation of wound healing in a solid organ. *Nat. Rev. Immunol.*, **14**(3), pp. 181–194.

Scholten, D., Trebicka, J., Liedtke, C. and Weiskirchen, R. (2015). The carbon tetrachloride model in mice. *Lab. Anim.*, 49, pp. 4–11.

Weber, L. W. D., Boll, M. and Stampfl, A. (2003). Hepatotoxicity and mechanism of action of haloalkanes: carbon tetrachloride as a toxicological model. *Crit. Rev. Toxicol.*, 33(2), pp. 105–136.

CHAPTER THREE

HEPATOCYTE AHR EXPRESSION IS REQUIRED FOR TCDD-INDUCED HSC ACTIVATION IN THE LIVER OF CCL_4 TREATED MICE

Abstract

The aryl hydrocarbon receptor (AhR) is a soluble, ligand-activated transcription factor that mediates the toxicity of 2,3,7,8-tetrachlorodibenzo-*p*-dioxin (TCDD). Chronic TCDD treatment has been shown to induce liver fibrosis, which is characterized by the activation of myofibroblasts, namely hepatic stellate cells (HSCs), and subsequent deposition of collagen. We previously reported that exposure to TCDD increased HSC activation during liver injury induced by chronic carbon tetrachloride (CCl_4) administration. However, it remains unclear if TCDD directly activates HSCs or if increased HSC activation results from TCDD-induced damage to parenchymal hepatocytes. The goal of this project was to determine the cell-specific consequences of TCDD treatment on HSC activation during liver fibrosis. To accomplish this, we used Cre-Lox recombination to generate male mice in which the AhR was removed from either hepatocytes or HSCs. In this study, mice were treated with 1.0 ml/kg CCl_4 every four days for 5 weeks, and TCDD (100 μg/kg) was administered during the final week. Results indicate that AhR functionality in hepatocytes is required for maximal HSC activation in CCl_4-treated mice. Likewise, TCDD treatment evoked a maximal inflammatory response in CCl_4-treated mice with a functional AhR in hepatocytes.

Additionally, TCDD treatment induced liver damage in CCl_4-treated mice only when hepatocytes possessed a functional AhR. Based on these findings, we conclude that maximum TCDD-induced HSC activation requires hepatocyte-specific AhR signaling. We further speculate that AhR-dependent events in hepatocytes increase HSC activation through a mechanism that involves increased liver damage and possibly inflammation.

Introduction

The aryl hydrocarbon receptor (AhR) is a ligand-activated transcription factor that belongs to the basic-helix-loop-helix (bHLH) Per/Arnt/Sim (PAS) superfamily of proteins (Beischlag *et al.*, 2008). As a bHLH-PAS protein, the AhR mediates gene expression for a wide array of biological functions such as developmental processes, xenobiotic metabolism and adaptation to environmental stress (Gu *et al.*, 2000; Beischlag *et al.*, 2008). In the absence of a bound ligand, the AhR localizes to the cytoplasm of a cell within a protein complex containing a p23, a XAP-molecule 2 and two heat shock protein 90 (Larigot *et al.*, 2018). However, upon binding to a ligand, the AhR translocates into the nucleus where it heterodimerizes with the aryl hydrocarbon nuclear translocator (ARNT) protein (Larigot *et al.*, 2018). This AhR/ARNT dimer then binds to the xenobiotic response element (XRE) in the promotor region of many genes to facilitate transcription (Larigot *et al.*, 2018). Alternate mechanisms of AhR activation have also been identified in which the AhR dimerizes with other transcriptional co-regulator proteins (Jackson *et al.*, 2015). It has also been shown that the AhR heterodimer complex can bind to non-XRE sites to mediate gene transcription (Huang & Elferink, 2012).

Accumulating evidence has implicated AhR signaling in mediating the progression of liver disease. For example, chronic exposure to 2,3,7,8-tetrachlorodibenzo-*p*-dioxin (TCDD), a prominent environmental contaminant and potent AhR agonist, has been shown to elicit liver fibrosis (Pierre *et al.*, 2014; Fader *et al.*, 2015). Chronic exposure of TCDD was also shown to induce steatosis and steatohepatitis (Fader *et al.*, 2015). Furthermore, in a mouse model of cholestasis induced by bile duct ligation, TCDD treatment was shown to increase hepatic bile acid and bilirubin levels, as

well as markers of liver injury, such as serum alanine aminotransferase (ALT) and aspartate aminotransferase (AST) activity (Pierre *et al.*, 2014). TCDD treatment was also shown to exacerbate steatosis in a mouse model of fatty liver induced by a high fat diet, as well as promote an increase in serum ALT and hepatic inflammatory cell infiltration (Duval *et al.*, 2017). We recently showed that the administration of TCDD elicits more pronounced markers of liver disease in a "two-hit" model where liver injury was initiated using carbon tetrachloride (CCl_4) (Lamb *et al.*, 2016b).

Administration of carbon tetrachloride (CCl_4) is a well-established model of liver injury that directly leads to the onset of liver fibrosis. In this model, CCl_4 is metabolized by cytochrome P4502E1 into a trichloromethyl radical ($CCl_3^{\bullet}$) thereby exerting oxidative stress on the liver tissue (Rechnagel & Glende, 1973). Chronic treatment of CCl_4 induces centrilobular necrosis (Bruckner *et al.*, 1986) and inflammation (Weber *et al.*, 2003) which ultimately leads to the activation of quiescent HSCs. When paired with CCl_4 treatment, administration of TCDD has been shown to increase liver injury as evidenced by increased hepatomegaly and increased serum ALT levels (Lamb *et al.*, 2016a). It was also shown that TCDD treatment exacerbated necroinflammation in the liver and elicited robust hepatic stellate cell (HSC) activation, the main hepatic cell type responsible for producing a liver fibrosis pathology (Lamb *et al.*, 2016a,b). Interestingly, despite observing an increase in liver injury, inflammation and HSC activation, exacerbated fibrosis was not observed with CCl_4/TCDD co-treatment (Lamb *et al.*, 2016b). It remains unclear what the cellular target of TCDD is, or how it increases markers of liver disease and HSC activation.

It is possible that administration of TCDD could directly activate HSCs in this liver injury model. Evidence to support this notion is that TCDD has been shown to activate human HSCs *in vitro* (Harvey *et al.*, 2016; Han *et al.*, 2017). For example, TCDD treatment was shown to increase cell proliferation (Harvey *et al.*, 2016) and αSMA expression, (Harvey *et al.*, 2016; Han *et al.*, 2017) both hallmark characteristics of activated HSCs. It stands to reason that TCDD might have a more profound effect on HSCs as the half-life of TCDD in these cells is 52 days, while the half-life in hepatocytes is 13 days (Håkansson & Hanberg, 1989). Although it is possible that TCDD acts directly on HSCs, we cannot dismiss the possibility that TCDD could activate HSCs indirectly.

Alternative mechanisms could also be responsible for eliciting HSC activation with TCDD treatment in a CCl_4-induced model of liver injury. For example, TCDD-induced hepatotoxicity such as hepatomegaly, elevated serum ALT, increased hydropic vacuolation and increased neutrophil infiltration were shown to be mediated by AhR signaling in hepatocytes (Walisser *et al.*, 2005). Because HSCs are known to become activated in response to hepatocyte apoptosis (Jiang & Török, 2013), it is possible that widespread livery injury exacerbated by TCDD is what activates HSCs. There is also some evidence to suggest that hepatocytes can produce proinflammatory chemokines in response to environmental stress which could result in increased activation of HSCs. For example, hepatocytes have been observed to release the neutrophil chemoattractant CXCL1 in response to peripheral cell necrosis (Su *et al.*, 2018). HSC activation via direct and indirect effects of TCDD in a liver injury model were assessed in this study.

In this study, we sought to identify the cellular target of TCDD and determine if markers of liver disease progression were exacerbated as a result of AhR signaling in

HSCs or hepatocytes. The objective of this study was to identify if HSC activation occurred as a direct TCDD effect, or if HSC activation occurred indirectly through increased liver injury and/or inflammation. To accomplish this, we used a Cre-lox system to create transgenic mice in which AhR functionality was knocked out of either HSCs or hepatocytes. By using Cre-recombinase under the control of a glial fibrillary acidic protein (GFAP) or albumin promotor, functionality of double-floxed AhR was ablated in HSCs and hepatocytes, respectively. Our results suggest that HSCs are not the direct cellular target of TCDD in mice. Rather TCDD-induced HSC activation occurs as a result of liver injury and inflammation mediated by AhR signaling in hepatocytes.

Materials and Methods

Generation of conditional AhR knockout mice

The following strains of mice were purchased from The Jackson Laboratory (Bar Harbor, Maine): mice that were homozygous for the floxed AhR allele ($Ahr^{fl/fl}$; strain B6.129S-$Ahr^{tm3.1Bra/J}$), mice that expressed Cre recombinase driven by the albumin gene promoter (Cre^{Alb}; strain B6.Cg-Tg(Alb-cre)21Mgn/J), and mice that expressed Cre recombinase driven by the human glial fibrillary acidic protein (GFAP) gene promoter (Cre^{GFAP}; strain FVB-Tg(GFAP-cre)25Mes/J). Male $Ahr^{fl/fl}$ mice were bred to female mice carrying either the Cre^{Alb} transgene or the Cre^{GFAP} transgene. Offspring that were heterozygous for the floxed Ahr allele and hemizygous for Cre were bred to $Ahr^{fl/fl}$ mice to produce mice with AhR-deficient hepatocytes (designated $Ahr^{\Delta Hep}$ mice) or with AhR-deficient HSCs and cholangiocytes (designated $Ahr^{\Delta HSC}$). Genotypes were determined using DNA extracted from an ear punch, and PCR was carried out according to the strain-specific genotyping protocols provided by The Jackson Laboratory. Animals were housed in a selective pathogen-free facility in a temperature- and humidity-controlled room with a 12:12 hr light-dark cycle and given ad libitum access to food and water.

Animal treatment

All animal studies were conducted with the approval of the Institutional Animal Care and Use Committee at Boise State University. Male $AhR^{\Delta Hep}$ or $AhR^{\Delta HSC}$ mice were used in experiments at 8 weeks of age. Age-matched $Ahr^{fl/fl}$ mice, which were phenotypically equivalent to wild-type mice, were used as controls. CCl_4 (Sigma-Aldrich, St. Louis, MO) was diluted 1:4 (v/v) in corn oil and administered by oral gavage (1

ml/kg) twice weekly for 5 weeks (10 treatments total; Figure 3.1). TCDD (≥98% purity; Cambridge Isotope Laboratories, Tewksbury, MA) was dissolved in anisole (1 mg/ml) and diluted in peanut oil to create a 20 µg/ml working stock. At the beginning of the fifth week, mice were gavaged with TCDD at 100 µg/kg body weight or with an equivalent volume of vehicle, which consisted of peanut oil spiked with anisole. This dose of TCDD was chosen because the mice used in these experiments expressed the d-allele of the AhR gene, which encodes an AhR protein with low ligand binding affinity (Supplementary Data, Supplementary Table 3.1; Poland et al., 1994). In order to produce TCDD toxicity, mice with this allele require a dose of TCDD that is approximately 10-fold higher than doses administered to mice with the more sensitive b-allele (Poland et al., 1994). In mice with the d-allele, 100 µg/kg of TCDD elicits classic endpoints of TCDD hepatotoxicity (Walisser et al., 2005) and is well below the LD50, which was determined to be 2,570 ug/kg (Chapman & Schiller, 1985). At the end of the fifth week (7 days after TCDD administration), mice were euthanized by isoflurane overdose followed by cervical dislocation. Blood was collected by cardiac puncture, and serum was extracted. The liver was excised and weighed. Sections from the liver were fixed in formalin buffer (PSL Equipment, Vista, CA) for paraffin-embedding or else embedded in optimal cutting temperature (OCT) compound and frozen. The remaining liver tissue was snap-frozen in liquid nitrogen and stored at -80°C until RNA was prepared.

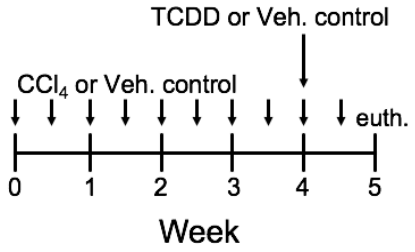

Figure 3.1 Mouse treatment schedule

Mice were gavaged 1.0 ml/kg of CCl_4 twice per week and received a single dose of 100 μg/kg TCDD during the final week of the experiment.

Alanine Aminotransferase (ALT) Activity Assay

Serum was diluted 1:10 in phosphate buffered saline (PBS). ALT content was measured using the Infinity™ ALT (GPT) Liquid Stable Reagent according to the manufacturer's protocol (Thermo Fisher Scientific, Waltham, MA). Samples were run in duplicate, and ALT content was expressed as activity in U/L.

Histological analysis

Formalin-fixed, paraffin-embedded liver tissue was cut into 5-μm sections at the Biomolecular Research Center at Boise State University. Tissue staining with hematoxylin and eosin and picrosirius red, as well as immunofluorescence staining to detect αSMA, were performed as previously described (Lamb et al., 2016b). Images were acquired using an Olympus BX45 dual-headed compound microscope, and densitometry was performed using ImageJ software (National Institute of Health, Bethesda, MD). To assess inflammation, images (100x magnification) were analyzed, and areas containing inflammatory cell nuclei were highlighted. Image J was used to quantify these areas, and the extent of inflammation was estimated based on the percent of highlighted area per total field. Five fields of view were assessed per liver sample. Liver damage was also

assessed using the Ishak modified histological activity scoring index. A pathologist from the Idaho Veterans Research and Education Foundation (IVREF) who was blinded to each treatment used picro-sirius red-stained sections to score for fibrosis (Ishak 0–6) and H&E-stained sections to score for periportal or periseptal interface hepatitis (Ishak 0–4), confluent necrosis (Ishak 0–6), focal lytic necrosis, apoptosis, and focal inflammation (Ishak 0–4) and portal inflammation (Ishak 0–4) (Ishak et al., 1995; Lamb et al., 2016b).

RNA isolation and quantitative real-time polymerase chain reaction (qPCR) analysis

Total RNA was extracted from liver tissues using an E.N.Z.A® Total RNA kit (Omega Bio-Tek, Norcross, GA), and purity was assessed by ultraviolet spectroscopy. First-strand cDNA was synthesized from 1 ug total RNA using an applied biosystems high capacity cDNA reverse transcription kit with random primers (Thermo Fisher Scientific, Waltham, MA). cDNA was quantified by qPCR using Roche FastStart Essential DNA Green Master hotstart reaction mix (Roche Diagnostics, Indianapolis, IN) with the primers listed in Table 3.1. Duplicate reactions from eight biological replicates per treatment group were amplified on a LightCycler® 96 thermocycler (Roche). Expression of mRNA for each target gene was normalized against *Gapdh*, and differences in gene expression were calculated using the $2^{-\Delta\Delta Ct}$ method (Livak et al., 2001).

Table 3.1 Primer Sequences

Gene	Primer sequence (5′ to 3′)	Annealing Temp. (°C)
$Ahr^{tm3.1Bra}$	GGT ACA AGT GCA CAT GCC TGC CAG TGG GAA TAA GGC AAG AGT GA	60
Alb (WT)	TGC AAA CAT CAC ATG CAC AC TTG GCC CCT TAC CAT AAC TG	60
Alb-Cre	GAA GCA GAA GCT TAG GAA GAT GG TTG GCC CCT TAC CAT AAC TG	60
αSMA	TCC TCC CTG GAG AAG AGC TAC TAT AGG TGG TTT CGT GGA TGC	60
Col1a1	GTC CCT GAA GTC AGC TGC ATA TGG GAC AGT CCA GTT CTT CAT	60
Col3a1	CCT GGT GGA AAG GGT GAA AT CGT GTT CCG GGT ATA CCA TTA G	62
Cyp1a1	GCC TTC ATT CTG GAG ACC TTC C CAA TGG TCT CTC CGA TGC	60
Cyp1b1	TGG CCT AAC CCA GAG GAC TT ATT GCA CTG ATG AGC GAG GA	60
Gapdh	CAA TGA CCC CTT CAT TGA CC GAT CTC GCT CCT GGA AGA TG	60
Ccl2	ACT GAA GCC AGC TCT CTC TTC CTC TTC CTT CTT GGG GTC AGC ACA GAC	60
Tgfb1	TGC TAA TGG TGG ACC GCA A CAC TGC TTC CCG AAT GTC TGA	55
Tgfb2	TGA GCC ACC AGA AGA ACA CG GCA GAT CCT GAG CAA GCT G	54

Quantification of hydroxyproline by LC/MS

Frozen liver tissue (10 mg) was homogenized in 100 µl reagent-grade water and hydrolyzed with 100 µl of 12 M HCl at 95°C for 20 hr. Debris was removed from hydrolyzed samples using Phree® phospholipid removal columns (Phenomex, Torrance, CA) (Lamb et al., 2016b). Linear calibration curves were created by spiking control samples with known concentrations of trans-4-hydroxy-L-proline (Sigma-Aldrich). Hydroxyproline levels were then analyzed by LC-MS as previously described (Lamb et al., 2016b) at the Biomolecular Research Center at Boise State University.

Hyaluronan binding protein (HABP) assay

Formalin-fixed, paraffin-embedded liver tissue was cut into 5-µm sections and rehydrated in CitroSolv™ Hybrid Solvent and Clearing Agent (Decon Labs, Inc., King of Prussia, PA) followed by immersion in a graded series of ethanol solutions, running water, and PBS. Endogenous biotin, biotin receptors, and avidin-binding sites were blocked with a commercially available kit (Vector Laboratories, Burlingame, CA), and tissues were incubated with normal goat serum (150 µl/10ml) in PBS for 20 min. Sections were then incubated with biotinylated-HABP (MilliporeSigma, Burlington, MA) at a 1:100 dilution in normal goat serum for 1 h at room temperature. After washing with PBS 4 times, the signal was amplified using VECTASTAIN® ABC reagent (Vector Laboratories) for 30 minutes. After 4 additional PBS washes, a second amplification step was performed using a 1:400 dilution of a TSA® fluorescein reagent (Perkin Elmer, Waltham, MA) for 5 min. Sections were then washed in PBS, and nuclei were counterstained with VECTASHIELD® mounting medium with DAPI (Vector Laboratories). Images of each liver were taken at 100x magnification using an Olympus BX51 fluorescence microscope with an Olympus BH2RFLT3 burner and an Olympus DP71 camera operated by DP Controller software (Olympus, Waltham, MA). ImageJ was used to quantify the area of fluorescence from three fields on each slide.

In situ zymography

Frozen, OCT-embedded liver tissue was cut into 7-µm thick sections, adhered to glass slides, and stored at -80°C for 18 h. Slides were then treated with developing buffer (100 mM Tris, pH 7.4, 100 mM NaCl, 5 mM CaCl2, 0.05% Brij® 35, 1 mM

phenylmethylsulfonyl fluoride (PMSF), and 0.1 mg/mL of gelatin conjugated to Oregon Green® 488 dye (Thermo Fisher). Serial sections were incubated in developing buffer containing 50 mM EDTA to inhibit calcium-dependent zinc-containing endopeptidase (matrix metalloproteinase) activity. Slides were then incubated in a humid chamber at 37°C for 22 hours, then rinsed three times in water. VECTASHIELD® with DAPI was applied to the slides. Images were taken at 100x magnification on an Olympus BX51 microscope. ImageJ was used to quantify the area of fluorescence from 5 fields from each slide.

Western Blotting

Liver tissue was homogenized as previously described (Lamb et al., 2016b). Protein concentration was determined, and 25 µg of protein from each sample was resolved on an 8% SDS-polyacrylamide gel and transferred to a polyvinylidene difluoride membrane. Membranes were incubated with anti-CYP1A1 or anti-GAPDH antibodies and species-specific, horseradish peroxidase-conjugated secondary antibodies (Santa Cruz Biotechnology, Dallas, TX). Bands were visualized using an enhanced chemiluminescent reagent (Thermo Fisher).

Statistical Analysis

Statistical analysis was performed using GraphPad Prism 7.0d (GraphPad Software, La Jolla, CA). Mean values were compared among genetic backgrounds and treatment using a two-way ANOVA and Bonferroni post hoc test. Differences were

considered significant when p values were ≤ 0.05. Unless otherwise stated, error bars on graphs represent standard error of the mean (SEM).

Results

To ensure that AhR-ablation had occurred in $AhR^{\Delta Hep}$ mice, we measured gene expression levels of the hallmark markers for AhR activation, *Cyp1a1* and *Cyp1b1* (Figure 3.2A, B). In $AhR^{fl/fl}$ mice, where TCDD was used to activate AhR, mRNA levels of *Cyp1a1* exceeded a minimum of 200-fold when compared to the vehicle treated mice. Similarly, $AhR^{fl/fl}$ mice treated with TCDD showed a minimum of 100-fold increase of *Cyp1b1* gene expression when compared to the vehicle treated mice. However, in $AhR^{\Delta Hep}$ mice where hepatocyte-specific AhR-ablation should have occurred, TCDD increased *Cyp1a1* and *Cyp1b1* mRNA levels by only 20-fold and 10-fold, respectively. The slight induction of *Cyp1a1* and *Cyp1b1* mRNA expression in $AhR^{\Delta Hep}$ mice can likely be attributed to AhR activation in non-parenchymal liver cells, such as HSCs, cholangiocytes, Kupffer cells and endothelial cells. Protein expression of *Cyp1a1* were verified by Western blot (Figure 3.2 C, D). Similar to the mRNA expression, cytochrome P4501A1 protein levels induced by TCDD in $AhR^{fl/fl}$ mice and markedly decreased in TCDD-treated $AhR^{\Delta Hep}$ mice. These results indicate that $AhR^{\Delta Hep}$ mice have decreased responsiveness to TCDD, as has been previously reported (Walisser *et al.*, 2005).

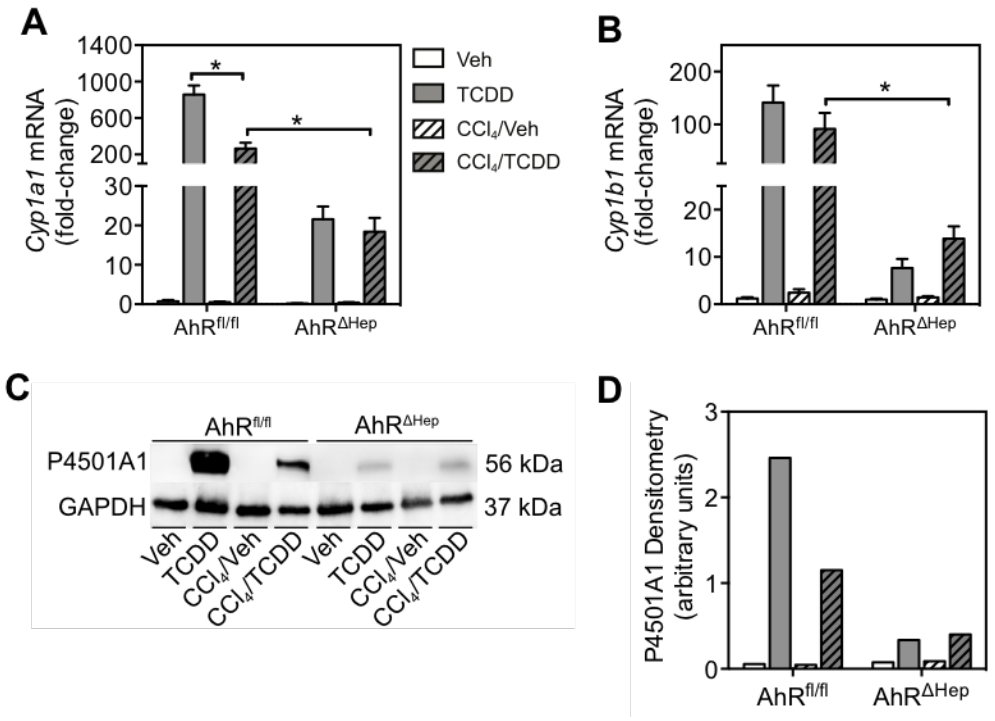

Figure 3.2 AhR activation is decreased in AhR$^{\Delta Hep}$ mice

TCDD-induced expression of *Cyp1a1* (A) and *Cyp1b1* (B) was used as an indicator of AhR activation in response to TCDD. Bars represent mean ± SEM (n=8). Asterisks (*) denote a significant difference ($p < 0.05$). Cytochrome P4501A1 protein expression levels were measured by Western blot (C) and quantified by pixel densitometry (D). Results are representative of three replicate assays.

We then sought to investigate how TCDD treatment impacted liver damage in mice treated with CCl_4. Gross hepatotoxicity was evaluated based on hepatomegaly, serum ALT, and confluent necrosis. The livers of CCl_4/TCDD-treated AhR$^{fl/fl}$ mice exhibited significant hepatomegaly when compared to CCl_4/Veh AhR$^{fl/fl}$ mice (Figure 3.3A). CCl_4/TCDD-treated AhR$^{\Delta Hep}$ mice showed no indication of hepatomegaly. Hepatocellular necrosis was measured based on serum ALT (Figure 3.3B). Treatment with CCl_4 or TCDD did not impact serum ALT levels. However, TCDD administration to CCl_4-treated AhR$^{fl/fl}$ mice significantly increased serum ALT levels. This increase in

serum ALT levels was completely absent in co-treated $AhR^{\Delta Hep}$ mice. Finally, we assessed mRNA expression for *Cyp2e1*, the gene encoding cytochrome P450 2E1 (Figure 3.3C). Cytochrome P450 2E1 metabolizes CCl_4 into $CCl_3^{\bullet}$, which induces liver injury through lipid peroxidation. Expression of *Cyp2e1* decreased in mice treated with CCl_4/Veh and co-treated with CCl_4/TCDD.

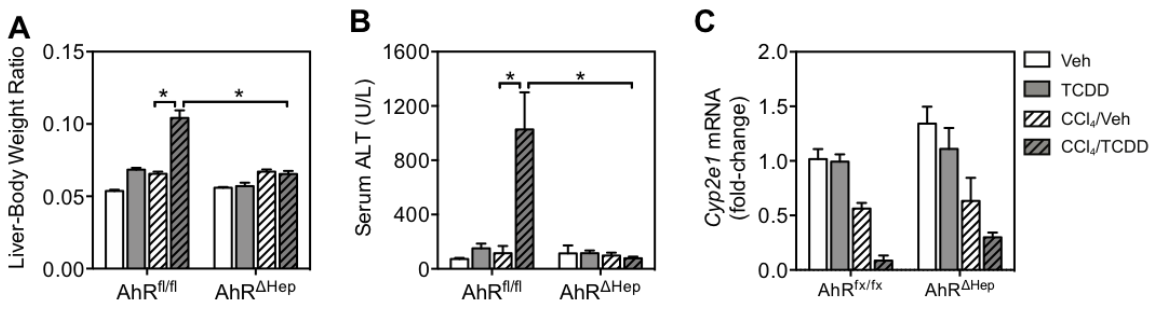

Figure 3.3 Hepatotoxic effects of TCDD in a CCl_4 liver injury model are absent in $AhR^{\Delta Hep}$ mice

Hepatotoxicity was assessed based on (A) liver-to-body weight ratios and (B) serum ALT levels. (C) *Cyp2e1* mRNA levels were measured using qRT-PCR. Bars represent mean ± SEM for mice (n=8). Asterisks (*) denote a significant difference ($p < 0.05$).

We determined to what extent hepatic inflammation impacted myofibroblast activation (Figure 3.4). Results indicate that treating mice with CCl_4/Veh elicited no significant hepatic inflammatory response, while TCDD treatment a minor inflammatory effect. However, CCl_4/TCDD treatment in $AhR^{fl/fl}$ mice, which possess hepatocytes with a functional AhR, elicited a robust inflammatory response (Figure 3.4A, B). A significant decrease in inflammation was observed in co-treated $AhR^{\Delta Hep}$ mice when compared to $AhR^{fl/fl}$ mice. The same trend was observed when assessing necroinflammation (Figure 3.4C). Necroinflammation was prominent in the CCl_4/TCDD-treated $AhR^{fl/fl}$ mice when compared against the CCl_4/Veh counterparts. When comparing co-treated $AhR^{\Delta Hep}$ mice

against the co-treated $AhR^{fl/fl}$ mice, we observed a significant decrease of necroinflammation in the $AhR^{\Delta Hep}$ mice. We looked at gene expression for monocyte chemoattractant protein 1 (*Ccl2*) and discovered that $AhR^{fl/fl}$ mice treated with CCl_4/TCDD expressed this gene in high abundance when compared against any other treatment group (Figure 3.4D). $AhR^{\Delta Hep}$ mice that underwent CCl_4/TCDD co-treatment showed practically no increase in *Ccl2* expression when compared against the other treatment groups in this genotype. TCDD increased the expression of the macrophage marker CD68 in $AhR^{fl/fl}$ mice but not in the $AhR^{\Delta Hep}$ mice. (Figure 3.4E).

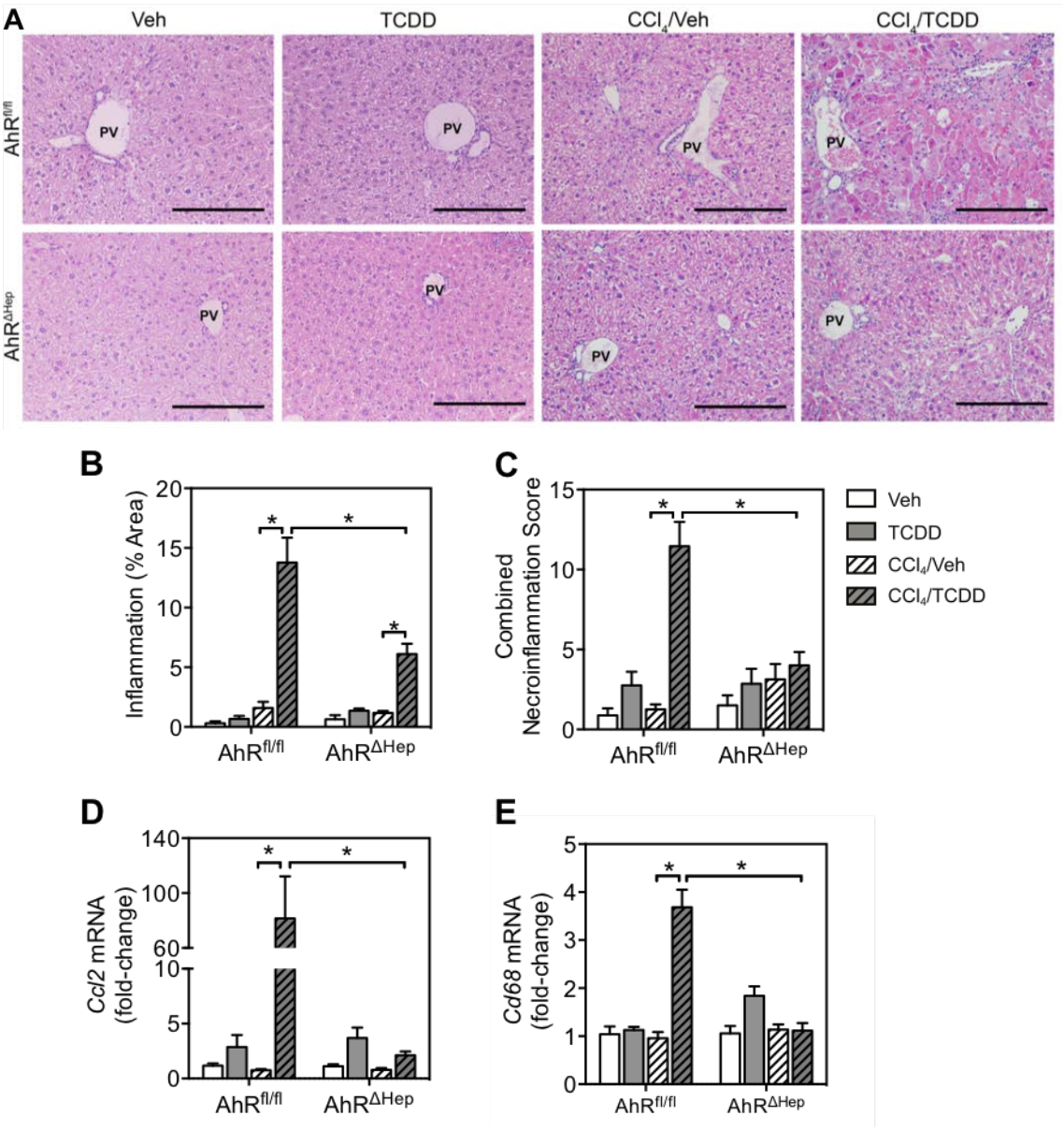

Figure 3.4 Hepatocyte-specific AhR ablation alleviates some of the inflammatory effects of TCDD

(A) H&E-stained liver tissue reveals the presence of inflammatory cells (200X magnification). Portal vein (PV) is labeled in each frame. Scale bars represent 250 μm. (B) Inflammation was quantified by selecting areas with inflammatory cells and expressing this as a function of percent area. Eight mice were assessed per treatment group and five fields were assessed per mouse. (C) A clinical pathologist scored tissue for necroinflammation using the modified Ishak scoring method. (D/E) Gene expression of the inflammatory chemoattractant CCL2 and macrophage marker CD68 was quantified using qRT-PCR. Bars represent mean ± SEM for mice (n=8). Asterisks (*) denote a significant difference ($p < 0.05$).

αSMA protein levels were assessed using immunofluorescence staining as a marker of HSC activation (Figure 3.5A, B). Results indicate that CCl_4/Veh and TCDD-alone did not elicit a robust HSC activation in either mouse genotype. In co-treated $AhR^{fl/fl}$ mice, HSC activation increased significantly compared to mice treated with CCl_4. However, in co-treated $AhR^{\Delta Hep}$ mice, only a slight increase in HSC activation was observed compared to mice treated with CCl_4. This could, in part, be due to the decreased inflammation seen in this group of mice to begin with. Markers of HSC activation were assessed using qRT-PCR (Figure 3.5C-E). Results from mRNA expression levels of αSMA were similar those of αSMA protein levels in immunofluorescence staining. We looked at mRNA expression of *Col1a1* and *Col3a1*, the major components of collagen type I and collagen type III, respectively. The expression levels of these genes were similar to those of αSMA, showing a rise in expression for co-treated $AhR^{fl/fl}$ mice, but not a significant increase for $AhR^{\Delta Hep}$ mice. These results indicate that HSC activation could be, at least partially, an indirect consequence mediated by AhR signaling in hepatocytes.

Activated HSCs are also known produce the ECM component hyaluronan (Vrochides *et al.*, 1996). Co-treated $AhR^{fl/fl}$ mice showed a marked increase in hyaluronan distribution throughout the liver (Figure 3.5). Results indicate that hyaluronan distribution shows a similar trend as HSC activation further validating that TCDD fails to elicit robust HSC activation if AhR is knocked out of hepatocytes. These results suggest that the AhR in hepatocytes is required for maximal response upon co-treatment.

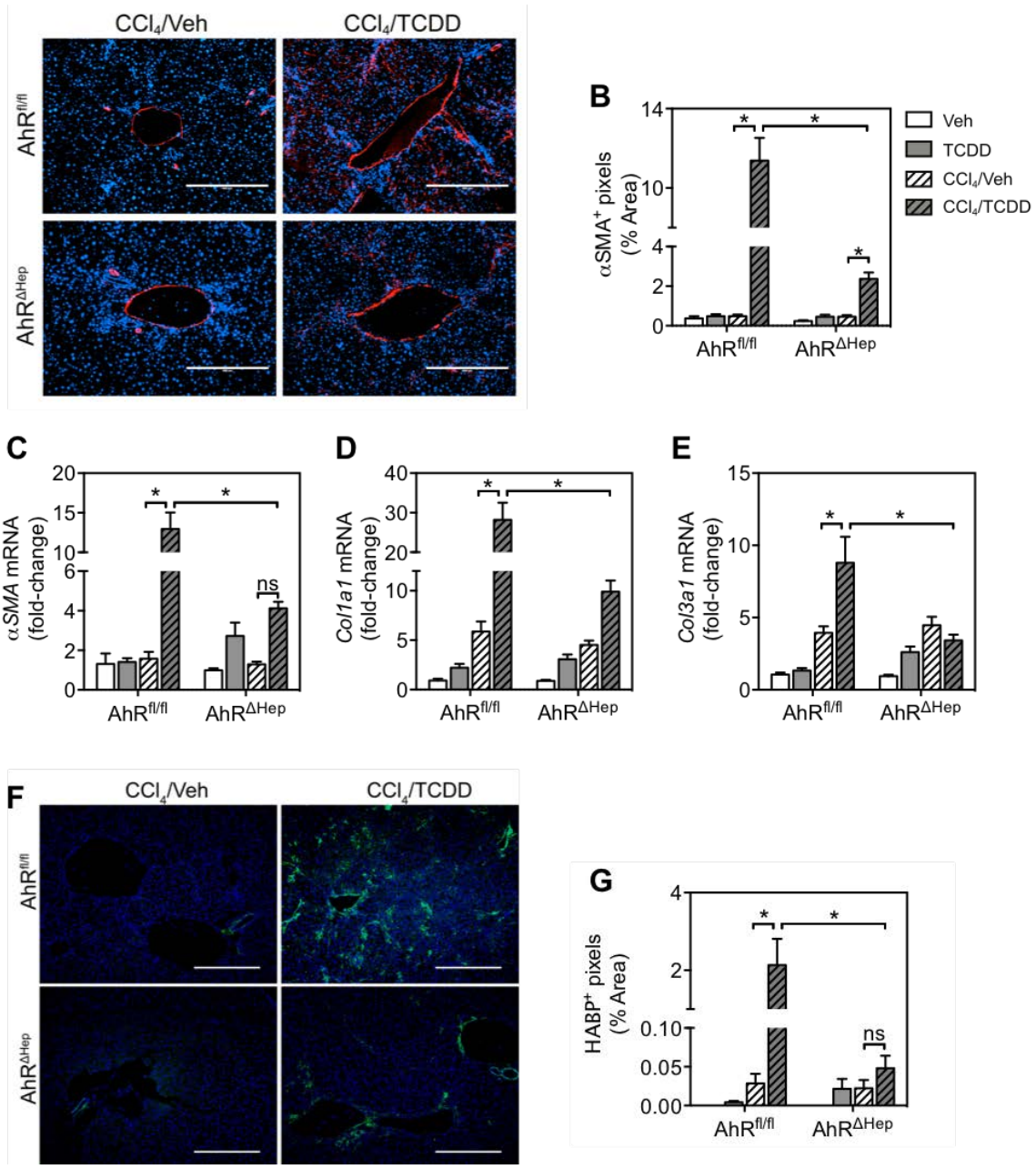

Figure 3.5 AhR signaling in hepatocytes is required for maximal HSC activation induced by TCDD

(A) Immunofluorescence staining was used to measure αSMA expression (red), which is a hallmark of HSC activation (100X magnification). Cell nuclei were counterstained with DAPI (blue). Scale bars represent 500 μm. (B) Pixel densitometry for αSMA immunofluorescence staining was assessed as percent of total fluorescence per field. Eight mice were assessed per treatment group and five fields were assessed per mouse. (C-E) mRNA levels of HSC activation markers in the mouse liver were measured by qRT-PCR. Bars represent mean ± SEM for mice (n=8). Asterisks (*) denote a significant difference ($p < 0.05$). (F) Immunofluorescence staining was conducted for HABP (green) to assess hyaluronic acid (100X magnification). Cell nuclei were counterstained with DAPI (blue). Scale bars represent 500 μm. (G) Pixel densitometry for HABP immunofluorescence staining was assessed as percent of total fluorescence per field. Four mice were assessed per treatment group and three fields were assessed per mouse. Bars represent mean ± SEM for mice (n=3). Asterisks (*) denote a significant difference ($p < 0.05$).

Despite all of these previous differences between the two genotypes, no overt differences were seen in levels of fibrosis (Figure 3.6A). Densitometry quantifying Sirius red histological staining showed a slight increase in collagen deposition between CCl_4/Veh and CCl_4/TCDD-treated in both genotypes of mice (Figure 3.6B). Hepatic hydroxyproline content demonstrated a similar trend, with mice that were co-treated with CCl_4/TCDD exhibiting an increase in hydroxyproline content when compared against the CCl_4/Veh group in the respective genotype (Figure 3.6C). Histological scoring also determined that fibrosis was similar between both co-treated genotypes of mice (Figure 3.6D). Assessment of gene expression for the pro-fibrotic markers *TFGβ1* and *TGFβ2*, indicated that co-treated $AhR^{fl/fl}$ mice showed a slight increase in expression when compared against the CCl_4/Veh-treated group in this genotype (Figure 3.6E, F). Gene expression did not increase for *TFGβ1* and *TGFβ2* in the $AhR^{\Delta Hep}$ mice. Taken together, all analyses indicated the same degree of fibrosis to be present in $AhR^{\Delta Hep}$ and $AhR^{fl/fl}$ mice.

Gelatinase activity was assessed to characterize ECM turnover (Figure 3.7). Our results suggest that TCDD treatment elicited slight gelatinase activity in both genotypes. Co-treatment of CCl_4/TCDD in the $AhR^{fl/fl}$ mice elicited widespread gelatinase activity throughout the entire liver. A minimal increase of gelatinase activity was observed in co-treated $AhR^{\Delta Hep}$ mice.

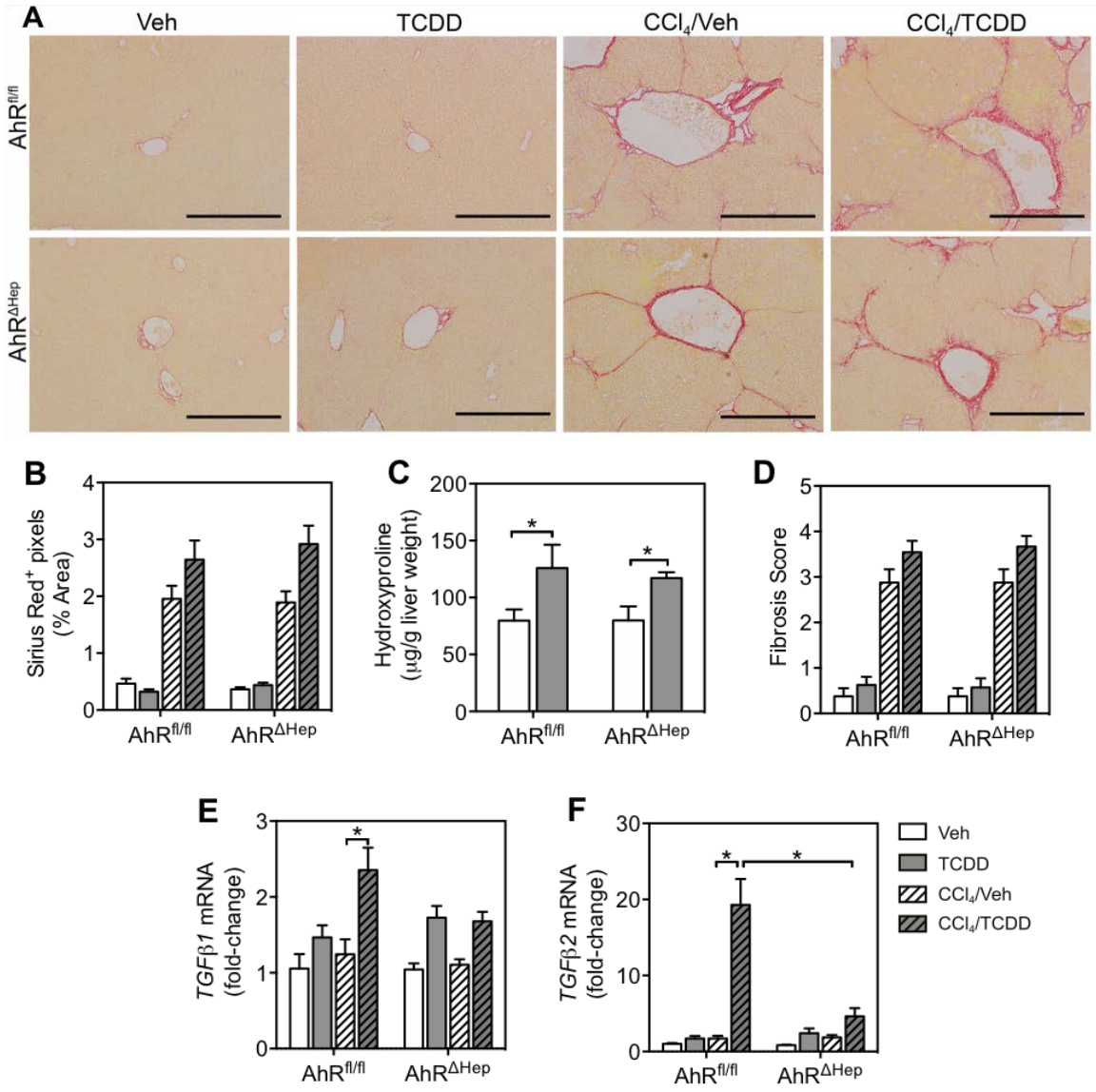

Figure 3.6 AhR signaling in hepatocytes has no overt impact on fibrosis induced by TCDD treatment

(A) Sirius Red staining was used to visualize collagen deposition in paraffin-embedded liver sections (100X magnification). Scale bars represent 500μm. (B) Densitometry was performed to quantify the amount of Sirius red staining present in each treatment group and was expressed as percent of total staining per field. Eight mice were assessed per treatment group and five fields were assessed per mouse. (C) Collagen content in each treatment group was further quantified by measuring the amount of hydroxyproline using tandem mass spectrometry. Five mice assessed for hydroxyproline content of the liver. (D) Sirius-red-stained liver tissue was scored according to the Ishak Modified Histological Activity Index. (E, F) mRNA levels of TGFβ1 and TGFβ2, both pro-fibrogenic growth factors, were assessed by qRT-PCR Bars represent mean ± SEM for mice (n=8). Asterisks (*) denote a significant difference ($p < 0.05$).

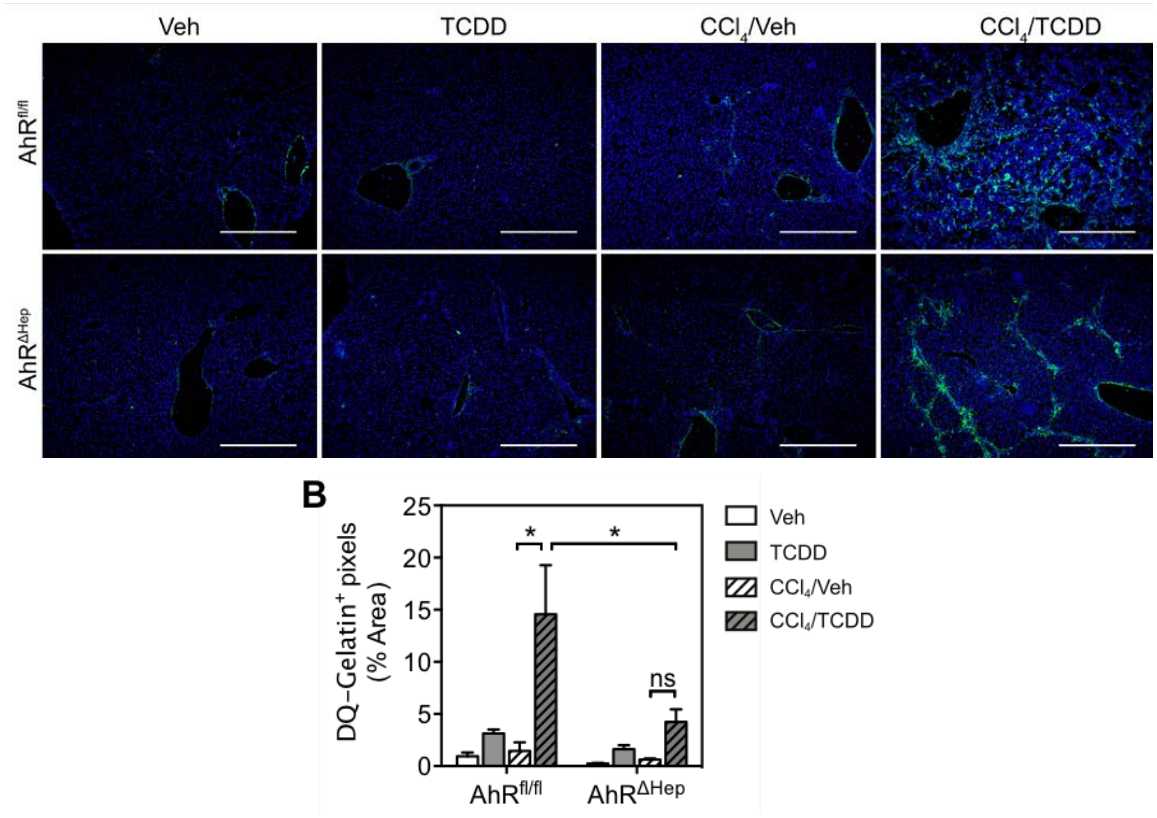

Figure 3.7 Gelatinase activity is diminished in mice lacking functional AhR in hepatocytes

(A) Gelatinase activity was assessed with DQ-Gelatin (green); 100X magnification. Cell nuclei were counterstained with DAPI (blue). Scale bars represent 500µm. (B) Pixel densitometry for DQ-Gelatin immunofluorescence staining was assessed as a percent of total fluorescence per field. Three mice were assessed per treatment group and five fields were assessed per mouse. Bars represent mean ± SEM for mice (n=8). Asterisks (*) denote a significant difference ($p < 0.05$).

AhR signaling was also assessed in mice lacking a functional AhR in HSCs (Figure 3.8). ALT levels in $AhR^{\Delta HSC}$ mice followed a similar trend as their $AhR^{fl/fl}$ counterparts, depicting only an increase of serum ALT upon co-treatment (Figure 3.8A). AhR activation was verified by measuring *Cyp1a1* mRNA expression (Figure 3.8B).

Knocking out the AhR from HSCs had a marginal effect on overall *Cyp1a1* transcription, as both $AhR^{\Delta HSC}$ and $AhR^{fl/fl}$ mice demonstrated similar expression levels amongst TCDD and CCl_4/TCDD treatment groups. When then assessed how AhR ablation in HSCs would contribute to liver inflammation (Figure 3.8C). Histopathological densitometry assessment indicated that only significant increases in inflammatory cell infiltration were similar in both genotypes of co-treated mice (Figure 3.8D). HSC activation was assessed by αSMA immunofluorescence staining (Figure 3.8E). We observed similar trends for αSMA content in the livers of $AhR^{\Delta HSC}$ and $AhR^{fl/fl}$ mice (Figure 3.8F). Only co-treated groups elicited markedly increased αSMA deposition through the liver. Lastly, we assessed if knocking out the AhR from HSCs alleviated fibrosis in the liver by staining histological slides with picro-sirius red (Figure 3.8G). Staining was quantified by densitometry (Figure 3.8H). We observed similar levels of picro-sirius red staining amongst all treatment groups that had undergone CCl_4/Veh and CCl_4/TCDD treatment.

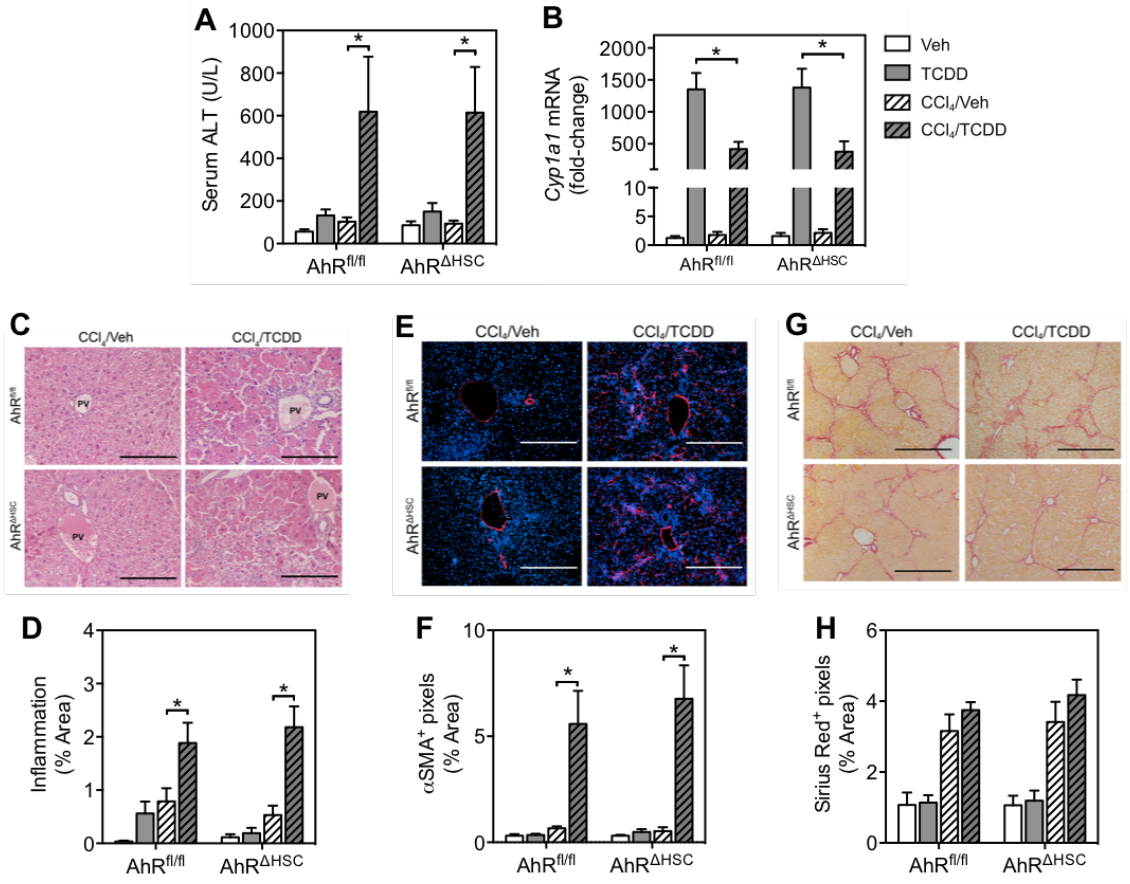

Figure 3.8 Knocking out AhR functionality from HSCs produces similar pathology to control mice.

(A) Hepatotoxicity was assessed using serum ALT. (B) AhR activation was verified by quantifying gene expression levels of *Cyp1a1*. (C) Inflammation was assessed using H&E staining (200X magnification). Scale bars represent 250 µm. (D) Inflammation was quantified using inflammatory cell densitometry denoted as percent area per frame. Eight mice were assessed per treatment group and five fields were assessed per mouse. (E) HSC activation was assessed using immunofluorescence staining to visualized αSMA (red); 100X magnification. Cell nuclei were counterstained with DAPI. Scale bars represent 500 µm. (F) Densitometry was used to quantify αSMA percent area per frame. Eight mice were assessed per treatment group and five fields were assessed per mouse. (G) Sirius red histological staining was used to visualize collagen deposition (100X magnification). Scale bars represent 500 µm. (H) Sirius red was quantified by densitometry. Staining is expressed as percent area per frame. Eight mice were assessed per treatment group and five fields were assessed per mouse. Bars represent mean ± SEM for mice (n=8). Asterisks (*) denote a significant difference ($p < 0.05$).

Discussion

The CDC reports that as of 2017, 4.5 million Americans suffer from chronic liver disease or cirrhosis. As the 12th leading cause of death in the United States, not only do chronic liver disease and cirrhosis have a major impact on human health, but they also cause a major economic burden on the American healthcare system. Treating liver fibrosis before it progresses into cirrhosis is crucial for a patient's health because fibrosis is generally regarded to be reversible, while cirrhosis is not. Fibrosis in the liver is mediated by HSCs, which are cells that remodel the ECM of the tissue in response to injury and inflammation. There is some evidence to suggest that activation of the AhR can regulate HSC activation (Yan *et al.*, 2019). A common method of activating the AhR experimentally is through TCDD administration. Furthermore, there is some evidence to suggest that TCDD treatment can modulate the activation of HSCs, however, it is unclear whether this happens through a direct mechanism, or if indirect processes such as necrosis and inflammation play a major role (Harvey *et al.*, 2016; Lamb *et al.*, 2016b; Han *et al.*, 2017.) Understanding the role AhR plays in mediating HSC activation is crucial because if HSC activation can be reversed, then liver fibrosis will not progress into cirrhosis.

In this study, we determined that AhR signaling in hepatocytes plays a role in mediating HSC activation with TCDD treatment. We discovered that for maximal HSC activation to occur in response to TCDD treatment, the AhR must be present in hepatocytes in our liver injury model. However, removal of the AhR from hepatocytes does not completely abolish HSC activation in an injured liver with TCDD treatment. In fact, HSC activation is still present, albeit very minimal, indicating that activation of

these cells must occur through multiple mechanisms. Interestingly, similar levels of liver fibrosis were observed despite seeing different levels of HSC activation upon CCl_4/TCDD co-treatment with the AhR either present or absent in hepatocytes. It is unclear why differences in HSC activation elicit a similar fibrogenic response. It is possible that increased gelatinase activity prevents a more robust fibrotic response in co-treated $AhR^{fl/fl}$ mice. Furthermore, the source of these gelatinase could be from inflammatory cells, which are known to release gelatinases and collagenases thereby having a major impact on ECM remodeling (Fallowfield *et al.*, 2007; Ramachandran *et al.*, 2012).

Our study also demonstrated that hepatoxic effects of TCDD must be mediated by hepatocytes. A previous study found similar results by showing that TCDD elicited almost no hepatotoxic effects in mice when the AhR was knocked out of hepatocytes (Walisser *et al.*, 2005). In that study, ALT levels were assessed from serum, and liver-to-body weight ratios were calculated. In both metrics, only wild-type strain of mice that had undergone TCDD treatment showed elevated markers of hepatoxicity. Our study demonstrated similar effects upon only treating with TCDD. However, mice that underwent co-treatment showed an even more remarkable trend. $AhR^{fl/fl}$ mice showed exponentially greater levels of serum ALT than compared against their $AhR^{\Delta Hep}$ mice counterparts. Similarly, $AhR^{fl/fl}$ mice that underwent co-treatment showed significantly higher liver-to-body weight ratios than their $AhR^{\Delta Hep}$ mice counterparts. These findings are interesting because they highlight a major role for AhR activation in exacerbating liver injury. It stands to reason that the hepatotoxic effects of TCDD in a liver injury model system are what drive HSCs to maximal activation. However, it also possible that

the observed hepatotoxic effects elicited a secondary response – such as inflammation – which ultimately mediated HSC activation.

Although liver injury can lead to HSC activation, inflammation is also known to modulate HSC activity (Tsuchida & Friedman, 2017). Our results suggest that inflammation could be a driving force for HSC activation. In this study, inflammatory markers were present in higher abundance in $AhR^{fl/fl}$ co-treated mice than in $AhR^{\Delta Hep}$ counterparts. It is possible that higher levels of inflammation were a driving factor leading to higher levels of HSC activation. These $AhR^{\Delta Hep}$ co-treated mice that demonstrated significantly reduced levels of inflammation also demonstrated reduced levels of HSC activation. This raises the possibility that HSC activation levels which were still present in $AhR^{\Delta Hep}$ co-treated mice were the direct result induced by the inflammation. The inflammation seen during liver injury could be a direct result of TCDD treatment, as TCDD is known to promote the induction of proinflammatory cytokines (Vogel *et al.*, 2007; Han *et al.*, 2017). On the other hand, it is possible that these reduced levels of inflammation in the $AhR^{\Delta Hep}$ co-treated mice are in response to the activated HSCs. Given that there is some evidence to suggest that HSCs can regulate hepatic inflammation, (Harvey *et al.*, 2013; Fujita & Narumiya, 2016; Fujita *et al.*, 2016) it stands to reason that the inflammation seen in these livers is secondary to HSC activation, and not vice-versa.

Taken together, our research demonstrates that there are multiple mechanisms for which TCDD elicits a robust HSC activation response in a liver injury model. We cannot rule out any direct effects TCDD might have on HSCs. Several studies have shown TCDD promotes HSC activation *in vitro* (Harvey *et al.*, 2016; Han *et al.*, 2017). Our data

shows that TCDD treatment in our $AhR^{\Delta Hep}$ mice elicits slight gene expression of *Cyp1a1* and *Cyp1b1*. This response must be attributed to other non-parenchymal cells in the liver still possessing a functional AhR. AhR signaling through these other cell types could play a role in mediating HSC activation. This includes AhR signaling within HSCs. It stands to reason that TCDD might have a more profound effect on HSCs as the half-life of TCDD in these cells is 52 days, while the half-life in hepatocytes is 13 days (Håkansson & Hanberg, 1989).

In conclusion, results from this study highlight a major role for hepatocyte-specific AhR signaling in mediating several pathologies associated with liver disease. TCDD-mediated liver toxicity and inflammation are heavily dependent on there being a functional AhR in hepatocytes. Furthermore, TCDD appears to elicit HSC activation through multiple mechanisms. However, differences in HSC activation do not necessarily elicit differences in the severity of fibrosis using a CCl_4/TCDD model. It appears that although AhR signaling in hepatocytes significantly impacts the severity of liver damage, inflammation and HSC activation, fibrosis levels remain consistent. This in part could be as a result of a more aggressive ECM remodeling. Future studies are needed to characterize how AhR signaling in hepatocytes directly affects these ECM remodeling events.

Acknowledgements

This work was supported by NIH Grant Nos. P20GM103408 and P20GM109095, National Science Foundation Grant Nos. 0619793 and 0923535; the MJ Murdock Charitable Trust; and the Idaho State Board of Education; the Society of Toxicology Diversity Initiatives Grant; and a seed grant from the ID-INBRE bioinformatics core.

Supplementary Data

AhR allele identification in $AhR^{\Delta Hep}$, and $AhR^{fl/fl}$ mice:

Whole DNA was isolated. The part of exon 11 containing the point mutation that distinguishes between the d and b allele was amplified using PCR (FWD: CGAAAGACTTAGCCATGAGC, RVS: GAAGTTACTGAGCAGGGAACC). The cleaned PCR products were quantified using the Qubit 2.0 Fluorometer. PCR products were prepared for sequencing using the BigDye® Terminator v3.1 Cycle Sequencing Kit (Applied Biosystems, Cat# 4337455) and sequenced on an Applied Biosystems 3130xl Genetic Analyzer with a 3130x*l*/3100 Genetic Analyzer 16-Capillary Array, 50 cm; sequencing basecalls were determined by Sequence Analysis Software v6.0 using the default analysis settings.

Supplementary Table 3.1 Genotype of AhR allele expressed in mice

Genotype	Exon 11 Sequence	Type of allele
$AhR^{fl/fl}$	GTGCAGAGTCGA	Ahr^{d-1} allele
$AhR^{\Delta Hep}$	GTGCAGAGTCGA	Ahr^{d-1} allele
$AhR^{\Delta HSC}$	GTGCAGAGTCGA	Ahr^{d-1} allele

References

Beischlag, T. V., Morales, J. L., Hollingshead, B. D. and Perdew, G. H. (2008). The aryl hydrocarbon receptor complex and the control of gene expression. *Crit. Rev. Eukaryot. Gene Expr.*, **18**(3), pp. 207–250.

Bruckner, J. V., Mackenzie, W. F., Muralidhara, S., Luthra, R., Kyle, G. M. and Acosta, D. (1986). Oral toxicity of carbon tetrachioride: Acute, subacute, and subchronic studies in rats. *Toxicol. Sci.*, **6**(1), pp. 16–34.

Chapman, D. E. and Schiller, C. M. (1985). Dose-related effects of 2,3,7,8-tetrachlorodibenzo-p-dioxin in C57BL/6J and DBA/2J mice. *Toxicol. Appl. Pharmacol.*, **78**(1), pp. 147–157.

Duval, C., Teixeira-Clerc, F., Leblanc, A. F., Touch, S., Emond, C., Guerre-Millo, M., Lotersztajn, S., Robert Barouki, Aggerbeck, M. and Coumoul, and X. (2017). Chronic exposure to low doses of dioxin promotes liver fibrosis development in the C57BL/6J diet-induced obesity mouse model. *Environ. Health Perspect.*, **125**(3), pp. 428–436.

Fader, K. A., Nault, R., Ammendolia, D. A., Harkema, J. R., Williams, K. J., Crawford, R. B., Kaminski, N. E., Potter, D., Sharratt, B. and Zacharewski, T. R. (2015). 2,3,7,8-tetrachlorodibenzo-p-dioxin alters lipid metabolism and depletes immune cell populations in the jejunum of C57BL/6 mice. *Toxicol. Sci.*, **148**(2), pp. 567–580.

Fallowfield, J. A., Mizuno, M., Kendall, T. J., Constandinou, C. M., Benyon, R. C., Duffield, J. S. and Iredale, J. P. (2007). Scar-associated macrophages are a major source of hepatic matrix metalloproteinase-13 and facilitate the resolution of murine hepatic fibrosis. *J. Immunol.*, **178**(8), pp. 5288–5295.

Fujita, T. and Narumiya, S. (2016). Roles of hepatic stellate cells in liver inflammation: a new perspective. *Inflam. Regen.*, **36**(1), pp. 1–6.

Fujita, T., Soontrapa, K., Ito, Y., Iwaisako, K., Moniaga, C. S., Asagiri, M., Majima, M. and Narumiya, S. (2016). Hepatic stellate cells relay inflammation signaling from sinusoids to parenchyma in mouse models of immune-mediated hepatitis.

Hepatology, **63**(4), pp. 1325–1339.

Gu, Y.-Z., Hogenesch, J. B. and Bradfield, C. A. (2000). The PAS superfamily: sensors of environmental and developmental signals. *Annu. Rev. Pharmacol. Toxicol.*, **40**, pp. 519–561.

Håkansson, H. and Hanberg, A. (1989). The distribution of [14C]-2,3,7,8-tetrachlorodibenzo-p-dioxin (TCDD) and its effect on the vitamin A content in parenchymal and stellate cells of rat liver. *J. Nutr.*, **119**(4), pp. 573–580.

Han, M., Liu, X., Liu, S., Su, G., Fan, X., Chen, J., Yuan, Q. and Xu, G. (2017). 2,3,7,8-Tetrachlorodibenzo-p-dioxin (TCDD) induces hepatic stellate cell (HSC) activation and liver fibrosis in C57BL6 mouse via activating Akt and NF-κB signaling pathways. *Toxicol. Lett.*, **273**, pp. 10–19.

Harvey, S. A. K., Dangi, A., Tandon, A. and Gandhi, C. R. (2013). The transcriptomic response of rat hepatic stellate cells to endotoxin: Implications for hepatic inflammation and immune regulation. *PLoS ONE*, **8**(12).

Harvey, W. A., Jurgensen, K., Pu, X., Lamb, C. L., Cornell, K. A., Clark, R. J., Klocke, C. and Mitchell, K. A. (2016). Exposure to 2,3,7,8-tetrachlorodibenzo-p-dioxin (TCDD) increases human hepatic stellate cell activation. *Toxicology*. **344**, pp. 26–33.

Huang, G. and Elferink, C. J. (2012). A novel nonconsensus xenobiotic response element capable of mediating aryl hydrocarbon receptor-dependent gene expression. *Mol. Pharmacol.*, **81**(3), pp. 338–347.

Ishak, K., Baptista, A., Bianchi, L., Callea, F., De Groote, J., Gudat, F., Denk, H., Desmet, V., Korb, G., MacSween, R. N. M., Phillips, M. J., Portmann, B. G., Poulsen, H., Scheuer, P. J., Schmid, M. and Thaler, H. (1995). Histological grading and staging of chronic hepatitis. *J. Hepatol.*, **22**(6), pp. 696–699.

Jackson, D. P., Joshi, A. D. and Elferink, C. J. (2015). Ah receptor pathway intricacies; signaling through diverse protein partners and DNA-motifs. *Toxicol. Res.*, **4**(5), pp. 1143–1158.

Jiang, J. X. and Török, N. J. (2013). Liver injury and the activation of the hepatic

myofibroblasts. *Curr. Pathobiol. Rep.*, **1**(3), pp. 215–223.

Lamb, C. L., Cholico, G. N., Perkins, D. E., Fewkes, M. T., Oxford, J. . T., Morrill, E. E. and Mitchell, K. A. (2016a). Aryl hydrocarbon receptor activation by TCDD modulates expression of extracellular matrix remodeling genes during experimental liver fibrosis. *Biomed Res. Int.*, **2016**.

Lamb, C. L., Cholico, G. N., Pu, X., Hagler, G. D., Cornell, K. A. and Mitchell, K. A. (2016b). 2,3,7,8-Tetrachlorodibenzo-p-dioxin (TCDD) increases necro-inflammation and hepatic stellate cell activation but does not exacerbate experimental liver fibrosis in mice. *Toxicol. Appl. Pharmacol.*, **311**, pp. 42–51.

Larigot, L., Juricek, L., Dairou, J. and Coumoul, X. (2018). AhR signaling pathways and regulatory functions. *Biochimie Open.*, **7**, pp. 1–9.

Livak, K. J. and Schmittgen, T. D. (2001). Analysis of relative gene expression data using real-time quantitative PCR and the $2^{-\Delta\Delta CT}$ method. *Methods*, **25**(4), pp. 402–408.

Pierre, S., Chevallier, A., Teixeira-Clerc, F., Ambolet-Camoit, A., Bui, L. C., Bats, A. S., Fournet, J. C., Fernandez-Salguero, P. M., Aggerbeck, M., Lotersztajn, S., Barouki, R. and Coumoul, X. (2014). Aryl hydrocarbon receptor-dependent induction of liver fibrosis by dioxin. *Toxicol. Sci.*, **137**(1), pp. 114–124.

Poland, A., Palen, D. and Glover, E. (1994). Analysis of the four alleles of the murine aryl hydrocarbon receptor. *Mol. Pharmacol.*, **46**, pp. 915–921.

Ramachandran, P., Pellicoro, A., Vernon, M. A., Boulter, L., Aucott, R. L., Ali, A., Hartland, S. N., Snowdon, V. K., Cappon, A., Gordon-Walker, T. T., Williams, M. J., Dunbar, D. R., Manning, J. R., Van Rooijen, N., Fallowfield, J. A., Forbes, S. J. and Iredale, J. P. (2012). Differential Ly-6C expression identifies the recruited macrophage phenotype, which orchestrates the regression of murine liver fibrosis. *Proc. Natl. Acad. Sci. U.S.A.*, **109**(46).

Rechnagel, R. O. and Glende, E. A. (1973). Carbon tetrachloride hepatotoxicity: An example of lethal cleavage. *CRC Crit. Rev. Toxicol.*, **2**(3), pp. 263–97.

Su, L., Li, N., Tang, H., Lou, Z., Chong, X., Zhang, C., Su, J. and Dong, X. (2018).

Kupffer cell-derived TNF-α promotes hepatocytes to produce CXCL1 and mobilize neutrophils in response to necrotic cells. *Cell Death Dis.*, **9**(3).

Tsuchida, T. and Friedman, S. L. (2017). Mechanisms of hepatic stellate cell activation. *Nat. Rev. Gastroenterol. Hepatol.*, **14**(7), pp. 397–411.

Vogel, C. F. A., Nishimura, N., Sciullo, E., Wong, P., Li, W. and Matsumura, F. (2007). Modulation of the chemokines KC and MCP-1 by 2,3,7,8-tetrachlorodibenzo-p-dioxin (TCDD) in mice. *Arch. Biochem. Biophys.*, **461**(2), pp. 169–175.

Vrochides, D., Papanikolaou, V., Pertoft, H., Antoniades, A. A. and Heldin, P. (1996). Biosynthesis and degradation of hyaluronan by nonparenchymal liver cells during liver regeneration. *Hepatology*, **23**(6), pp. 1650–1655.

Walisser, J. A., Glover, E., Pande, K., Liss, A. L. and Bradfield, C. A. (2005). Aryl hydrocarbon receptor-dependent liver development and hepatotoxicity are mediated by different cell types. *Proc. Natl. Acad. Sci. U.S.A.*, **102**(49), pp. 17858–17863.

Weber, L. W. D., Boll, M. and Stampfl, A. (2003). Hepatotoxicity and mechanism of action of haloalkanes: carbon tetrachloride as a toxicological model. *Crit. Rev. Toxicol.*, **33**(2), pp. 105–136.

Yan, J., Tung, H.-C., Li, S., Niu, Y., Garbacz, W. G., Lu, P., Bi, Y., Li, Y., He, J., Xu, M., Ren, S., Monga, S. P., Schwabe, R. F., Yang, D. and Xie, W. (2019). Aryl hydrocarbon receptor signaling prevents activation of hepatic stellate cells and liver fibrogenesis in mice. *Gastroenterology*, pp. 1–14.

CHAPTER FOUR

TRANSCRIPTOME RNA-SEQ REVEALS NON-ALCOHOLIC FATTY LIVER DISEASE MEDIATED BY AHR ACTIVATION IN A CCL_4-INDUCED LIVER INJURY MODEL

Abstract

Non-alcoholic fatty liver disease (NAFLD) is a spectrum of disorders ranging from simple steatosis to non-alcoholic steatohepatitis (NASH). Complications from NASH include the development of fibrosis or cirrhosis. During fibrosis, chronic injury and inflammation drive the activation of myofibroblast precursors, namely hepatic stellate cells (HSCs), which produce collagen. We have previously shown that AhR activation by 2,3,7,8-tetrachlorodibenzo-*p*-dioxin (TCDD) increases HSC activation *in vitro* and in a mouse model of liver fibrosis elicited by chronic carbon tetrachloride (CCl_4) administration. The goal of this project was to determine the cell-specific consequences of TCDD/AhR signaling on the progression of liver disease. Initial results demonstrated that CCl_4/TCDD co-treatment in double floxed control mice ($AhR^{fl/fl}$) led to an end state pathology possessing steatosis, inflammation and fibrosis. Mice with AhR knock-out from hepatocytes ($AhR^{\Delta Hep}$) however alleviated these pathologies except for fibrosis. To elucidate what molecular mechanisms might different liver pathologies in control mice but not in $AhR^{\Delta Hep}$ mice, RNA-seq was conducted. In this study, mice were treated with 1.0 ml/kg CCl_4 every four days for 5 weeks, and TCDD (100 μg/kg) was

administered during the final week of the experiment. RNA-seq revealed that co-treatment of CCl_4 and TCDD produced a NAFLD-like gene expression profile in $AhR^{fl/fl}$ mice, consistent with our pathological data. Further investigation revealed changes in gene expression promoting liver triglyceride accumulation in co-treated $AhR^{fl/fl}$ mice, but not in $AhR^{\Delta Hep}$ mice. Dysregulation of glucose metabolism is a risk factor for the development of NAFLD. RNA-seq revealed glycolysis-, gluconeogenesis-, and glycogen synthesis-related genes to be transcriptionally inactive in $AhR^{fl/fl}$ mice and unchanged in $AhR^{\Delta Hep}$ mice. Based on these findings, we conclude that AhR signaling in hepatocytes is essential for promoting NAFLD progression in a liver injury model system.

Introduction

Non-alcoholic fatty liver disease (NAFLD) is prevalent in approximately one-third of the population and is characterized by excessive lipid accumulation in the liver (steatosis) of individuals who consume little to no alcohol (Loomba & Sanyal, 2013). NAFLD refers to a spectrum of histological conditions, ranging from simple steatosis to non-alcoholic steatohepatitis (NASH), in which steatosis is accompanied by hepatocyte ballooning, lobular inflammation, and varying degrees of fibrosis. NAFLD/NASH patients with progressive fibrosis are at increased risk for developing cirrhosis, liver failure, and hepatocellular carcinoma (Neuman *et al.*, 2014). NAFLD has become a major concern for public health as it is projected to be the most common cause of liver transplantation needs by the year 2030 (Jayakumar, 2018).

The aryl hydrocarbon receptor (AhR) is a ubiquitously expressed, ligand-activated transcription factor that is widely recognized for mediating the toxicity of environmental contaminants, including benzopyrene, coplanar polychlorinated biphenyls (PCBs) and dioxins (Duval *et al.*, 2018). The AhR can also be activated by endogenous metabolic, dietary and microbial ligands (Seok *et al.*, 2018). Several compelling lines of evidence indicate that AhR activity may contribute to the development of NAFLD. For example, mice with a constitutively active AhR (C-AhR) were found to exhibit spontaneous hepatic steatosis that was attributed to the AhR-mediated induction of CD36 (fatty acid translocase) (Lee *et al.*, 2010; Angrish *et al.*, 2012). Steatosis was accompanied by decreased fatty acid oxidation, increased peripheral fat mobilization, and increased hepatic oxidative stress. Similarly, exposure of mice to the high-affinity, exogenous AhR ligand 2,3,7,8-tetrachlorodibenzo-*p*-dioxin (TCDD) was found to elicit steatohepatitis,

based on increased hepatic triglyceride levels and liver pathology with ballooning degeneration, lobular inflammation, and microvesicular steatosis (Lu *et al.*, 2011).

Activation of the AhR can also impact fibrogenesis, which is a wound-healing response characterized by the deposition of extracellular matrix proteins such as collagen. AhR deficiency is associated with increased collagen deposition and liver fibrosis, which indicates that endogenous AhR activity may be important for limiting fibrogenesis (Fernandez-Salguero *et al.*, 1995; Fernandez-Salguero *et al.*, 1997; Zaher *et al.*, 1998; Peterson *et al.*, 2000). This is supported by recent reports that AhR activation with the endogenous ligand 2-(1′H-indole-3′-carbonyl)-thiazole-4-carboxylic acid methyl ester (ITE) suppressed liver fibrosis in mice treated with carbon tetrachloride (CCl_4) (Yan *et al.*, 2019). In contrast, exogenous activation of the AhR with TCDD is associated with increased fibrogenesis. For example, chronic treatment of mice with TCDD produced liver fibrosis, increased production of the pro-fibrogenic soluble mediator transforming growth factor-beta (TGFβ), and increased inflammation and myofibroblast activation, all of which were not observed in AhR knockout mice treated with TCDD (Pierre *et al.*, 2014).

Despite the prevalence of NAFLD, only a small portion of patients will develop inflammation, progressive fibrosis, and chronic liver disease (Bertot & Adams, 2016). Although NAFLD pathogenesis is not yet fully understood, risk factors include obesity, dyslipidemia, and insulin resistance (Loomba & Sanyal, 2013). A “two-hit hypothesis” has been proposed for NAFLD progression, in which a “first hit,” such as insulin resistance, obesity or genetic factors, causes excess triglycerides to accumulate in the liver, which sensitizes the organ to a “second hit” (oxidative stress, proinflammatory

cytokines, mitochondrial dysfunction), leading to inflammation and fibrogenesis (Marra & Lotersztajn, 2013). Another hypothesis is that interruption of triglyceride synthesis initiates free fatty acid (FA)-mediated lipotoxicity, which then leads to NASH and fibrosis (Jou *et al.*, 2008; Trauner *et al.*, 2010). It has been proposed that exposure to environmental contaminants could contribute to NAFLD progression (Marrero *et al.*, 2005; Zein *et al.*, 2011). It is possible that TCDD-induced AhR activation could function much like the second hit and increase progression to NASH and advanced liver injury. For example, in a mouse model of diet induced obesity, chronic administration of a low dose of TCDD increased liver fibrosis and steatosis and altered gene expression related to hepatic lipid metabolism (Duval *et al.*, 2017). Mice in this study were treated with carbon tetrachloride (CCl_4) for four weeks to produce mild liver damage and fibrosis. Then, mice were given a single dose of TCDD at the beginning of the fifth week. At the end of the 5-week experiment, it was observed that TCDD exacerbated liver damage, steatosis, inflammation, myofibroblast activation, and expression of fibrogenesis-related genes, consistent with advanced liver disease (Lamb *et al.*, 2016; Chapter 3).

In this study, we tested the hypothesis that acute exposure to TCDD provides the second hit needed to cause NAFLD progression in CCl_4-treated mice. We used RNA-sequencing to identify differentially expressed genes between CCl_4-treated mice with and without TCDD. Genes pertaining to insulin signaling, glucose metabolism and lipid homeostasis were severely modulated in CCl_4-treated mice with TCDD. Furthermore, progression of NAFLD, and dysregulation of NAFLD-associated genes were found to be absent when the AhR was conditionally knocked-out from hepatocytes. Results from this study highlight a cell-specific role for AhR signaling in regulating NAFLD progression.

Animal Treatment:

Mice with AhR-deficient hepatocytes ($AhR^{\Delta Hep}$) were created using a Cre-Lox system as previously described (Chapter 3). Double AhR floxed mice were used as controls ($AhR^{fl/fl}$). Treatment groups (n=8) were set up with mice that were 8 weeks of age. Briefly, mice were treated twice per week with 1 ml/kg CCl_4 (Sigma-Aldrich, St. Louis, MO) diluted 1:4 in corn oil by gavage for a total of 5 weeks. During the final week, mice were gavaged with 100 μg/kg TCDD (Cambridge Isotope Laboratories, Andover, MA) diluted in peanut oil or peanut oil alone (Veh). Necropsies were performed at the end of week 5 and mouse livers were excised out and snap-frozen in liquid nitrogen. Mice were housed in a 12:12 h light:dark cycle, with food and water available *ad libitum*. All animal experiments were approved by the Institutional Animal Care and Use Committee at Boise State University and were conducted in compliance with the regulations and institutional policies that govern animal care and use.

Histopathology:

Histopathological slides were prepared as previously described (Chapter 3). Briefly, 5μm paraffin embedded sections were stained with hematoxylin and eosin (H&E) for visualization of steatosis. Slides were imaged on an Olympus BX45 dual headed compound microscope at 400x magnification.

Glucose Quantitation Assay:

Serum glucose was quantified using a glucose colorimetric assay kit according to the manufacturer's specifications (Cayman Chemical, Ann Arbor MI). Quantitation for each sample (n=5) was conducted in duplicate.

Triglyceride Quantitation Assay:

Triglyceride content from total liver homogenate was quantified using a triglyceride colorimetric assay kit (Cayman Chemical, Ann Arbor MI). Quantitation for each sample (n=5) was conducted in duplicate.

RNA Extraction:

RNA was extracted from cryogenically stored total liver (20 mg). Samples were homogenized using a dounce homogenizer and total RNA was extracted using an E.N.Z.A.® Total RNA kit (Omega Bio-Tek, Norcross, GA). Quality of RNA was verified on a 2100 Bioanalyzer using with an RNA 6000 Nano kit (Agilent, Santa Clara, CA).

RNA-sequencing, Mapping and Analysis:

RNA-sequencing was performed at the University of Oregon, GC3F (https://gc3f.uoregon.edu/). Briefly, Illumina libraries from three biological replicates (n = 3) were prepared using a QuantSeq 3' mRNA-Seq Library Prep Kit (Lexogen, Vienna, Austria)., after which, all samples were sequenced using an Illumina Hiseq 4000 sequencer. Reads of 1 × 75 bp were demultiplexed and adapter sequences were removed

using Trim Galore v0.5.0. Trimmed reads were then assessed for quality using FASTQC v0.11.8. Reads were then mapped to a mouse reference genome (version GRCm38.p6) using Hisat2 v2.1.0 (Kim *et al.*, 2015). Gene counts were determined using HTSeq v0.11.0 (Anders *et al.*, 2015) after which, counts were normalized using the median-of-ratios method with Deseq2 v1.22.2 (Love *et al.*, 2014). Genes with an adjusted p-value < 0.05 were considered differentially expressed. Differentially expressed genes (DEGs) were enriched for KEGG pathways using the ClueGO plug-in v2.5.1 (Bindea *et al.*, 2009) in Cytoscape v3.7.0 (Shannon *et al.*, 2003). Pathways with an FDR-adjusted p-value < 0.05 were considered enriched.

Qualitative real-time RT-PCR:

Qualitative real-time PCR (qRT-PCR) was conducted as previously described (Chapter 3). Briefly, cDNA libraries were prepared from isolated RNA using an Applied Biosystems High Capacity cDNA Reverse Transcription kit (Thermo Fisher Scientific, Waltham, MA). Gene-specific primer sets (Table 4.1) were used in conjunction with Roche FastStart Essential DNA Green Master (Roche, Indianapolis, IN). Five biological replicates were used per treatment group. Gene expression was normalized to GAPDH and was quantified using the $2^{-\Delta\Delta Cq}$ (fold-change) method normalized to the $AhR^{fl/fl}$ Veh treatment group.

Table 4.1 Primer Sequences

Gene	Primer sequence (5′ to 3′)	Temp. (°C)
Cd68	CCA ATT CAG GGT GGA AGA AA CTC GGG CTC TGA TGT AGG TC	52
Dgat2	GCG CTA CTT CCG AGA CTA CTT GGG CCT TAT GCC AGG AAA CT	59
G6pc	TTC AAG TGG ATT CTG TTT GG AGA TAG CAA GAG TAG AAG TGA C	53
Gapdh	CAA TGA CCC CTT CAT TGA CC GAT CTC GCT CCT GGA AGA TG	60
Gys2	GAG GCT GAG AGG GAT CGG CTA AA TGG ACT TGG GGC AGC TCA TTT	60
Insr	TTT GTC ATG GAT GGA GGC TA CCT CAT CTT GGG GTT GAA CT	54
Irs1	TCC CAA ACA GAA GGA GGA TG CAT TCC GAG GAG AGC TTT TG	54
Mttp	AGC CAG TGG GCA TAG AAA ATC GGT CAC TTT ACA ATC CCC AGA G	57
Pklr	CCG CAT CTA CAT TGA CGA CG CCG TGT TCC ACT TCG GTC AC	53
Slc2a2	ACC GGG ATG ATT GGC ATG TT GGA CCT GGC CCA ATC TCA AA	57

Statistical Analysis:

Analyses were conducted using GraphPad Prism 7.0d (GraphPad Software, La Jolla, CA). Multiple comparisons between treatment groups were conducted using a two-way ANOVA followed by a Bonferroni's test. Statistical significance is reported in data with $p < 0.05$.

Results

RNA-sequencing was conducted to assess differences in transcriptomes between TCDD-treated $AhR^{fl/fl}$ and $AhR^{\Delta Hep}$ mice in our model system utilizing TCDD with CCl_4-induced liver injury. Specifically, we tried to identify what transcriptional changes occurred when the AhR was activated upon liver injury and what role AhR played in hepatocytes. RNA samples from each mouse liver had an average read depth of 12 M resulting in about 9.7 M high quality reads. When comparing the gene expression profiles of $AhR^{fl/fl}$ mice livers that had undergone CCl_4/Veh or CCl_4/TCDD, it was determined that 8,022 genes were differently expressed. When comparing the gene expression profiles of co-treated $AhR^{\Delta Hep}$ mice against the CCl_4/Veh, 1,128 genes were differentially expressed genes (Figure 4.1). These differences in sheer number of DEGs between the two mice genotypes indicate that AhR signaling in hepatocytes plays a major in mediating a major role of liver pathology progression in a CCl_4/TCDD model system.

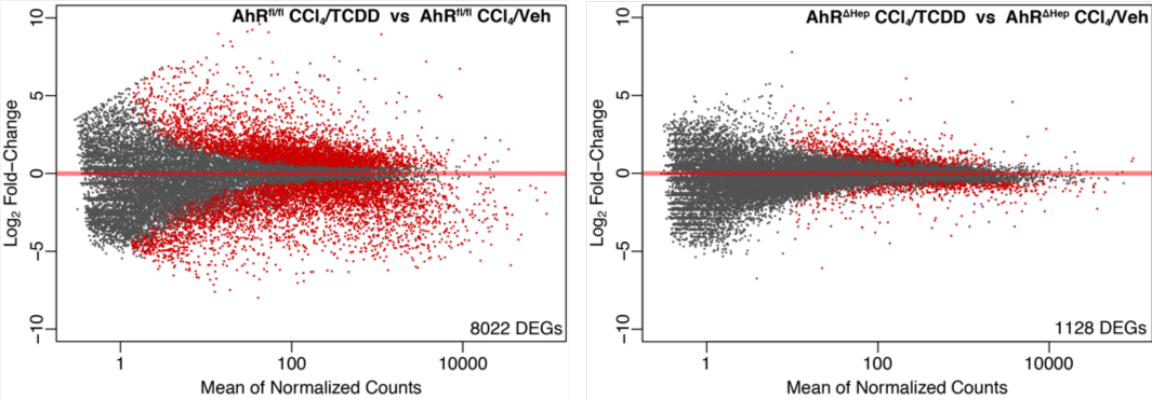

Figure 4.1 Knocking out AhR functionality from hepatocytes greatly reduces modulation of gene expression upon TCDD treatment in a liver injury model

MA-plots depicting differentially expressed genes (red markers) per pairwise comparison in RNA-seq data. Pairwise comparisons are defined in the top right corner. Number of differentially expressed genes are listed in the bottom right corner.

To elucidate what might have caused these major discrepancies in number of differentially expressed genes between the treatment groups, we enriched DEGs for KEGG pathways. Enrichment data for $AhR^{fl/fl}$ co-treated mice (referenced against CCl_4/Veh $AhR^{fl/fl}$ mice) proved to have 51 KEGG pathways with an enrichment p-value < 0.05 (Supplementary Table 4.1). Alternatively, when enriching DEGs for co-treated $AhR^{\Delta Hep}$ mice (referenced against CCl_4/Veh $AhR^{\Delta Hep}$ mice), only the pathway for *D-glutamine and D-glutamate metabolism* was enriched (data not shown). It is remarkable that TCDD treatment in a CCl_4 liver injury model has strikingly different effects on transcript expression in mice that have a functional AhR in hepatocytes when compared against mice that do not have a functional AhR in hepatocytes.

The most significant enriched KEGG pathway for the $AhR^{fl/fl}$ co-treatment group compared against $AhR^{fl/fl}$ CCl_4/Veh was Non-Alcoholic Fatty Liver Disease (NAFLD). Significant enriched KEGG pathways pertaining to NAFLD are depicted in Table 4.2. We had never considered that we might be promoting the onset of NAFLD in our CCl_4 liver injury model system upon treatment with TCDD. We therefore looked for overt markers of NAFLD progression in histopathological data. The first stage of NAFLD is steatosis, characterized by the accumulation of fat droplets in the hepatocytes of the liver. H&E stained slides were used to assess steatosis in our model system (Figure 4.2). Histopathological scoring for steatosis was then conducted by a pathologist (Table 4.3). All non-Veh treatment groups elicited at least a mild steatosis pathology. However, TCDD and CCl_4/TCDD treated $AhR^{fl/fl}$ mice demonstrated a more pronounced pathological response, with the co-treated group showing a significant increase against the CCl_4-only treatment group. Based on this evidence, it stands to reason that steatosis is exacerbated in a liver injury model when AhR activation occurs.

Table 4.2 Enriched KEGG Pathways from DEGs related to NAFLD

KEGG Pathway	Nr. Enriched Genes	Upreg. Genes	Downreg. Genes	% Assoc. Gene	-Log(P)
Non-alcoholic fatty liver disease (NAFLD)	103	30	73	68.21	12.80
Pyruvate metabolism	32	8	24	84.21	6.76
Fatty acid degradation	35	1	34	70.00	3.71
Insulin signaling pathway	73	42	31	52.14	1.98

Differentially expressed genes in $AhR^{fl/fl}$ CCl_4/TCDD (compared against $AhR^{fl/fl}$ CCl_4/Veh) were enriched for KEGG pathways. NAFLD was the most significant pathway. Depicted pathways are those relevant to NAFLD. A full list of enriched pathways is available in Supplementary Table 1.

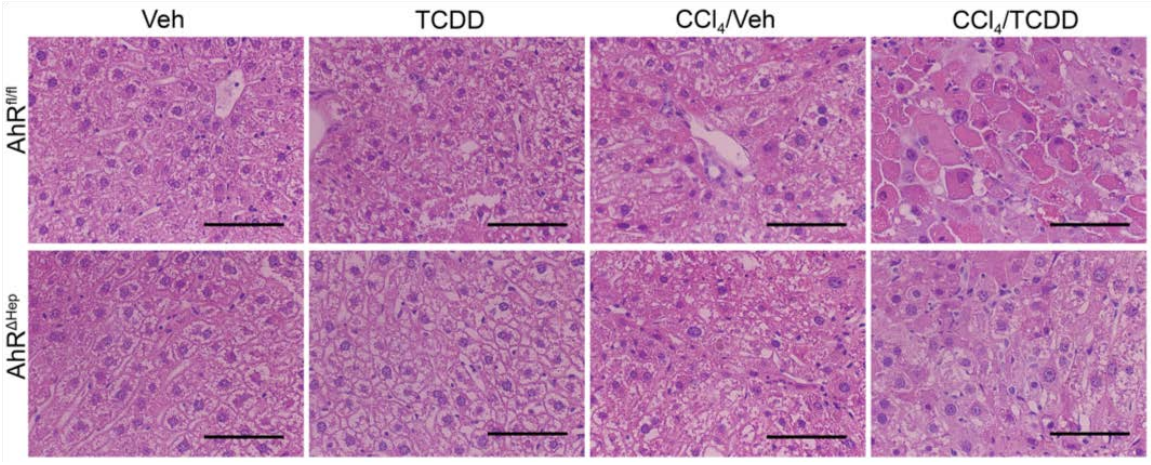

Figure 4.2 TCDD treatment worsens steatosis in mice with liver injury

H&E liver sections were assessed for steatosis (400X magnification). Scale bar represents 100μm.

Table 4.3 Histopathological scoring results

	Veh		TCDD		CCl_4/Veh		CCl_4/TCDD	
	$AhR^{fl/fl}$	$AhR^{\Delta Hep}$	$AhR^{fl/fl}$	$AhR^{\Delta Hep}$	$AhR^{fl/fl}$	$AhR^{\Delta Hep}$	$AhR^{fl/fl}$	$AhR^{\Delta Hep}$
Steatosis (0–6)	0.63 ± 0.32	0.25 ± 0.16	2.75 ± 0.37	1.29 ± 0.29	1.29 ± 0.36	1.38 ± 0.42	3.18 ± 0.62[a]	2.11 ± 0.20
Combined Necroinflammation Score (0-18)†	0.88 ± 0.44	1.50 ± 0.63	2.75 ± 0.86	2.86 ± 0.94	1.29 ± 0.36	3.13 ± 0.97	11.45 ± 1.53[a]	4.00 ± 0.85[b]
Fibrosis Score (0–6)†	0.38 ± 0.18	0.38 ± 0.18	0.63 ± 0.18	0.57 ± 0.20	3.00 ± 0.31	2.88 ± 0.30	3.55 ± 0.25	3.67 ± 0.24

The Ishak scoring method was used to assess histopathological sections for gross markers of steatosis, necroinflammation and fibrosis (Ishak *et al.*, 1995). Values represent mean ± SEM. [a]*p*-value < 0.05 when compared against $AhR^{fl/fl}$ CCl_4/Veh. [b]*p*-value < 0.05 when compared against $AhR^{fl/fl}$ CCl_4/TCDD. Eight individual mice were assessed were histological scoring. †Histological sections for these data can be found in Chapter 3.

Histopathological markers for later stages of NAFLD were assessed. Histopathological scoring for inflammation and fibrosis can be found in Table 4.3. The most robust necroinflammatory response was observed in co-treated $AhR^{fl/fl}$ mice. A necroinflammatory pathology was also observed in co-treated $AhR^{\Delta Hep}$ mice, however, the response is significantly reduced when compared against the $AhR^{fl/fl}$ counterpart. A different trend was observed for fibrosis, however. CCl_4/Veh induced a fibrosis pathology in either genotype. This seemed reasonable as CCl_4 metabolism and toxicity is not dependent on AhR signaling. However, a similar degree of fibrosis was observed in co-treated mice in either genotype. This was unexpected because CCl_4/TCDD treatment in $AhR^{fl/fl}$ mice elicited greater levels of steatosis and inflammation.

To investigate what molecular mechanisms might have yielded the co-treated $AhR^{fl/fl}$ mice to demonstrate a more aggressive steatosis response, we conducted RNA-seq and assessed gene sets involved in lipid metabolism (Figure 4.3A). Expression of genes pertaining to lipid accumulation showed both an upregulation and downregulation trend. *Cd36* is a fatty transporter that was upregulated in most treatment groups, more than likely leading to a larger intake of circulating lipids. *Mttp* encodes the protein microsomal triglyceride transfer protein which is essential for the formation of LDLs and VLDLs. These lipoproteins are essential for the release and circulation of triglycerides from the liver. RNA-seq reveals that *Mttp* gene expression was inhibited in co-treated $AhR^{fl/fl}$ mice. Triglycerides are synthesized by two evolutionary unrelated enzymes DGAT1 and DGAT2. RNA-seq reveals that gene expression of *Dgat1* was almost unchanged across treatment groups and expression of *Dgat2* was downregulated in co-treated $AhR^{fl/fl}$ mice. qRT-PCR was used to verify gene expression levels of *Cd36*, *Mttp*,

and *Dgat2*. *Cd36* qRT-PCR results are very similar to RNA-seq data. Although not statistically significant, an increase in expression of *CD36* was observed in co-treated $AhR^{fl/fl}$ mice compared against their CCl_4/Veh counterparts. Expression of *Mttp* was observed to decrease in either co-treated treatment group, although only co-treated $AhR^{fl/fl}$ mice showed a significant decrease. Gene expression for *Dgat2* decreased slightly with most treatment groups compared against Veh, although co-treated $AhR^{fl/fl}$ mice showed a significant decrease when compared against their CCl_4/Veh counterparts. Fatty acid synthesis was also assessed using RNA-seq. Although all fatty acid synthesis genes in co-treated $AhR^{fl/fl}$ mice were found to have been downregulated, *Acaca* and *Acacb*, both genes encoding the rate limiting enzyme acetyl-CoA carboxylase were found to be profoundly downregulated. Similarly, most genes involved in β-oxidation were downregulated in co-treated $AhR^{fl/fl}$ mice. Total liver triglycerides were assessed in all treatment groups (Figure 4.4). TCDD and CCl_4/TCDD treated mice in $AhR^{fl/fl}$ genotype showed the greatest increase in liver triglyceride content, with co-treated $AhR^{fl/fl}$ mice showing a significant increase when compared against the CCl_4/Veh counterparts. These results are show a strikingly similar trend when compared against the steatosis scoring conducted by a pathologist.

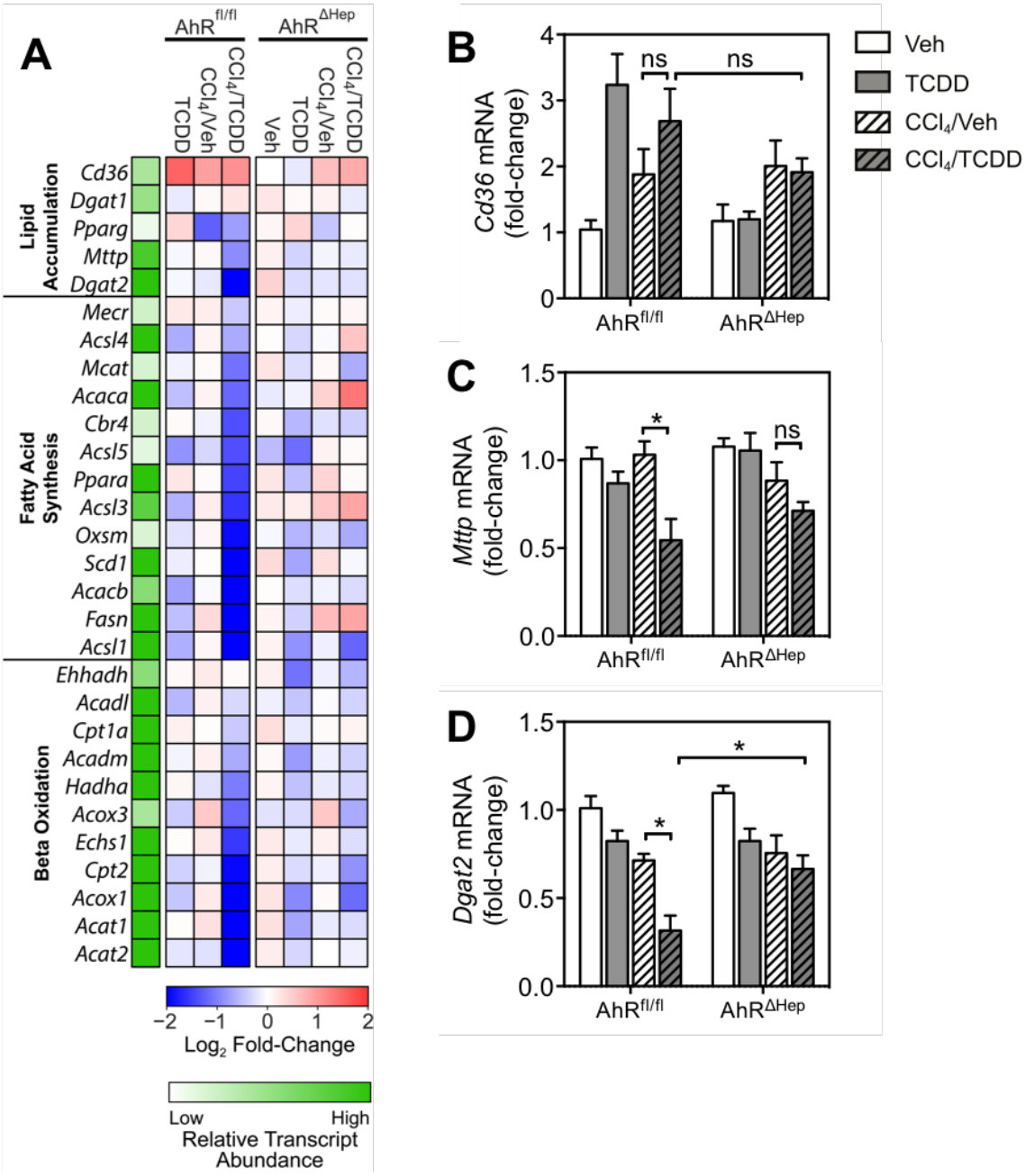

Figure 4.3 AhR signaling impedes fatty acid metabolism in control mice treated with TCDD in a liver injury model

(A) Gene expression for markers of lipid metabolism was measured using RNA-seq from total liver homogenate. All treatment groups were compared against $AhR^{fl/fl}$ Veh for relative expression. **(B-D)** Genes pertaining to lipid homeostasis were assessed via qRT-PCR. Bars represent mean ± SEM for mice (n=5). Asterisks (*) denote a significant difference ($p < 0.05$).

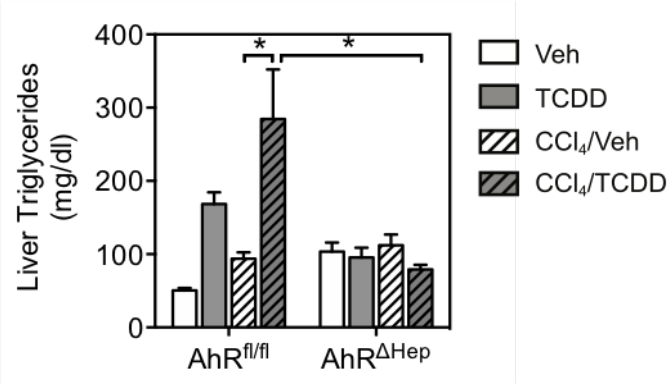

Figure 4.4 Liver triglyceride accumulation occurs in control mice with upon TCDD treatment

Steatosis is defined as the accumulation of fat droplets within hepatocytes. Liver triglycerides were quantified from total liver homogenates. Bars represent mean ± SEM for mice (n = 5). Asterisks (*) denote a significant difference ($p < 0.05$).

There is some evidence to suggest that NAFLD is associated with dysregulation of insulin signaling (Marchesini *et al.*, 1999; Pagano *et al.*, 2002; Lomonaco *et al.*, 2012). RNA-seq was used to assess expression of genes associated with insulin signaling (Figure 5A). Gene expression for both the insulin receptor (*Insr*) and insulin receptor substrate (*Irs1*) were found to decrease upon co-treatment in either genotype, however, a more profound decrease was observed in $AhR^{fl/fl}$ mice. When bound to the insulin receptor, insulin receptor substrate recruits binding of p85/p55 proteins (*Pik3r1*, *Pik3r2*, *Pik3r3*). Expression of these three genes remained almost unchanged for *Pik3r2* and showed a decrease in co-treated $AhR^{fl/fl}$ mice for *Pik3r1* and *Pik3r3*. PI3-kinases (*Pik3ca*, *Pik3cb*, *Pik3cd*) are then recruited and bind to p85 which produce the cell signaling molecule PIP_3. Gene expression for only *Pik3cd* increased with co-treatment in both genotypes, while expression for the other two genes remained unchanged for all treatment groups. Upon release, PIP_3 binds to phosphoinositide dependent kinase (*Pdpk1*), which then phosphorylates atypical protein kinase C (*Prkci*, *Prkcz*) and protein kinase B (*Akt1*, *Akt2*,

Akt3). Gene expression of *Pdpk1* remained unchanged across all treatment groups. Expression of *Prkci* overall remained unchanged, while *Prkcz* showed a large decrease in expression for the co-treated $AhR^{fl/fl}$ mice. Atypical protein kinase C functions to activate SREBP-1C (*Srebf1*) which activates fatty acid synthesis and glycolysis. *Srebf1* expression was found to decrease in co-treated $AhR^{fl/fl}$ mice. Glycogen synthesis is largely controlled by protein kinase B. Hepatocytes mainly produce *Akt2* (Morales-Ruiz *et al.*, 2017) which was found to decrease in gene expression in both co-treated groups. Hepatic stellate cells (HSCs) mainly produce *Akt1* but can also produce *Akt3* if the cells are activated (Morales-Ruiz *et al.*, 2017). Expression for both of these genes increased in mainly co-treated $AhR^{fl/fl}$ mice. All three isoforms of protein kinase B activate PP1. The PP1 complex then activates glycogen synthase. The two hepatic regulatory subunits of PP1 – *Ppp1r3b* and *Ppp1r3c* – were found to greatest decrease in expression in co-treated $AhR^{fl/fl}$ mice, although a decrease can be seen in other treatment groups as well.

RNA-seq gene expression for key mediators in insulin signaling and glucose intake were verified by qRT-PCR (Figure 5B/C). Although not statistically significant, TCDD, CCl_4, and CCl_4/TCDD treated $AhR^{fl/fl}$ mice all showed a decrease in *Insr* expression, with the greatest decrease occurring in the co-treated mice. Although a slight decrease for *Insr* gene expression was observed in $AhR^{\Delta Hep}$ mice, it was not as much of a decrease as that seen in the $AhR^{fl/fl}$ mice. *Irs1* gene expression in $AhR^{fl/fl}$ mice was observed to decrease with TCDD or CCl_4/TCDD treatment, while only co-treated $AhR^{\Delta Hep}$ mice showed a decrease.

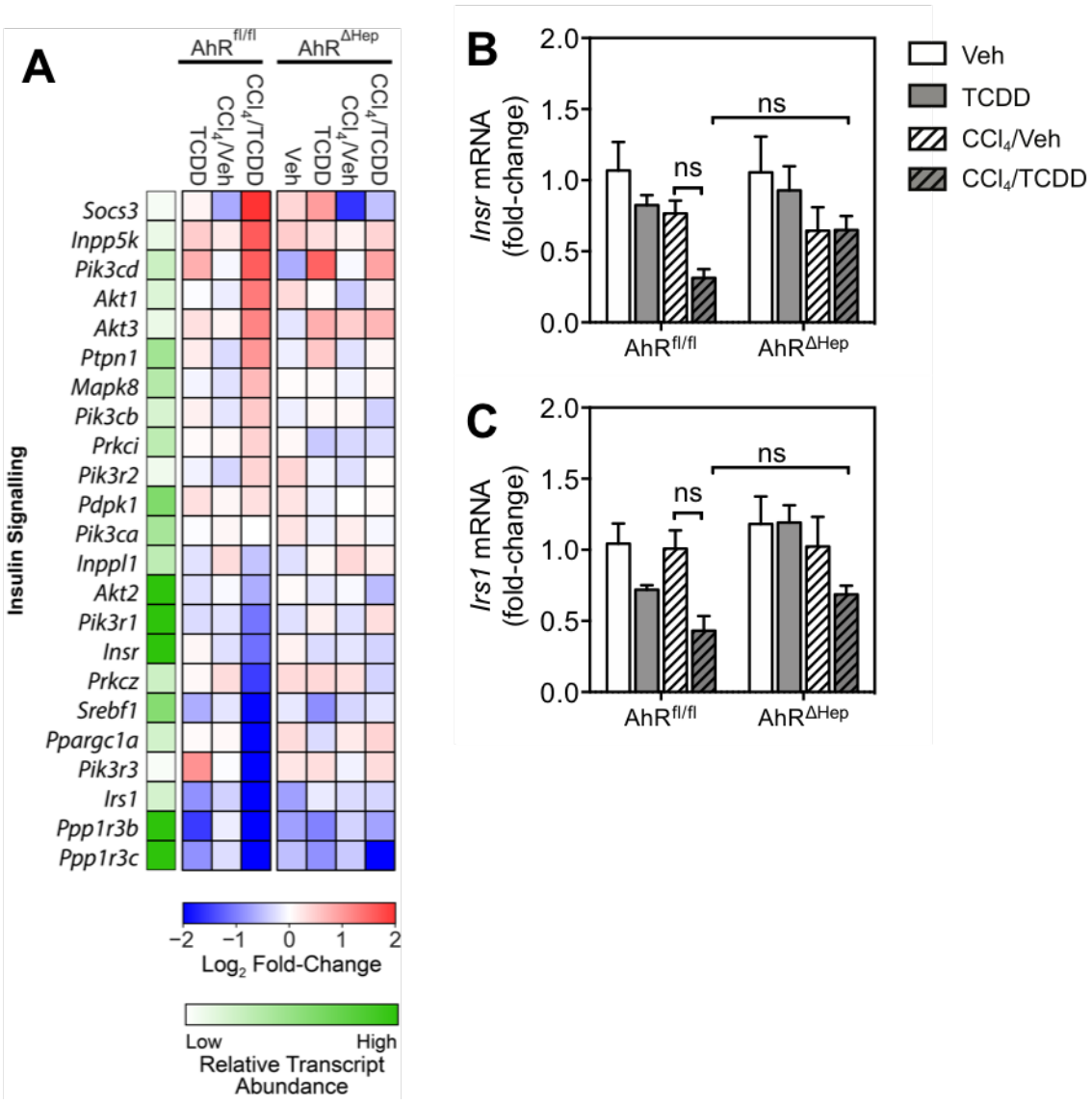

Figure 4.5 Insulin signaling is impeded in control mice that were treated with TCDD in a liver injury model

Dysregulation of glucose metabolism is a risk factor for the development of NAFLD. Insulin signaling plays a major role in glucose uptake of cells. **(A)** RNA-sequencing was used to assess insulin signaling from total liver homogenates. All treatment groups were compared against $AhR^{fl/fl}$ Veh for relative expression. (**B/C)** qRT-PCR was used to verify gene expression levels of select genes pertaining to insulin signaling. Bars represent mean ± SEM for mice (n=5). Asterisks (*) denote a significant difference ($p < 0.05$).

Because changes in gene expression for insulin signaling were severely dysregulated in co-treated $AhR^{fl/fl}$ mice, we investigated glucose levels in the serum of

mice (Figure 4.6). Serum glucose levels were fairly consistent across all treatment levels except for co-treated $AhR^{fl/fl}$ mice, which depicted hypoglycemic levels. Changes in insulin signaling probably resulted in changes of blood serum glucose levels leading to the possibility that glucose metabolism was altered in the liver.

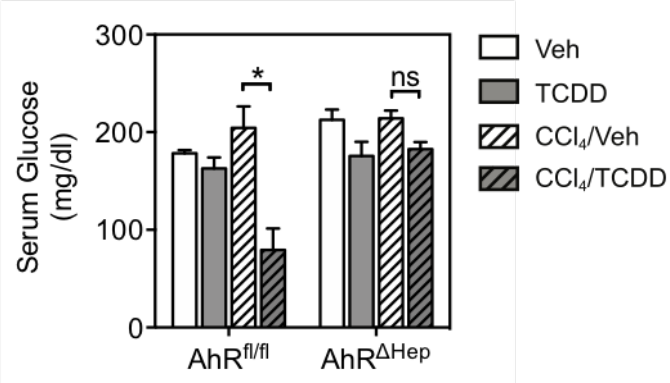

Figure 4.6 Co-treated control mice demonstrate decreased levels of serum glucose

Serum glucose levels were evaluated in mice at the end of the study. Bars represent mean ± SEM for mice (n=5). Asterisks (*) denote a significant difference ($p < 0.05$).

We investigated dysregulation of glucose metabolism using RNA-seq (Figure 4.7A). Select gene expression can be observed in a metabolic pathway in Supplementary Figure 1. Glucose metabolism begins with transport of the sugar across the cell membrane. In the liver, glucose transport occurs in an insulin-independent manner through the use of the constitutively expressed glucose transporters GLUT2 (*Slc2a2*) and GLUT9 (*Slc2a9*). Although most treatment groups showed a slight increase in gene expression for *Slc2a2*, co-treated $AhR^{fl/fl}$ mice showed downregulation of this gene. Similarly, expression of *Slc2a9* was found to greatly decrease in co-treated $AhR^{fl/fl}$ mice.

An important regulatory step in glycolysis involves the conversion of glucose to glucose-6-phosphate. In the liver, this step is controlled primarily by Glucokinase (*Gck*), a low affinity isoform of hexokinase that is typically upregulated with elevated blood glucose. Gene expression of *Gck* was profoundly decreased in the co-treated $AhR^{fl/fl}$ mice, consistent with decreased levels of serum glucose in this set of mice. Another important regulatory step in glycolysis involves the production of pyruvate from phosphoenolpyruvate by the enzyme pyruvate kinase. There are four isoforms of this enzyme encoded by two genes, *Pklr* and *Pkm*. In the liver, this step of glycolysis is primarily catalyzed by the isoform PKL, an alternatively spliced product of *Pklr*. Our data suggests that expression of this gene decreased in co-treated $AhR^{fl/fl}$ mice but slightly increased in co-treated $AhR^{\Delta Hep}$ mice. The gene *Pkm* encodes the two isoforms PKM1 and PKM2 and are primarily expressed in muscle and brain, but can be expressed in liver during circumstances of cell proliferation such as during tumorigenesis (Mendez-Lucas *et al.*, 2017). Interestingly, *Pkm* gene expression increased with TCDD and CCl_4/TCDD treatment in both genotypes, although the increase was greatest in $AhR^{fl/fl}$ mice. We also assessed gene expression changes in gluconeogenesis. The enzymes controlling the two regulatory steps, fructose-bisphosphatase 1 (*Fkp1*) and glucose-6-phosphatase (*G6pc*) both showed a decrease in gene expression in co-treated $AhR^{fl/fl}$ mice, and minimal changes across other treatment groups.

Long term storage of glucose involves the production of glycogen in the liver and skeletal muscle. Glycogen synthesis is regulated primarily by the enzyme glycogen synthase (*Gys1*, *Gys2*), in which this enzyme polymerizes glucose onto a nucleation site on the protein glycogenin (*Gyg*). *Gys2* expression decreased in only co-treated $AhR^{fl/fl}$

mice, while *Gys1* showed a slight increase in only co-treated $AhR^{\Delta Hep}$ mice. Interestingly, *Gyg* expression increased at least slightly in most treatment groups, with the greatest increase seen in co-treated $AhR^{fl/fl}$ mice. Gene expression regulatory steps in glucose metabolism were verified with qRT-PCR (Figure 4.7B-E). Gene expression for *Slc2a2* was found to slightly decrease in co-treated $AhR^{fl/fl}$ mice and slightly increase in co-treated $AhR^{\Delta Hep}$ mice. Pklr expression was shown to decrease with TCDD and CCl_4/TCDD treatment in $AhR^{fl/fl}$ mice, while a slight increase was observed in co-treated $AhR^{\Delta Hep}$ mice. *G6pc* gene expression decreased in both genotypes of co-treated mice. Lastly, *Gys2* expression decreased with TCDD and CCl_4/TCDD treatment in $AhR^{fl/fl}$ mice, with a greater decrease seen in the co-treatment group.

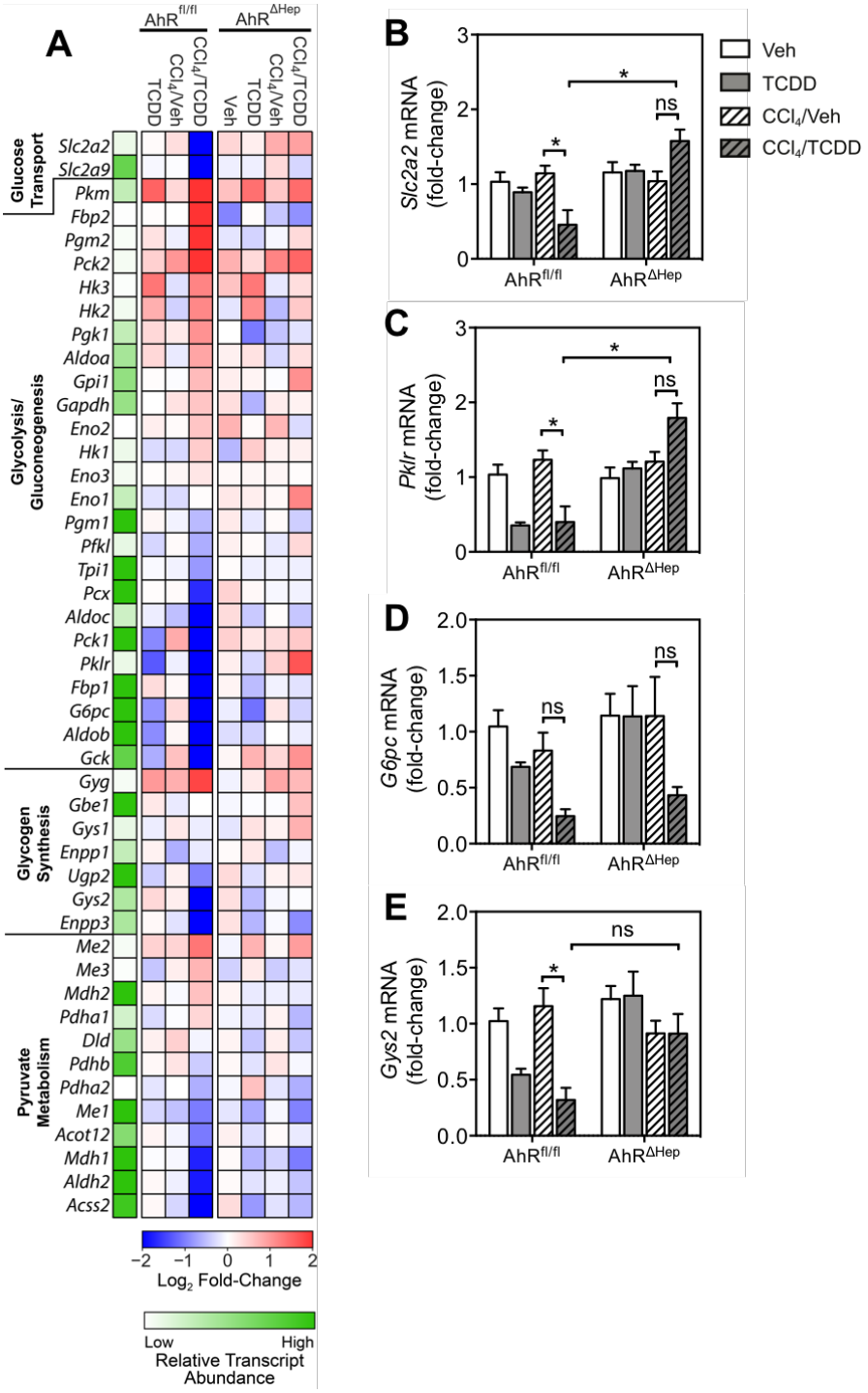

Figure 4.7 AhR signaling dysregulates central carbon metabolism in co-treated control mice.

(A) Glucose metabolism was assessed using RNA-seq from total liver homogenates. **(B)** qRT-PCR was also conducted to evaluate gene expression levels of the non-insulin dependent GLUT transporter SLC2A2 (GLUT2). **(C-E)** qRT-PCR was used to validate regulatory steps in glycolysis, gluconeogenesis, and glycogen synthesis. Bars represent mean ± SEM for mice (n=5). Asterisks (*) denote a significant difference ($p < 0.05$).

Discussion

We previously showed that administering a single dose of TCDD to mice with CCl_4-induced liver damage resulted in contrasting pathologies between $AhR^{fl/fl}$ (control) mice and $AhR^{\Delta Hep}$ mice (hepatocyte-specific AhR knockdown) (Chapter 3). In this previous study, it was verified that liver toxicity mediated by TCDD, as demonstrated by increased hepatomegaly, elevated serum ALT levels, and increased confluent necrosis, relies on AhR signaling in hepatocytes. Furthermore, this study demonstrated that TCDD treatment partially mediates liver inflammation in mice with CCl_4-induced liver damage. This inflammation, in part, occurs through AhR signaling in hepatocytes, as $AhR^{\Delta Hep}$ mice showed a partial, albeit not total, decrease in liver inflammation when compared against their $AhR^{fl/fl}$ counterparts. Furthermore, we demonstrated that AhR signaling in hepatocytes is required for a maximal HSC activation when mice were co-treated with CCl_4/TCDD. HSC activation (which occurs in response to liver injury and inflammation) was greater in co-treated $AhR^{fl/fl}$ mice than in $AhR^{\Delta Hep}$ mice. It stands to reason that higher levels of HSC activation observed in co-treated $AhR^{fl/fl}$ mice are a result of the higher levels of hepatic injury and inflammation observed in this same treatment group. Furthermore, because the AhR functions as a transcription factor, gene expression could be altered by TCDD in our model system that elicit cellular dysfunction and ultimately induce hepatic necrosis and inflammation. We conducted RNA-sequencing to identify these transcriptional changes in gene expression.

Enrichment of differentially expressed genes in TCDD treated $AhR^{fl/fl}$ mice that had CCl_4-induced liver injury suggested that a high number of genes pertaining to non-alcoholic fatty liver disease (NAFLD) had been modulated. NAFLD progression begins

with simple steatosis, which is an accumulation of fats packaged into lipid vacuoles in the hepatocytes of the liver. Several studies have demonstrated that administration of TCDD can result in steatosis. For example, subchronic administration of TCDD (30 μg/kg) for 28 days has been shown to induce lipid accumulation in the livers of mice, as demonstrated by oil red O histopathological staining (Nault *et al.*, 2016). In another study where mice were fed a high fat diet for 14 weeks, which itself promotes hepatic steatosis, weekly administration of TCDD (5 μg/kg) for the final 6 weeks resulted in increased triglyceride content of liver (Duval *et al.*, 2017). Our results suggest that a single dose of TCDD administered to mice with CCl_4-induced liver damage also promotes steatosis as we observed increased liver triglyceride levels in co-treated $AhR^{fl/fl}$ mice. Furthermore, TCDD did not induce triglyceride accumulation when the AhR was knocked out of hepatocytes, suggesting that AhR signaling in hepatocytes drives TCDD-induced lipid accumulation in the liver.

Previous studies have demonstrated that dietary or circulating lipids are the major source of fatty acids that accumulate in the liver in response to TCDD treatment (Angrish *et al.*, 2012; Yao *et al.*, 2016). In these studies, it was shown that TCDD induces gene transcriptional upregulation of the fatty acid (FA) transporter *Cd36* allowing for circulating fatty acids to be in taken into the liver (Lee *et al.*, 2010; Yao *et al.*, 2016; Nault *et al.*, 2017). Our data is in agreement with these other studies, demonstrating that TCDD treatment in mice with CCl_4-induced liver injury elicits gene transcriptional upregulation of *Cd36*, suggesting that circulating fatty acids are a source of lipids for hepatic steatosis in our model. Furthermore, our data also suggest that TCDD administration inhibits *de novo* fatty acid synthesis which is in agreement with other

studies as well (Lee *et al.*, 2010; Angrish *et al.*, 2012; Tanos *et al.*, 2012; Nault *et al.*, 2017). Steatosis occurs not only because of increased lipid storage but also because of decreased lipid usage and export. TCDD has been shown to inhibit β-oxidation of free fatty acids (Lee *et al.*, 2010; Nault *et al.*, 2017) as well as inhibit secretion of very low density lipoproteins (VLDL) containing triglycerides (Nault *et al.*, 2017). TCDD administration to mice with CCl_4-induced liver injury elicited transcriptional downregulation of genes pertaining to β-oxidation, suggesting that the degradation of free fatty acids was impaired in our study. Furthermore, genes pertaining to triglyceride synthesis and export, such as *Dgat2* and *Mttp*, respectively, decreased in expression with TCDD treatment. Overall, transcriptional data in our study suggests that TCDD promotes steatosis through the accumulation of circulating fatty acids while preventing degradation or export of lipids. Furthermore, these transcriptional changes in lipid metabolism are not observed in $AhR^{\Delta Hep}$ mice suggesting that TCDD steatosis in mice through AhR signaling in hepatocytes.

Accumulation of free fatty acids has been shown to be lipotoxic in rodent models when triglyceride synthesis was inhibited (Listenberger *et al.*, 2003; Yamaguchi *et al.*, 2007). In one of these studies, obese mice that underwent DGAT2 antisense oligonucleotide treatment demonstrated decreased levels of steatosis than their untreated counterparts due to decreased triglyceride vacuolation (Yamaguchi *et al.*, 2007). However, these mice with decreased steatosis went on to develop increased lobular necroinflammation and fibrosis, while demonstrating increased hepatic free FAs and markers of lipid peroxidation (Yamaguchi *et al.*, 2007). Free FAs in the liver are typically non-covalently bound to soluble fatty acid carriers termed fatty acid binding proteins

(FABPs). FABPs function to sequester free FAs and aid in their transport and metabolism. Recent studies have shown that FABP1, the predominant FABP in the liver, functions to reduce the lipotoxic effect of free FAs (Guzmán et al., 2013). Co-treated $AhR^{fl/fl}$ mice in our study demonstrated a $\log_2$ fold-change of -3.94 for the expression of *Fabp1* when compared against vehicle treated $AhR^{fl/fl}$ mice (data not shown). It is possible that the necroinflammation observed in our mice co-treated with CCl_4/TCDD is a direct result of free FA lipotoxicity, as mice in this treatment group demonstrated gene transcriptional patterns of increased FA uptake and decreased lipid export along with decreased expression of *Fabp1*.

Lipid metabolism in the liver is closely regulated by insulin signaling. Furthermore, insulin resistance has been linked to the development of NAFLD (Marchesini *et al.*, 1999; Pagano *et al.*, 2002; Lomonaco *et al.*, 2012). Since lipid metabolism appeared to be severely dysregulated in our model, we assessed in insulin signaling which regulates not only lipid metabolism in the liver, but also glucose metabolism. RNA-seq enrichment data indicated that insulin signaling was downregulated on a transcriptional level while repressors of insulin signaling were upregulated. These changes in insulin signaling potentially impact glucose metabolism, as is seen in patients with NAFLD. For example, silencing SREBP-1C, a downstream insulin signaling target, reduces expression of glycogen synthesis related genes (Ruiz *et al.*, 2014). Our data suggests that a single dose of TCDD decreases in *Srebf1* expression in $AhR^{fl/fl}$ mice with CCl_4-induced liver injury. Furthermore, a study suggested that overexpression of the insulin targets PPP1R3B and PPP1R3C both promote glycogen storage (Agius, 2015). PPP1R3B and PPP1R3C are both the hepatic regulatory

components of PP1, a phosphatase which activates glycogen synthase. Our data suggests that treatment with TCDD downregulates the expression of the hepatic regulatory components of PP1, *Ppp1r3b* and *Ppp1r3c*, which indicates suppression of glycogen production. It is unclear whether glycogen reserves had been depleted, however, it stands to reason that because hypoglycemia was observed in our co-treated $AhR^{fl/fl}$ mice, this treatment group must have depleted hepatic glycogen stores. However, it is important to note that these observations were not present in co-treated $AhR^{\Delta Hep}$ mice, indicating that the negative consequences of AhR signaling in a CCl_4 liver injury model occurs presumably through the AhR in the hepatocytes.

In summary, our results suggest that TCDD treatment elicits a NAFLD-like phenotype in mice with CCl_4-induced liver injury. Furthermore, NAFLD progression is dependent on AhR signaling in hepatocytes in this model. Our results suggest that TCDD treatment elicits steatosis by enhancing free FA uptake and impeding the export of triglycerides. This buildup of free FAs has the potential to elicit oxidative stress (Friedman *et al*., 2018) which could be a driving factor for promoting the necroinflammation observed in our model. Although our study demonstrated that a single dose of TCDD administered to mice with CCl_4-liver injury is enough to promote the onset of NAFLD, the exact changes in gene expression that ultimately drive liver injury and inflammation remain unknown.

Acknowledgements

This work was supported by NIH Grant Nos. P20GM103408 and P20GM109095, National Science Foundation Grant Nos. 0619793 and 0923535; the MJ Murdock Charitable Trust; and the Idaho State Board of Education; the Society of Toxicology Diversity Initiatives Grant; and a seed grant from the ID-INBRE bioinformatics core.

Supplementary Data

Supplementary Table 4.1 Enriched KEGG Pathways from DEGs

KEGG Pathway	Nr. Genes	% Assoc. Gene	-Log(P)
Non-alcoholic fatty liver disease (NAFLD)	103	68.21	12.80
Complement and coagulation cascades	63	71.59	8.75
Parkinson disease	89	61.80	7.33
Huntington disease	112	57.73	7.01
Pyruvate metabolism	32	84.21	6.76
Oxidative phosphorylation	83	61.94	6.73
Peroxisome	57	67.85	6.36
Alzheimer disease	101	57.71	6.15
Thermogenesis	125	53.87	5.44
Propanoate metabolism	26	83.87	5.14
Valine, leucine and isoleucine degradation	40	71.42	4.82
Fatty acid degradation	35	70.00	3.71
Prion diseases	26	76.47	3.64
Glyoxylate and dicarboxylate metabolism	24	77.41	3.36
Arginine and proline metabolism	34	68.00	3.25
AGE-RAGE signaling pathway in diabetic complications	59	58.41	3.24
Tryptophan metabolism	32	69.56	3.13
Focal adhesion	102	51.25	2.88
Small cell lung cancer	54	58.69	2.83
p53 signaling pathway	44	61.97	2.81
ErbB signaling pathway	50	59.52	2.78
Glycine, serine and threonine metabolism	28	70.00	2.76
Glutathione metabolism	40	62.50	2.70
FoxO signaling pathway	72	54.54	2.69
Fc gamma R-mediated phagocytosis	51	58.62	2.64
Proteoglycans in cancer	103	50.49	2.53
Autophagy	70	53.84	2.40
Salmonella infection	46	58.97	2.39
AMPK signaling pathway	68	53.96	2.35
Ferroptosis	28	68.29	2.35
Chronic myeloid leukemia	45	59.21	2.31
Apoptosis	72	52.94	2.24
Insulin signaling pathway	73	52.14	1.98
Protein processing in endoplasmic reticulum	83	50.92	1.94
Cholesterol metabolism	31	63.26	1.93
Histidine metabolism	18	75.00	1.93
B cell receptor signaling pathway	42	58.33	1.85
Bile secretion	42	58.33	1.85
Drug metabolism	49	56.32	1.85
Arginine biosynthesis	15	78.94	1.85
Osteoclast differentiation	67	52.34	1.83
Insulin resistance	59	53.63	1.82
Colorectal cancer	49	55.68	1.81
Pancreatic cancer	43	57.33	1.75
Retinol metabolism	50	54.94	1.70
Citrate cycle (TCA cycle)	22	68.75	1.70
Legionellosis	35	60.34	1.70
Cysteine and methionine metabolism	31	62.00	1.69
PPAR signaling pathway	47	55.29	1.58
TNF signaling pathway	58	52.72	1.53
Central carbon metabolism in cancer	37	57.81	1.42

Differentially expressed genes in $AhR^{fl/fl}$ CCl_4/TCDD (compared against $AhR^{fl/fl}$ CCl_4/Veh) were enriched for KEGG pathways.

References

Agius, L. (2015). Role of glycogen phosphorylase in liver glycogen metabolism. *Mol. Aspects Med.*, **46**, pp. 34–45.

Anders, S., Pyl, P. T. and Huber, W. (2015). HTSeq-A Python framework to work with high-throughput sequencing data. *Bioinformatics*, **31**(2), pp. 166–169.

Angrish, M. M., Mets, B. D., Jones, A. D. and Zacharewski, T. R. (2012). Dietary fat is a lipid source in 2,3,7,8-tetrachlorodibenzo-p-dioxin (TCDD)-elicited hepatic steatosis in C57BL/6 mice. *Toxicol. Sci.*, **128**(2), pp. 377–386.

Bertot, L. C. and Adams, L. A. (2016). The natural course of non-alcoholic fatty liver disease. *Int. J. Mol. Sci.*, **17**(5).

Bindea, G., Mlecnik, B., Hackl, H., Charoentong, P., Tosolini, M., Kirilovsky, A., Fridman, W., Pagès, F., Trajanoski, Z. and Galon, J. (2009). ClueGO : a Cytoscape plug-in to decipher functionally grouped gene ontology and pathway annotation networks. *Bioinformatics*, **25**(8), pp. 1091–1093.

Duval, C., Blanc, E. and Coumoul, X. (2018). Aryl hydrocarbon receptor and liver fibrosis. *Curr. Opin. Toxicol.*, **8**, pp. 8–13.

Duval, C., Teixeira-Clerc, F., Leblanc, A. F., Touch, S., Emond, C., Guerre-Millo, M., Lotersztajn, S., Robert Barouki, Aggerbeck, M. and Coumoul, and X. (2017). Chronic exposure to low doses of dioxin promotes liver fibrosis development in the C57BL/6J diet-induced obesity mouse model. *Environ. Health Perspect.*, **125**(3), pp. 428–436.

Fernandez-Salguero, P. M., Pineau, T., Hilbert, D. M., McPhail, T., Lee, S. S. T., Kimura, S., Nebert, D. W., Rudikoff, S., Ward, J. M. and Gonzalez, F. J. (1995). Immune system impairment and hepatic fibrosis in mice lacking the dioxin-binding Ah receptor. *Science*, **268**, pp. 722–726.

Fernandez-Salguero, P. M., Ward, J. M. and Gonzalez, F. J. (1997). Lesions of aryl-hydrocarbon receptor deficient mice. *Vet. Pathol.*, **34**, pp. 605–614.

Friedman, S. L., Neuschwander-Tetri, B. A., Rinella, M. and Sanyal, A. J. (2018).

Mechanisms of NAFLD development and therapeutic strategies. *Nat. Med.*, **24**(7), pp. 908–922.

Guzmán, C., Benet, M., Pisonero-Vaquero, S., Moya, M., García-Mediavilla, M. V., Martínez-Chantar, M. L., González-Gallego, J., Castell, J. V., Sánchez-Campos, S. and Jover, R. (2013). The human liver fatty acid binding protein (FABP1) gene is activated by FOXA1 and PPARα; And repressed by C/EBPα: Implications in FABP1 down-regulation in nonalcoholic fatty liver disease. *Biochim. Biophys. Acta*, **1831**(4), pp. 803–818.

Jayakumar, S. (2018). Liver transplantation for non-alcoholic fatty liver disease-a review. *AME Med. J.*, **3**(29).

Jou, J., Choi, S. S. and Diehl, A. M. (2008). Mechanisms of disease progression in nonalcoholic fatty liver disease. *Semin. Liver. Dis.*, **28**(4), pp. 370–379.

Kim, D., Langmead, B. and Salzberg, S. L. (2015). HISAT: a fast spliced aligner with low memory requirements. *Nat. Methods*, **12**(4), pp. 357–360.

Lamb, C. L., Cholico, G. N., Pu, X., Hagler, G. D., Cornell, K. A. and Mitchell, K. A. (2016). 2,3,7,8-Tetrachlorodibenzo-p-dioxin (TCDD) increases necro-inflammation and hepatic stellate cell activation but does not exacerbate experimental liver fibrosis in mice. *Toxicol. Appl. Pharmacol.* Elsevier Inc., **311**, pp. 42–51.

Lee, J. H., Wada, T., Febbraio, M., He, J., Matsubara, T., Jae, M., Gonzalez, F. J. and Xie, W. (2010). A novel role for the dioxin receptor in fatty acid metabolism and hepatic steatosis. *Gastroenterology*, **139**(2), pp. 653–663.

Listenberger, L. L., Han, X., Lewis, S. E., Cases, S., Farese, R. V., Ory, D. S. and Schaffer, J. E. (2003). Triglyceride accumulation protects against fatty acid-induced lipotoxicity. *Proc. Natl. Acad. Sci. U.S.A.*, **100**(6), pp. 3077–3082.

Lomonaco, R., Ortiz-Lopez, C., Orsak, B., Webb, A., Hardies, J., Darland, C., Finch, J., Gastaldelli, A., Harrison, S., Tio, F. and Cusi, K. (2012). Effect of adipose tissue insulin resistance on metabolic parameters and liver histology in obese patients with nonalcoholic fatty liver disease. *Hepatology*, **55**(5), pp. 1389–1397.

Loomba, R. and Sanyal, A. J. (2013). The global NAFLD epidemic. *Nat. Rev. Gastroenterol. Hepatol.*, **10**(11), pp. 686–690.

Love, M. I., Huber, W. and Anders, S. (2014). Moderated estimation of fold change and dispersion for RNA-seq data with DESeq2. *Genome Biol.*, **15**(12), p. 550.

Lu, H., Cui, W. and Klaassen, C. D. (2011). Nrf2 protects against 2,3,7,8-tetrachlorodibenzo-p-dioxin (TCDD)-induced oxidative injury and steatohepatitis. *Toxicol. Appl. Pharmacol.*, **256**(2), pp. 122–135.

Marchesini, G., Brizi, M., Morselli-Labate, A. M., Bianchi, G., Bugianesi, E., McCullough, A. J., Forlani, G. and Melchionda, N. (1999). Association of nonalcoholic fatty liver disease with insulin resistance. *Am. J. Med.*, **107**(5), pp. 450–455.

Marra, F. and Lotersztajn, S. (2013). Pathophysiology of NASH: Perspectives for a targeted treatment. *Curr. Pharm. Des.*, **19**(29), pp. 5250–5269.

Marrero, J. A., Fontana, R. J., Fu, S., Conjeevaram, H. S., Su, G. L. and Lok, A. S. (2005). Alcohol, tobacco and obesity are synergistic risk factors for hepatocellular carcinoma. *J. Hepatol.*, **42**(2), pp. 218–224.

Mendez-Lucas, A., Li, X., Hu, J., Che, L., Song, X., Jia, J., Wang, J., Xie, C., Driscoll, P. C., Tschaharganeh, D. F., Calvisi, D. F., Yuneva, M. and Chen, X. (2017). Glucose catabolism in liver tumors induced by c-MYC can be sustained by various PKM1/PKM2 ratios and pyruvate kinase activities. *Cancer Res.*, **77**(16), pp. 4355–4364.

Morales-Ruiz, M., Santel, A., Ribera, J. and Jiménez, W. (2017). The role of Akt in chronic liver disease and liver regeneration. *Semin. Liver. Dis.*, **37**(1), pp. 11–16.

Nault, R., Fader, K. A., Ammendolia, D. A., Dornbos, P., Potter, D., Sharratt, B., Kumagai, K., Harkema, J. R., Lunt, S. Y., Matthews, J. and Zacharewski, T. (2016). Dose-dependent metabolic reprogramming and differential gene expression in TCDD-elicited hepatic fibrosis. *Toxicol. Sci.*, **154**(2), pp. 253–266.

Nault, R., Fader, K. A., Lydic, T. A. and Zacharewski, T. R. (2017). Lipidomic evaluation of aryl hydrocarbon receptor-mediated hepatic steatosis in male and

female mice elicited by 2,3,7,8-tetrachlorodibenzo-p-dioxin. *Chem. Res. Toxicol.*, **30**(4), pp. 1060–1075.

Neuman, M. G., Cohen, L. B. and Nanau, R. M. (2014). Biomarkers in nonalcoholic fatty liver disease. *Can. J. Gastroenterol. Hepatol.*, **28**(11), pp. 607–618.

Pagano, G., Musso, G., Pacini, G., Gambino, R., Mecca, F., Depetris, N., Cassader, M., David, E., Cavallo-Perin, P. and Rizzetto, M. (2002). Nonalcoholic steatohepatitis, insulin resistance, and metabolic syndrome: Further evidence for an etiologic association. *Hepatology*, **35**(2), pp. 367–372.

Peterson, T. C., Hodgson, P., Fernandez-Salguero, P. M., Neumeister, M. and Gonzalez, F. J. (2000). Hepatic fibrosis and cytochrome P450: experimental models of fibrosis compared to AHR knockout mice. *Hepatol. Res.*, **17**(2), pp. 112–125.

Pierre, S., Chevallier, A., Teixeira-Clerc, F., Ambolet-Camoit, A., Bui, L. C., Bats, A. S., Fournet, J. C., Fernandez-Salguero, P. M., Aggerbeck, M., Lotersztajn, S., Barouki, R. and Coumoul, X. (2014). Aryl hydrocarbon receptor-dependent induction of liver fibrosis by dioxin. *Toxicol. Sci.*, **137**(1), pp. 114–124.

Ruiz, R., Jideonwo, V., Ahn, M., Surendran, S., Tagliabracci, V. S., Hou, Y., Gamble, A., Kerner, J., Irimia-Dominguez, J. M., Puchowicz, M. A., DePaoli-Roach, A., Hoppel, C., Roach, P. and Morral, N. (2014). Sterol regulatory element-binding protein-1 (SREBP-1) is required to regulate glycogen synthesis and gluconeogenic gene expression in mouse liver. *J. Biol. Chem.*, **289**(9), pp. 5510–5517.

Seok, S. H., Ma, Z. X., Feltenberger, J. B., Chen, Hongbo, Chen, Hui, Scarlett, C., Lin, Z., Satyshur, K. A., Cortopassi, M., Jefcoate, C. R., Ge, Y., Tang, W., Bradfield, C. A. and Xing, Y. (2018). Trace derivatives of kynurenine potently activate the aryl hydrocarbon receptor (AHR). *J. Biol. Chem.*, **293**(6), pp. 1994–2005.

Shannon, P., Markiel, A., Ozier, O., Baliga, N. S., Wang, J. T., Ramage, D., Amin, N., Schwikowski, B. and Ideker, T. (2003). Cytoscape: A Software Environment for Integrated Models of Biomolecular Interaction Networks. *Genome Res.*, **13**, pp. 2498–2504.

Tanos R., Murray I. A., Smith P. B., Patterson A., Perdew G. H. (2012). Role of the Ah receptor in homeostatic control of fatty acid synthesis in the liver. *Toxicol. Sci.*, **129**(2):372–379.

Trauner, M., Arrese, M. and Wagner, M. (2010). Fatty liver and lipotoxicity. *Biochim. Biophys. Acta.*, **1801**(3), pp. 299–310.

Yamaguchi, K., Yang, L., McCall, S., Huang, J., Xing, X. Y., Pandey, S. K., Bhanot, S., Monia, B. P., Li, Y. X. and Diehl, A. M. (2007). Inhibiting triglyceride synthesis improves hepatic steatosis but exacerbates liver damage and fibrosis in obese mice with nonalcoholic steatohepatitis. *Hepatology*, **45**(6), pp. 1366–1374

Yan, J., Tung, H.-C., Li, S., Niu, Y., Garbacz, W. G., Lu, P., Bi, Y., Li, Y., He, J., Xu, M., Ren, S., Monga, S. P., Schwabe, R. F., Yang, D. and Xie, W. (2019). Aryl hydrocarbon receptor signaling prevents activation of hepatic stellate cells and liver fibrogenesis in mice. *Gastroenterology*, pp. 1–14.

Yao, L., Wang, C., Zhang, Xu, Peng, L., Liu, W., Zhang, Xuejiao, Liu, Y., He, J., Jiang, C., Ai, D. and Zhu, Y. (2016). Hyperhomocysteinemia activates the aryl hydrocarbon receptor/CD36 pathway to promote hepatic steatosis in mice. *Hepatology*, **64**(1), pp. 92–105.

Zaher, H., Fernandez-Salguero, P. M., Letterio, J., Sheikh, M. S., Fornace, A. J., Roberts, A. B. and Gonzalez, F. J. (1998). The involvement of aryl hydrocarbon receptor in the activation of transforming growth factor-β and apoptosis. *Mol. Pharmacol.*, **54**(2), pp. 313–321.

Zein, C. O., Unalp, A., Colvin, R., Liu, Y. C. and McCullough, A. J. (2011). Smoking and severity of hepatic fibrosis in nonalcoholic fatty liver disease. *J. Hepatol.*, **54**(4), pp. 753–759.

CHAPTER 5: CONCLUSION

Concluding Remarks

The AhR is an interesting receptor as it is widely known for mediating toxicity of TCDD and other chemicals, yet many of the mechanisms remain unknown. One of the reasons it has been difficult to identify specific mechanisms of TCDD toxicity is that the direct cellular targets are not necessarily clear, and many of the toxic effects appear to be tissue-specific. Furthermore, while TCDD toxicity is attributed to AhR-mediated changes in gene expression, mechanisms of transcriptional regulation by the AhR are not necessarily straightforward. The goal of this project was to use mice with cell-specific AhR knockdown to determine how TCDD impacted individual types of cells in the liver. Furthermore, we used global transcriptome analysis to determine how removing AhR signaling in a particular type of liver cell impacted TCDD-induced transcriptional changes.

The research described in Chapter 3 focused on understanding how TCDD exposure impacted the activation to HSCs, which are the central mediators of liver fibrosis. We previously found that TCDD treatment increased HSC activation *in vitro*, which led us to speculate that these cells were direct targets for TCDD (Harvey *et al.*, 2016). Work from our lab also determined that TCDD increased HSC activation in mice with CCl_4-induced liver injury (Lamb *et al.*, 2016). These findings led us to speculate that HSCs could be a direct cellular target of TCDD. This notion is supported by the finding

that TCDD has a half-life of 52 days in HSCs, which is four times longer than the half-life in hepatocytes (13 days) (Håkansson & Hanberg, 1989). Increased duration of exposure to TCDD increases the likelihood that these cells will be impacted by TCDD. However, results from this study indicate that, whatever is happening to HSCs in TCDD-treated mice is not occurring through direct effects on these cells. In other words, TCDD treatment probably does not induce HSC activation directly, based on our finding that TCDD exacerbated HSC activation in CCl_4-treated mice regardless of whether or not HSCs contained the AhR. Furthermore, removing the AhR from HSCs had no impact on liver damage and inflammation, which are the two main drivers for HSC activation (Tsuchida & Friedman, 2017). It seems likely that TCDD increases either one or both of these processes to exacerbate HSC activation in CCl_4-treated mice. Under these circumstances, it would be accurate to say that TCDD *indirectly* increases HSC activation in the injured liver. Furthermore, we found evidence that these indirect effects are mediated by AhR signaling in hepatocytes. We found that knocking out the AhR from hepatocytes completely abolished the hepatonecrotic effects of TCDD and diminished hepatic inflammation, which corresponded to lower levels of HSC activation. From these results, we envision a model in which TCDD treatment exacerbates injury and inflammation in an already injured liver to exacerbate HSC activation.

Another major finding of this work is that administration of TCDD to CCl_4-treated mice produced histopathological endpoints and gene expression profiles that are consistent with non-alcoholic fatty liver disease (NAFLD) and, more specifically, a subset of this disease called non-alcoholic steatohepatitis (NASH). Although the precise mechanisms that underlie NAFLD/NASH development are unknown, they are perhaps

best explained by a “multiple-hit” mechanism. Under this model, dietary, environmental, and genetic factors collectively promote the development of insulin resistance, obesity and changes in gut microbiota, which in turn result in NAFLD pathologies (Tilg & Moschen, 2010). Insulin resistance has been shown to promote fatty acid (FA) uptake in the liver (Bugianesi *et al.*, 2010). Accumulation of free fatty acids cause lipotoxicity, which exerts oxidative stress and subsequent mitochondrial dysfunction (Cusi, 2009). Few studies have explored the possibility that exposure to TCDD could be a sufficient “hit” for producing NAFLD in a predisposed (i.e., CCl_4-injured) liver. Our results demonstrate that exposure of CCl_4-treated mice to TCDD produced endpoints of NAFLD/NASH, whereas no evidence of NAFLD was found in mice treated with either CCl_4 or TCDD alone. Furthermore, RNA sequencing revealed that CCl_4/TCDD-treated mice also had dysregulated insulin signaling, and insulin resistance is a known risk factor for NAFLD development. FA metabolism was also altered in these mice, as evidenced by increased gene expression for fatty acid translocase (*Cd36*), and decrease expression of all genes related to β-oxidation. Based on transcriptome data alone, it is impossible to determine if hepatic FA levels increased lipotoxicity. However, one could speculate that an increased expression of fatty acid translocase would increase peripheral FA intake into the liver, and a decrease in β-oxidation would prevent subsequent degradation of these FAs. These events would be expected to increase lipotoxicity, which could be another mechanism by which TCDD produces NASH. Finally, we found that TCDD have no impact on NAFLD development if the AhR was conditionally knocked out of hepatocytes. Thus, results from this study raise the possibility that TCDD exposure could

function as one of the “hits” required to promote the development of NAFLD, and that this occurs through AhR signaling in hepatocytes.

Future Directions

One of the biggest questions that arose as a result of this project was *why does TCDD activate certain gene networks in a damaged liver but not in a healthy liver?* For example, transcriptome analysis revealed that 8022 genes were differentially expressed when a single dose of TCDD was administered to CCl_4-treated mice (Chapter 4). However, when a single dose of TCDD was administered to mice with a healthy liver, only 255 genes were differentially expressed (data not shown). This raises the intriguing possibility that, when activated by TCDD, the AhR binds to different XREs, and possibly even more XREs, in the injured liver compared to a healthy liver.

TCDD could induce AhR to bind to a more diverse repertoire of XREs in an injured liver through the increased accessibility of XREs. This could occur as a result of liver injury itself, as oxidative stress has been shown to induce heterochromatin loss (Kreuz, 2016). Loss of tightly packed chromatin could expose more XREs that the AhR can bind to, which would increase the diversity of gene expression. In addition, TCDD treatment has been shown to increase histone acetylation, which promotes the formation of euchromatin to expose the promoter regions for the genes *Cyp1a1* and *Cyp1b1* (Morgan & Whitlock., 1992; Okino & Whitlock, 1995; Beedanagari *et al.*, 2010). The histone acetyltransferase protein p300 was identified to be responsible for these acetylation events (Beedanagari *et al.*, 2010). Since TCDD has already been shown to directly induce chromatin remodeling events around the promoter regions of *Cyp1a1* and

Cyp1b1, it stands to reason that other promoter regions would also be affected. Proving that AhR-regulated gene expression in an injured liver is more diverse due to increased accessibility of chromatin binding sites could be achieved by identifying AhR binding locations in the injured and healthy liver. ChIP-sequencing (ChIP-seq) is a method used to determine interactions between proteins and DNA. It harnesses both capabilities of chromatin immunoprecipitation (ChIP) and next generation sequencing, and would enable the selective sequencing of the specific DNA fragments that were bound to the AhR. By using this method, it would be possible to enrich locations of the genome for which AhR bound in a healthy vs an unhealthy liver. Results from these ChIP-seq studies could prove that the TCDD-activated AhR is more transcriptionally active in an injured liver than in a healthy liver.

In addition to chromatin remodeling, it would be useful to look at DNA methylation between a healthy and an unhealthy liver. DNA methylation is an epigenetic modification in which cytosine residues throughout a genome are methylated. DNA methylation events occur at CpG sites, which are sites in which a cytosine is immediately followed by a guanine (Moore *et al.*, 2013). Furthermore, most (~70%) promoters reside within CpG islands, which are areas in a genome that are rich in CpG sites (Saxonov *et al.*, 2006). Methylation of CpG sites has been shown to induce gene silencing (Bird, 2002). A study looking at differential methylation sites in patients with advanced NAFLD found that 69,247 sites were differentially methylated when compared to patients with mild NAFLD (Murphy *et al.*, 2013). Approximately 70% of those sites were determined to be *hypomethylated*, although the mechanisms remain unclear as to why such aggressive demethylation occurs. This raises the possibility that patients with

advanced NAFLD could have different transcription patterns compared to healthy patients, simply because of differences in DNA methylation. In our study, TCDD was shown to induce a NAFLD-like pathology in mice with pre-existing (CCl_4-induced) liver injury, and this corresponded to a radically different transcriptome compared to mice treated with CCl_4 alone. Furthermore, the genetic sequence for XREs (the location in which activated AhR canonically binds to) is 5'-GCGTG-3', which itself contains one CpG. It stands to reason that TCDD could induce differences in transcription patterns by promoting the onset of NAFLD and subsequent demethylation of the genome, potentially in regions that are rich in XREs. Bisulfite sequencing is a method used to identify areas of methylation within a genome. This method utilizes a bisulfite treatment of DNA to convert any unmethylated cytosines to uracil prior to sequencing. Using this method, it would be possible to determine if promoter regions of genes were demethylated after TCDD treatment. Demethylation of promoter regions could indicate that downstream genes were more transcriptionally active. Furthermore, data from this study could be compared against data from a ChIP-seq study to determine if AhR binding occurs more frequently in areas of hypomethylation in CCl_4/TCDD-treated mice.

Results from future studies could shed light on mechanisms of AhR-mediated gene regulation and provide information about how such regulation could differ depending on the disease. This information will be important for identifying mechanisms of toxicity of exogenous AhR ligands, such as TCDD, which often elicit tissue-specific effects. Furthermore, understanding how the AhR regulates transcription in the presence of confounding factors, such as inflammation, oxidative stress or fibrogenesis, will be particularly important for the development of novel AhR ligands for therapeutic use.

References

Beedanagari, S. R., Taylor, R. T., Bui, P., Wang, F., Nickerson, D. W. and Hankinson, O. (2010). Role of epigenetic mechanisms in differential regulation of the dioxin-Inducible Human CYP1A1 and CYP1B1 Genes. *Mol. Pharmacol.*, **78**(4), pp. 608–616.

Bird, A. (2002). DNA methylation patterns and epigenetic memory. *Genes Dev.*, **16**, pp. 16–21.

Bugianesi, E., Moscatiello, S., Ciaravella, M. F. and Marchesini, G. (2010). Insulin resistance in nonalcoholic fatty liver disease. *Curr. Pharm. Des.*, **16**, pp. 1941–1951.

Cusi, K. (2009). Role of insulin resistance and lipotoxicity in non-alcoholic steatohepatitis. *Clin. Liver Dis.*, **13**, pp. 545–563.

Håkansson, H. and Hanberg, A. (1989). The distribution of [14C]-2,3,7,8-tetrachlorodibenzo-p-dioxin (TCDD) and its effect on the vitamin A content in parenchymal and stellate cells of rat liver. *J. Nutr.*, **119**(4), pp. 573–580.

Harvey, W. A., Jurgensen, K., Pu, X., Lamb, C. L., Cornell, K. A., Clark, R. J., Klocke, C. and Mitchell, K. A. (2016). Exposure to 2,3,7,8-tetrachlorodibenzo-p-dioxin (TCDD) increases human hepatic stellate cell activation. *Toxicology.*, **344**, pp. 26–33.

Kreuz, S. (2016). Oxidative stress signaling to chromatin in health and disease. *Epigenomics*, **8**, pp. 843–862.

Lamb, C. L., Cholico, G. N., Pu, X., Hagler, G. D., Cornell, K. A. and Mitchell, K. A. (2016). 2,3,7,8-Tetrachlorodibenzo-p-dioxin (TCDD) increases necro-inflammation and hepatic stellate cell activation but does not exacerbate experimental liver fibrosis in mice. *Toxicol. Appl. Pharmacol.*, **311**, pp. 42–51.

Moore, L. D., Le, T. and Fan, G. (2013). DNA methylation and its basic function. *Neuropsychopharmacology*. Nature Publishing Group, **38**(1), pp. 23–38.

Morgan, J. E. and Whitlock, J. P. (1992). Transcription-dependent and transcription-

independent nucleosome disruption induced by dioxin. *Proc. Natl. Acad. Sci. U.S.A.*, **89**(December), pp. 11622–11626.

Murphy, S. K., Yang, H., Moylan, C. A., Pang, H., Dellinger, A., Abdelmalek, M. F., Garrett, M. E., Ashley-Koch, A., Suzuki, A., Tillmann, H. L., Hauser, M. A. and Diehl, A. M. (2013). Relationship between the methylome and transcriptome in patients with non-alcoholic fatty liver disease. *Gastroenterology*, **145**(5), pp. 1076–1087.

Okino, S. T. and Whitlock, J. P. (1995). Dioxin induces localized, graded changes in chromatin structure: implications for Cyp1A1 gene transcription. *Mol. Cell. Biol.*, **15**(7), pp. 3714–3721.

Saxonov, S., Berg, P. and Brutlag, D. L. (2006). A genome-wide analysis of CpG dinucleotides in the human genome distinguishes two distinct classes of promoters. *Proc. Natl. Acad. Sci. U.S.A.*, **103**(5), pp. 1412–1417.

Tilg, H. and Moschen, A. R. (2010). Evolution of inflammation in nonalcoholic fatty liver disease: The multiple parallel hits hypothesis. *Hepatology*, **52**(5), pp. 1836–1846.

Tsuchida, T. and Friedman, S. L. (2017). Mechanisms of hepatic stellate cell activation. *Nat. Rev. Gastroenterol. Hepatol.*, **14**(7), pp. 397–411.